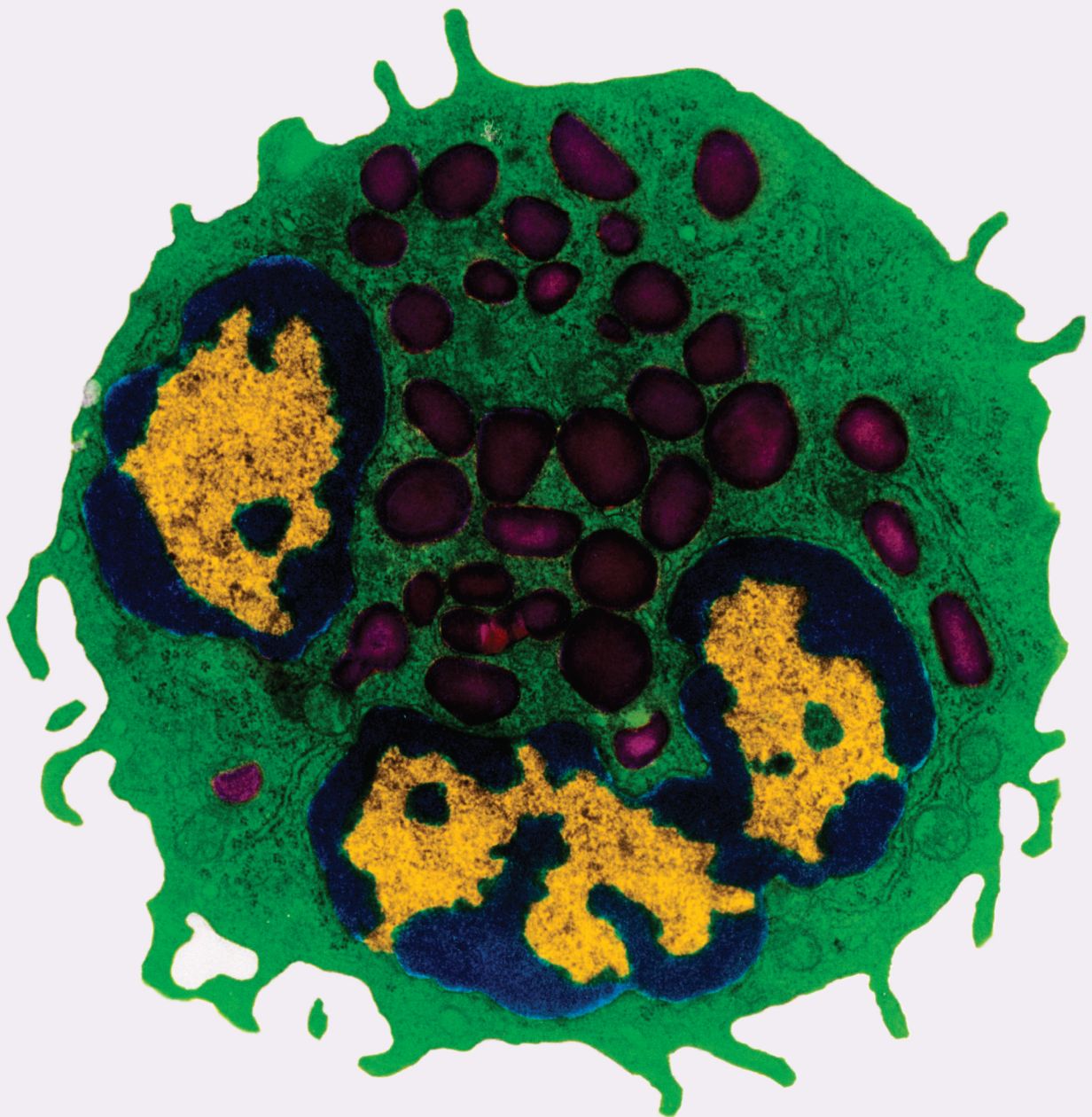


Regulation of Inflammation in Myocardial Ischemia-Reperfusion

Lead Guest Editor: Alessio Rungatscher

Guest Editors: Bruno Podesser and Johann Wojta





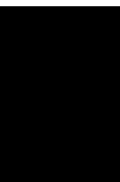
Regulation of Inflammation in Myocardial Ischemia-Reperfusion

Mediators of Inflammation

Regulation of Inflammation in Myocardial Ischemia-Reperfusion

Lead Guest Editor: Alessio Rungatscher


Guest Editors: Bruno Podesser and Johann Wojta







Copyright © 2020 Hindawi Limited. All rights reserved.

This is a special issue published in "Mediators of Inflammation." All articles are open access articles distributed under the Creative Commons Attribution License, which permits unrestricted use, distribution, and reproduction in any medium, provided the original work is properly cited.

Chief Editor



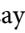




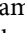
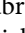
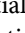
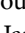
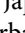
Anshu Agrawal , USA

Associate Editors

Carlo Cervellati , Italy
Elaine Hatanaka , Brazil
Vladimir A. Kostyuk , Belarus
Carla Pagliari , Brazil



Academic Editors

Amedeo Amedei , Italy
Emiliano Antiga , Italy
Tomasz Brzozowski , Poland
Daniela Caccamo , Italy
Luca Cantarini , Italy
Raffaele Capasso , Italy
Calogero Caruso , Italy
Robson Coutinho-Silva , Brazil
Jose Crispin , Mexico
Fulvio D'Acquisto , United Kingdom
Eduardo Dalmarco , Brazil
Agnieszka Dobrzyn, Poland
Ulrich Eisel , The Netherlands
Mirvat El-Sibai , Lebanon
Giacomo Emmi , Italy
Claudia Fabiani , Italy
Fabíola B Filippin Monteiro , Brazil
Antonella Fioravanti , Italy
Tânia Silvia Fröde , Brazil
Julio Galvez , Spain
Mirella Giovarelli , Italy
Denis Girard, Canada
Markus H. Gräler , Germany
Oreste Gualillo , Spain
Qingdong Guan , Canada
Tommaso Iannitti , United Kingdom
Byeong-Churl Jang, Republic of Korea
Yasumasa Kato , Japan
Cheorl-Ho Kim , Republic of Korea
Alex Kleinjan , The Netherlands
Martha Lappas , Australia
Ariadne Malamitsi-Puchner , Greece
Palash Mandal, India
Joilson O. Martins , Brazil
Donna-Marie McCafferty, Canada
Barbro N. Melgert , The Netherlands


Paola Migliorini , Italy
Vinod K. Mishra , USA
Eeva Moilanen , Finland
Elena Niccolai , Italy
Nadra Nilsen , Norway
Sandra Helena Penha Oliveira , Brazil
Michal A. Rahat , Israel
Zoltan Rakonczay Jr. , Hungary
Marcella Reale , Italy
Emanuela Roscetto, Italy
Domenico Sergi , Italy
Mohammad Shadab , USA
Elena Silvestri, Italy
Carla Sipert , Brazil
Helen C. Steel , South Africa
Saravanan Subramanian, USA
Veendamali S. Subramanian , USA
Taina Tervahartiala, Finland
Alessandro Trentini , Italy
Kathy Triantafilou, United Kingdom
Fumio Tsuji , Japan
Maria Letizia Urban, Italy
Giuseppe Valacchi , Italy
Kerstin Wolk , Germany
Soh Yamazaki , Japan
Young-Su Yi , Republic of Korea
Shin-ichi Yokota , Japan
Francesca Zimetti , Italy

Contents



The Prognostic Impact of Circulating Regulatory T Lymphocytes on Mortality in Patients with Ischemic Heart Failure with Reduced Ejection Fraction

Andreas Hammer , Patrick Sulzgruber, Lorenz Koller, Niema Kazem, Felix Hofer, Bernhard Richter, Steffen Blum, Martin Hülsmann, Johann Wojta , and Alexander Niessner
Research Article (7 pages), Article ID 6079713, Volume 2020 (2020)




Ischemia/Reperfusion Injury: Pathophysiology, Current Clinical Management, and Potential Preventive Approaches

César Daniel Sánchez-Hernández, Lucero Aidé Torres-Alarcón, Ariadna González-Cortés, and Alberto N. Peón 
Review Article (13 pages), Article ID 8405370, Volume 2020 (2020)


Analysis of Myocardial Ischemia Parameters after Coronary Artery Bypass Grafting with Minimal Extracorporeal Circulation and a Novel Microplegia versus Off-Pump Coronary Artery Bypass Grafting

Luca Koechlin , Urs Zenklusen, Thomas Doebele, Bejtush Rrahmani, Brigitta Gahl, Thibault Schaeffer, Denis Berdajs, Friedrich S. Eckstein, and Oliver Reuthebuch 
Research Article (8 pages), Article ID 5141503, Volume 2020 (2020)




Bretschneider (Custodiol®) and St. Thomas 2 Cardioplegia Solution in Mitral Valve Repair via Anterolateral Right Thoracotomy: A Propensity-Modelled Comparison

Constantin Mork , Luca Koechlin , Thibault Schaeffer, Lena Schoemig, Urs Zenklusen, Brigitta Gahl, Oliver Reuthebuch, Friedrich S. Eckstein, and Martin T. R. Grapow 
Research Article (7 pages), Article ID 5648051, Volume 2019 (2019)



Post-TTM Rebound Pyrexia after Ischemia-Reperfusion Injury Results in Sterile Inflammation and Apoptosis in Cardiomyocytes

Giang Tong , Nalina N. A. von Garlen, Sylvia J. Wowro, Phuong D. Lam, Jana Krech, Felix Berger, and Katharina R. L. Schmitt
Research Article (10 pages), Article ID 6431957, Volume 2019 (2019)

Neutrophil Extracellular Trap Components Associate with Infarct Size, Ventricular Function, and Clinical Outcome in STEMI

Ragnhild Helseth , Christian Shetelig, Geir Øystein Andersen, Miriam Sjøstad Langseth, Shanmuganathan Limalanathan, Trine B. Opstad, Harald Arnesen, Pavel Hoffmann , Jan Eritsland, and Ingebjørg Seljeflot 
Research Article (10 pages), Article ID 7816491, Volume 2019 (2019)

Enhanced Activity by NKCC1 and Slc26a6 Mediates Acidic pH and Cl⁻ Movement after Cardioplegia-Induced Arrest of db/db Diabetic Heart

Minjeong Ji, Seok In Lee, Sang Ah Lee, Kuk Hui Son , and Jeong Hee Hong 
Research Article (12 pages), Article ID 7583760, Volume 2019 (2019)

Research Article

The Prognostic Impact of Circulating Regulatory T Lymphocytes on Mortality in Patients with Ischemic Heart Failure with Reduced Ejection Fraction

Andreas Hammer ¹, Patrick Sulzgruber,¹ Lorenz Koller,¹ Niema Kazem,¹ Felix Hofer,¹ Bernhard Richter,¹ Steffen Blum,¹ Martin Hülsmann,¹ Johann Wojta ^{1,2} and Alexander Niessner¹

¹Division of Cardiology, Department of Internal Medicine II, Medical University of Vienna, Austria

²Ludwig Boltzmann Cluster for Cardiovascular Research, Vienna, Austria

Correspondence should be addressed to Johann Wojta; johann.wojta@meduniwien.ac.at

Received 24 July 2019; Accepted 6 January 2020; Published 10 February 2020

Academic Editor: Markus H. Gräler

Copyright © 2020 Andreas Hammer et al. This is an open access article distributed under the Creative Commons Attribution License, which permits unrestricted use, distribution, and reproduction in any medium, provided the original work is properly cited.

Background. Heart failure with reduced ejection fraction (HFrEF) constitutes a global health issue. While proinflammatory cytokines proved to have a pivotal role in the development and progression of HFrEF, less attention has been paid to the cellular immunity. Regulatory T lymphocytes (Tregs) seem to have an important role in the induction and maintenance of immune homeostasis. Therefore, we aimed to investigate the impact of Tregs on the outcome in HFrEF. **Methods.** We prospectively enrolled 112 patients with HFrEF and performed flow cytometry for cell phenotyping. Individuals were stratified in ischemic (iHFrEF, $n = 57$) and nonischemic etiology (niHFrEF, $n = 55$). Cox regression hazard analysis was used to assess the influence of Tregs on survival. **Results.** Comparing patients with iHFrEF to niHFrEF, we found a significantly lower fraction of Tregs within lymphocytes in the ischemic subgroup (0.42% vs. 0.56%; $p = 0.009$). After a mean follow-up time of 4.5 years, 32 (28.6%) patients died due to cardiovascular causes. We found that Tregs were significantly associated with cardiovascular survival in the entire study cohort with an adjusted HR per one standard deviation (1-SD) of 0.60 (95% CI: 0.39-0.92; $p = 0.017$). A significant inverse association of Tregs and cardiovascular mortality in patients with iHFrEF with an adj. HR per 1-SD of 0.59 (95% CI: 0.36-0.96; $p = 0.034$) has been observed, while this association was not evident in the nonischemic subgroup (adj. HR per 1-SD of 0.62 (95% CI: 0.17-2.31); $p = 0.486$). **Conclusion.** Our results indicate a potential influence of Tregs in the pathogenesis and progression of iHFrEF, fostering the implication of cellular immunity in iHFrEF pathophysiology and proving Tregs as a predictor for long-term survival among iHFrEF patients. A preview of this study has been presented at a meeting of the European Society of Cardiology earlier this year.

1. Introduction

Heart failure with reduced ejection fraction (HFrEF) represents a major health issue in western-industrialized countries with an estimated prevalence of more than 37 million people worldwide [1]. As multifaceted syndrome caused by structural damage and subsequent dysfunction of the cardiac tissue, it is mainly promoted via inflammatory response triggered by cardiac tissue damage and functional remodeling [2–5]. In this regard, there has been growing evidence of

close pathophysiological links between the progression of HFrEF and both local and peripheral proinflammatory states. Inflammatory biomarkers such as high-sensitivity C-reactive protein (hsCRP) or cytokines were found to have a major predictive potential on the development and progression of HFrEF. However, while data on peripheral cytokines has been widely investigated, less attention has been paid to the association of cellular immunity. In this regard, T lymphocytes were recently found among cardiac tissue in both patients with ischemic and nonischemic HFrEF—suggesting

their importance in the modulation of cardiac remodeling driven by inflammatory stimuli [6, 7]. It is well investigated that exaggerated immune activity is closely related to HFrEF severity and patient outcome by an increase of proinflammatory cytokines and both activation and recruitment of several T cell lines [8–10]. Among these, intrinsic proinflammatory stimuli, mostly TNF- α and its involvement in cardiac remodeling through the recruitment of further—especially cytotoxic—T cell populations, have recently been identified as an independent predictor for outcome in HFrEF individuals [11]. As a major modulator of the inflammatory response, regulatory T cells (Tregs) induce and maintain immune homeostasis through TGF- β , IL-2, and IL-10. It consequently suppresses T cell activation, proliferation, and cytokine production and therefore inhibits an exaggerated immune response and most importantly potentially unjustified tissue damage and cardiac fibrosis. Considering the strong association of T lymphocytes and outcome in HFrEF, it seems intuitive that regulatory Tregs might have a major impact on the limitation of inflammation-triggered local tissue damage, cardiac fibrosis, and subsequently the outcome of patients at risk. Therefore, we aimed to investigate the impact of regulatory T cells on patient outcome in HFrEF.

2. Methods

2.1. Study Population. Within the present investigation, we prospectively enrolled 112 patients with HFrEF between January 2008 and December 2010 at a specialized outpatient department for the management of heart failure of the Medical University of Vienna, Department of Cardiology (Austria). All patients received an optimal and personalized medical treatment approach in accordance to the latest guidelines of the European Society of Cardiology (ESC). The presence of HFrEF was defined in accordance to the current guidelines of the ESC for the management of heart failure: New York Heart Association functional classification (NYHA) \geq II and either left ventricular ejection fraction (LVEF) $<$ 40% and/or N-terminal pro B-type natriuretic peptide (NT-proBNP) values $>$ 500 pg/ml. Ischemic HFrEF was classified as acquired heart failure based on significant coronary vessel disease and/or prior acute myocardial infarction. Patients presenting with any kind of inflammatory conditions, active infections, autoimmune diseases, or malignancies were not eligible for study inclusion. The total study population was stratified into two subgroups according to etiology—ischemic (iHFrEF, $n = 57$) and nonischemic etiology (niHFrEF, $n = 55$). Peripheral venous blood samples of all 112 subjects were available for flow cytometry analysis. Participants were followed prospectively until December 2014 or until the primary endpoint was reached. No patient was lost during this period. All participants gave written informed consent for enrollment. The study protocol was approved by the ethics committee of the Medical University of Vienna and complies with the Declaration of Helsinki. Data reporting was performed according to the STROBE and MOOSE guidelines.

2.2. Data Acquisition and Flow Cytometry. At the time of study enrollment, the patient characteristics were assessed; additionally, peripheral venous blood samples were taken and available for all study participants. All patients were enrolled in a stable condition free of any signs of congestion of acute cardiac ischemia. In patients presenting with ischemic HFrEF, the definition of heart failure was made at least 6 weeks after the acute ischemic event to overcome selection bias based on postinfarction myocardial stunning as recommended by the European Society of Cardiology [12, 13]. Routine laboratory parameters were analyzed and processed according to the local standards of the Department of Laboratory Medicine of the Medical University of Vienna. In addition, cells from fresh EDTA blood samples were stained with APC-Cy7-conjugated Anti-CD4 (BD Biosciences, San Jose, CA, USA) and FITC-conjugated Anti-CD8. Regulatory T cells were identified via their intracellular forkhead-box protein P3 (Fox-P3) and CD25 expression using PE-conjugated Anti-Fox-P3 (BioLegend, San Diego, CA, USA) as well as APC-conjugated Anti-CD25 (BioLegend, San Diego, CA, USA) in a second FACS panel. Stained cells were analyzed using a BD FACS Canto II Flow Cytometer System and FACSDiva software.

2.3. Follow-Up and Study Endpoints. The primary study endpoint was defined as cardiovascular mortality. The cause of death was evaluated by screening the national registry of death and revision of death certificated for the classification of cardiovascular mortality. Causes of death were specified according to the International Statistical Classification of Disease and Related Health Problem 10th revision (ICD-10). Cardiovascular mortality was determined as sudden cardiac death, fatal myocardial infarction, death after cardiovascular intervention, stroke, and causes of death effected from cardiac diseases.

2.4. Statistical Analysis. Categorical values were illustrated in counts and the respective percentage, continuous data as median and interquartile range (IQR). Categorical data are analyzed using the chi-square test, continuous data using the Kruskal-Wallis and Mann-Whitney U test. Cox regression hazard analysis was used to assess the influence of Tregs on survival. Accordingly, the influence of Tregs is presented as hazard ratio (HR) and the respective confidence interval (CI) which refers to an increase per one standard deviation (1-SD) in continuous values. To exclude all potential confounders, the multivariate model was adjusted for age, gender, and NT-proBNP. Moreover, survival curves of cardiovascular mortality were generated as the Kaplan-Meier plot. In statistical hypothesis, testing a p value of >0.05 (2-sided) was considered significant. A sample size of 100 patients (50 per group) was calculated to identify an assumed relative risk increase in mortality by 30% (power 80%, alpha 0.05). STATA 11 software (StataCorp LP, College Station, TX, USA) and PASW 18.0 (IBM SPSS, Armonk, NY, USA) were applied for statistical analysis.

The datasets gathered and analyzed during the current study are available from the corresponding author on reasonable request.

TABLE 1: Baseline characteristics.

	Total collective	Ischemic HFrEF (<i>n</i> = 57)	Nonischemic HFrEF (<i>n</i> = 55)	<i>p</i> value
Age, years (IQR)	65.6 (57.1-70.7)	66.6 (57.7-70.8)	61.9 (56.4-70.7)	0.094
Male gender, <i>n</i> (%)	84 (75.7)	47 (82.5)	37 (69.1)	0.098
BMI, kg/m ² (IQR)	28.1 (24.6-31.3)	28.7 (25.3-31.9)	27.5 (24.1-30.8)	0.994
Diabetes mellitus, <i>n</i> (%)	42 (38.2)	23 (41.1)	19 (32.5)	0.478
Hypertension, <i>n</i> (%)	76 (68.5)	43 (75.4)	33 (61.8)	0.187
Current smoker, <i>n</i> (%)	20 (18.0)	11 (19.3)	9 (16.4)	0.682
Hypercholesterolemia, <i>n</i> (%)	59 (53.2)	39 (68.4)	20 (36.4)	0.002
Coronary vessel disease, <i>n</i> (%)	59 (53.2)	57 (100.0)	2 (3.6)	<0.001
Atrial fibrillation, <i>n</i> (%)	56 (50.5)	28 (49.1)	28 (51.9)	0.774
Left ventricular ejection fraction				0.802
>40%, <i>n</i> (%)	27 (32.7)	18 (32.7)	19 (35.8)	
30-40%, <i>n</i> (%)	39 (36.4)	21 (38.2)	18 (34.0)	
<30%, <i>n</i> (%)	32 (29.9)	16 (29.1)	16 (30.2)	
Nt-proBNP, pg/ml (IQR)	1120 (443-2632)	1353 (449-3105)	851 (431-2117)	0.790
eGFR, ml/min/1.73m ² (IQR)	45.9 (35.0-54.7)	38.9 (32.2-50.2)	52.4 (41.9-59.9)	0.823
CRP, mg/dl (IQR)	0.36 (0.18-0.71)	0.32 (0.18-0.66)	0.37 (0.16-0.83)	0.520

Categorical data are presented as counts and percentages, continuous as median and IQR (interquartile range). Categorical data are analyzed using the chi-square test, continuous data using the Kruskal-Wallis test.

TABLE 2: Distribution of T cell subsets.

	Ischemic HFrEF	Nonischemic HFrEF	<i>p</i> value
Total lymphocytes (IQR)	2811 (2032-3753)	2986 (2260-4507)	0.183
% regulatory T cells within lymphocytes (IQR)	0.42 (0.30-0.68)	0.56 (0.39-0.80)	0.009
% CD4 ⁺ T cells within lymphocytes (IQR)	7.1 (5.2-10.4)	6.3 (4.2-8.3)	0.080
% CD3 ⁺ T cells within lymphocytes (IQR)	71.7 (67.6-76.6)	71.6 (65.8-77.5)	0.707
% CD8 ⁺ T cells within lymphocytes (IQR)	22.9 (17.7-34.2)	22.1 (14.1-32.3)	0.273

Continuous data are presented as median (interquartile range) and were compared between subgroups using the Mann-Whitney *U* test.

3. Results

3.1. Baseline Characteristics. A detailed description of the entire study population (*n* = 112) and stratified in iHFrEF (*n* = 57) and niHFrEF (*n* = 55) is illustrated in Table 1. In short, the average age was 65.6 years (IQR: 57.1-70.1) and 75% of participants were male. Comparing individuals with iHFrEF and niHFrEF, we observed a balanced cardiovascular risk profile in both groups, with regard to hypertension and type II diabetes mellitus. As expected, iHFrEF individuals presented with increased rates of hypercholesterolemia (iHFrEF: 68.4% vs. niHFrEF: 36.4%; *p* = 0.002) and coronary vessel disease (iHFrEF: 3.6% vs. niHFrEF: 100.0%; *p* < 0.001). Additionally, disease severity indicated via left ventricular ejection fraction (LVEF; *p* = 0.802) and N-terminal pro-Brain Natriuretic Peptide (Nt-proBNP; *p* = 0.790) were found to be comparable between types of HFrEF.

3.2. Distribution of T Cell Subsets. While the fraction of CD4⁺ (*p* = 0.080), CD3⁺ (*p* = 0.707), and CD8⁺ (*p* = 0.273) cells within T lymphocytes was comparable between iHFrEF and niHFrEF, a significantly higher fraction of Tregs was observed within the niHFrEF subgroup (iHFrEF: 0.42% vs. niHFrEF: 0.56%; *p* = 0.009; see Table 2).

3.3. Survival Analysis

3.3.1. Cox Regression Analysis. After a mean follow-up time of 4.5 years, 32 (28.6%) patients died due to cardiovascular causes. We observed a significant inverse association of the fraction of Tregs with cardiovascular mortality in the entire study population with a crude HR per 1-SD of 0.53 (95% CI: 0.36-0.79; *p* = 0.002). Interestingly, while the predictive potential of Tregs was lost in the niHFrEF (crude HR per 1-SD of 0.41 (95% CI: 0.12-1.44, *p* = 0.163)) subgroup, its prognostic effect remained stable within the iHFrEF population (crude HR per 1-SD of 0.57 (95% CI: 0.36-0.96, *p* = 0.019)). Of note, the association remained stable even after comprehensive adjustment for potential confounders (adj. HR per 1-SD of 0.59 (95% CI: 0.36-0.96, *p* = 0.034), Table 3).

3.3.2. Kaplan-Meier Survival Curves. The Kaplan-Meier survival curves according to tertiles of frequencies of Tregs were plotted and compared using the log-rank test in the total study collective, as well as patients stratified in iHFrEF and niHFrEF. Tertiles were stratified in 1 = low, 2 = mid, and 3 = high frequencies of Tregs. A period of 55 months was observed. The cardiovascular mortality event rate stratified

TABLE 3: Outcome analysis.

Cardiovascular mortality	Crude HR (95% CI)	<i>p</i> value	Adjusted HR (95% CI)	<i>p</i> value
Entire study cohort	0.53 (0.36-0.79)	0.002	0.60 (0.39-0.92)	0.017
Ischemic HFrEF	0.57 (0.35-0.91)	0.019	0.59 (0.36-0.96)	0.034
Nonischemic HFrEF	0.41 (0.12-1.44)	0.163	0.62 (0.17-2.31)	0.486

Cox proportional hazard model for % regulatory T cells within lymphocytes in patients with iHFrEF and niHFrEF. Hazard ratios (HR) for continuous variables refer to a 1-SD increase. The multivariate model was adjusted for age, gender, and NT-proBNP.

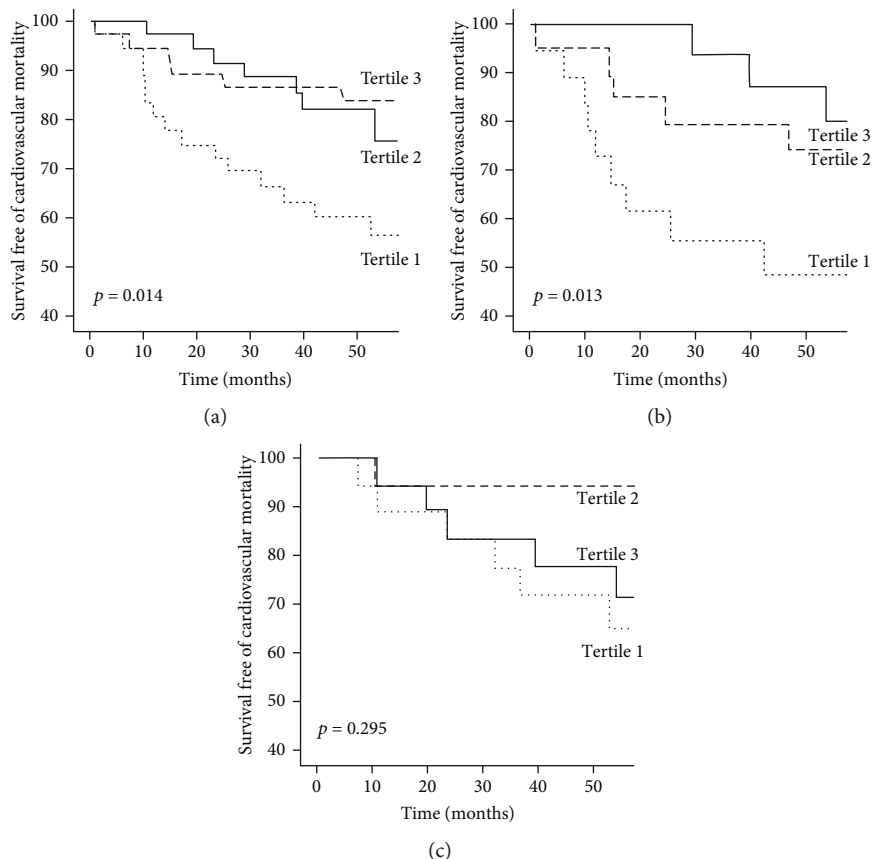


FIGURE 1: Survival curves of cardiovascular mortality. The Kaplan-Meier plots showing survival free of cardiovascular mortality in the total study collective (a) and patients stratified in ischemic HFrEF (b) as well as nonischemic HFrEF (c) according to tertiles of frequencies of regulatory T cells. Tertile 1 = low; tertile 2 = mid; tertile 3 = high.

by Treg fraction within the entire study population was 42.5% (low) vs. 24% (mid) vs. 16% (high) ($p = 0.014$; see Figure 1(a)). Moreover, a cardiovascular event rate of 52.5% (low) vs. 26% (mid) vs. 20% (high) ($p = 0.013$; see Figure 1(b)) was found in patients with iHFrEF. Patients with niHFrEF presented a cardiovascular mortality rate of 36% vs. 6% vs. 29% (tertile 1-3) ($p = 0.295$; see Figure 1(c)).

4. Discussion

To the best of our knowledge, the present investigation mirrors the first and largest in literature that highlighted a clear association of Tregs and patient outcome in HFrEF. Additionally, we were able to highlight that the observed effect of risk prediction is mainly attributed to ischemic etiology of HFrEF.

Recently, proinflammatory cytokines proved to have a pivotal role in the development and progression of HFrEF—however, less attention has been paid to the impact of cellular immunity. Shear stress and inflammatory mediators released by damaged myocardial tissue encourage sterile inflammation among myocytes and subsequently cardiac fibrosis [14] in HFrEF. Besides affecting the cardiac tissue itself, released cytokines proved to indirectly impact other organs as well [14, 15]. Moreover, the observation has been made that patients with HFrEF show elevated levels of inflammatory cytokines, such as IL-1 β and IL-6 and TNF- α [16]. The latter correlates with disease severity, but generally, cytokines and their receptors seem to be a predictor of mortality in patients with progressed HFrEF [8, 16].

IL-1 β promotes increased proliferation of monocytes in the spleen and monocytoysis through the stimulation of stem

cells in the bone marrow [17, 18]. Additionally, TNF-alpha modifies inflammation in the musculoskeletal system and adipose tissue [19, 20]. Both mentioned cytokines are also able to downregulate the expression of Ca^{2+} regulation genes in myocytes [21, 22]. This subsequently leads to a direct negative inotropic effect through disturbed intracellular Ca^{2+} homeostasis and therefore promotes cardiac remodeling, loss of LVEF, and tissue fibrosis in HFrEF [23, 24]. Furthermore, it has been illustrated that TNF-alpha and IL-1 β are able to upregulate angiotensin II type 1 receptors on cardiac fibroblasts which additionally supports fibrosis [25, 26].

It is well established that the neurohumoral mechanism through the β -adrenergic nervous system and the renin angiotensin aldosterone system is trying to preserve the required cardiac function; however, this can lead to inflammation in other organs [27, 28]. Angiotensin II and catecholamine release that further stimulates the monocytopoiesis in the spleen and subsequently through long-term vasoconstriction skeletal muscle is harmed due to inadequate perfusion; thus, further inflammation is induced [29, 30]. Intestinal organs may suffer from underperfusion which potentially results in increased mucosal permeability and subsequently promotes systemic inflammation through translocation of bacteria and toxins into the blood stream [31–33]. Generally, inflammation leads to apoptosis of cardiomyocytes, myofibroblast differentiation, hypertrophy, endothelial dysfunction, and ultimately to myocardial remodeling and therefore dysfunction of the left ventricle [14, 15]. Thus, inflammatory processes, whether cardiac or systemic (e.g., obesity and rheumatoid arthritis), can trigger HFrEF through variable pathophysiological mechanisms.

Treg cells are the most important immune regulators and defined as $\text{CD4}^+\text{CD25}^+\text{Foxp3}^+$ T cells. The intracellular transcription factor Foxp3 is a master regulator of Treg function and development and at present the most reliable molecular marker for Tregs. Moreover, it is vital for the identification of Tregs, as a T cell subset cannot be independently defined by their CD25 receptor surface expression [34].

This specific regulatory T cell population plays a pivotal role in fostering immune homeostasis and disruption of function or development is a primary cause of inflammatory and autoimmune diseases, e.g., rheumatoid arthritis. Tregs have been documented in inflammatory or damaged muscle tissue and atherosclerotic plaques [35, 36]. Through the secretion of anti-inflammatory cytokines such as TGF- β , IL-10, and IL-35, they prevent further progression of atherosclerosis and postinfarction inflammation [37–39]. In terms of myocardial infarction, genetic ablation of Foxp3^+ Tregs leads to pronounced infiltration by proinflammatory T cells and thus severe cardiac inflammation and impaired cardiac function [40].

In addition, Tregs foster the healing process after myocardial infarction by modulating monocyte and macrophage differentiation [40]. The tissue regenerative effect of Tregs has been subject of emerging studies, but the specific mechanism of recruitment, and how they utilize regulatory effects within various local environments, remains yet unknown [41].

Our results further support the idea of cellular immunity in iHFrEF pathophysiology and corroborate Tregs as a predictor for long-term survival among iHFrEF patients. Higher levels of Tregs apparently contributed to a better overall survival. In our study collective, the niHFrEF subgroup showed both elevated levels of Tregs and better survival. In contrast, we found lower levels of Tregs and thus worse outcome within the iHFrEF subgroup. This observation supports previous findings [36], which documented reduced frequencies of circulating Tregs and also compromised function of Tregs in patients presenting with HFrEF. The latter, however, was not subject of the present study but would be interesting for further investigation.

Furthermore, the specific cause of the observed differences between the niHFrEF and iHFrEF subgroup remains unclear. A possible explanation for lower Treg counts in patients presenting with iHFrEF could be due to the inflammatory origin of the disease. iHFrEF is clearly related to atherosclerosis, which is driven by endothelial cell activation and plaque inflammation predominately mediated by Th1 cells [42]. In addition, an augmentation of the Th17/Treg ratio has been reported in ischemic heart tissue [43, 44]. The importance of this ratio has been discovered in other autoinflammatory diseases and could be related to plasticity of CD4^+ T cell lineage differentiation [45]. Recently, the possibility of conversion to other phenotypes was discovered and lead to revision of the concept of terminally differentiated effector T cell lineage [46]. Thus, the influence of cell plasticity could have an important meaning in iHFrEF and would be an intriguing area for further investigation.

Previous research has also found decreased frequencies of Tregs in patients with nonischemic HFrEF [47]. However, the pathogenesis of niHFrEF is much more diverse than in iHFrEF due to its multifactorial causes, which are not limited to autoinflammatory etiology. Various other factors, for example, genetic predisposition or virus infections have been suggested as causes of niHFrEF. Moreover, no etiology can be found in the majority of cases and cardiomyopathy is considered idiopathic [48].

Overall, there is evidence for inflammatory processes in both etiologies of HFrEF, but the inflammatory component is apparently more dominant in iHFrEF due to its origin in atherosclerosis. Thus, it seems plausible that a lower frequency of Tregs is more closely associated with a worse outcome in the iHFrEF than in the niHFrEF subgroup. Cell plasticity and conversion to proinflammatory CD4^+ cells could be a possible explanation for the lower Treg fraction in iHFrEF.

4.1. Limitations. The major limitation of the present study mirrors its small sample size. However, considering the performed methodology and flow cytometry, a satisfactory number of participants has been enrolled.

5. Conclusion

The frequency of Tregs in patients with iHFrEF was found to have a strong and inverse association with mortality in HFrEF. The present investigation supports the hypothesis

that Tregs are an independent predictor of cardiovascular mortality in HFREF patients. Most importantly, we extended the current knowledge by demonstrating that their prognostic potential is mainly attributed via the predictive effect in iHFREF while there was no effect observed in niHFREF. Our results indicate a clear influence of Tregs in the pathogenesis and progression of HFREF—especially in individuals presenting with iHFREF, fostering the implication of cellular immunity in its pathophysiology. Tregs mirror an independent predictor for long-term survival among iHFREF patients. Future investigations are needed to clarify the exact predictive mechanism of Tregs in HFREF.

Data Availability

The data used to support the findings of this study are available from the corresponding author upon request.

Conflicts of Interest

The authors declare that they have no conflicts of interest.

Authors' Contributions

Andreas Hammer and Patrick Sulzgruber contributed equally in this work.

Acknowledgments

The study was supported and received funding for materials by the “Association for the Promotion of Research in Atherosclerosis, Thrombosis and Vascular Biology” (Vienna, Austria), the Special Research Program (SFB) of the FWF (Vienna, Austria), and the Ludwig Boltzmann Institute for Cardiovascular Research (Vienna, Austria).

References

- [1] B. Ziaieian and G. C. Fonarow, “Epidemiology and aetiology of heart failure,” *Nature Reviews Cardiology*, vol. 13, no. 6, pp. 368–378, 2016.
- [2] A. K. Schroer and W. D. Merryman, “Mechanobiology of myofibroblast adhesion in fibrotic cardiac disease,” *Journal of Cell Science*, vol. 128, no. 10, pp. 1865–1875, 2015.
- [3] S. Van Linthout and C. Tschöpe, “Inflammation - cause or consequence of heart failure or both?,” *Current Heart Failure Reports*, vol. 14, no. 4, pp. 251–265, 2017.
- [4] S. A. Dick and S. Epelman, “Chronic heart failure and inflammation: what do we really know?,” *Circulation Research*, vol. 119, no. 1, pp. 159–176, 2016.
- [5] D. Westermann, D. Lindner, M. Kasner et al., “Cardiac inflammation contributes to changes in the extracellular matrix in patients with heart failure and normal ejection fraction,” *Circulation. Heart Failure*, vol. 4, no. 1, pp. 44–52, 2011.
- [6] A. Abbate, E. Bonanno, A. Mauriello et al., “Widespread myocardial inflammation and infarct-related artery patency,” *Circulation*, vol. 110, no. 1, pp. 46–50, 2004.
- [7] T. Nevers, A. M. Salvador, A. Grodecki-Pena et al., “Left ventricular T-cell recruitment contributes to the pathogenesis of heart failure,” *Circulation Heart Failure*, vol. 8, no. 4, pp. 776–787, 2015.
- [8] A. Deswal, N. J. Petersen, A. M. Feldman, J. B. Young, B. G. White, and D. L. Mann, “Cytokines and cytokine receptors in advanced heart failure: an analysis of the cytokine database from the vesnarinone trial (VEST),” *Circulation*, vol. 103, no. 16, pp. 2055–2059, 2001.
- [9] R. Ferrari, T. Bachetti, R. Confortini et al., “Tumor necrosis factor soluble receptors in patients with various degrees of congestive heart failure,” *Circulation*, vol. 92, no. 6, pp. 1479–1486, 1995.
- [10] M. Rauchhaus, W. Doehner, D. P. Francis et al., “Plasma cytokine parameters and mortality in patients with chronic heart failure,” *Circulation*, vol. 102, no. 25, pp. 3060–3067, 2000.
- [11] L. Koller, B. Richter, G. Goliash et al., “CD4⁺CD28^{null} cells are an independent predictor of mortality in patients with heart failure,” *Atherosclerosis*, vol. 230, no. 2, pp. 414–416, 2013.
- [12] H. Søholm, J. Lønborg, M. J. Andersen et al., “Repeated echocardiography after first ever ST-segment elevation myocardial infarction treated with primary percutaneous coronary intervention—is it necessary?,” *European Heart Journal Acute Cardiovascular Care*, vol. 4, no. 6, pp. 528–536, 2015.
- [13] B. Ibanez, S. James, S. Agewall et al., “2017 ESC guidelines for the management of acute myocardial infarction in patients presenting with ST-segment elevation: the task force for the management of acute myocardial infarction in patients presenting with ST-segment elevation of the European Society of Cardiology (ESC),” *European Heart Journal*, vol. 39, no. 2, pp. 119–177, 2018.
- [14] J. W. Jahng, E. Song, and G. Sweeney, “Crosstalk between the heart and peripheral organs in heart failure,” *Experimental & Molecular Medicine*, vol. 48, no. 3, article e217, 2016.
- [15] G. Loncar, S. Fulster, S. von Haehling, and V. Popovic, “Metabolism and the heart: an overview of muscle, fat, and bone metabolism in heart failure,” *International Journal of Cardiology*, vol. 162, no. 2, pp. 77–85, 2013.
- [16] G. Torre-Amione, S. Kapadia, C. Benedict, H. Oral, J. B. Young, and D. L. Mann, “Proinflammatory cytokine levels in patients with depressed left ventricular ejection fraction: a report from the studies of left ventricular dysfunction (SOLVD),” *Journal of the American College of Cardiology*, vol. 27, no. 5, pp. 1201–1206, 1996.
- [17] H. B. Sager, T. Heidt, M. Hulsmans et al., “Targeting interleukin-1 β reduces leukocyte production after acute myocardial infarction,” *Circulation*, vol. 132, no. 20, pp. 1880–1890, 2015.
- [18] S. Honsho, S. Nishikawa, K. Amano et al., “Pressure-mediated hypertrophy and mechanical stretch induces IL-1 release and subsequent IGF-1 generation to maintain compensative hypertrophy by affecting Akt and JNK pathways,” *Circulation Research*, vol. 105, no. 11, pp. 1149–1158, 2009.
- [19] S. Gielen, V. Adams, S. Mobius-Winkler et al., “Anti-inflammatory effects of exercise training in the skeletal muscle of patients with chronic heart failure,” *Journal of the American College of Cardiology*, vol. 42, no. 5, pp. 861–868, 2003.
- [20] B. Wang, J. R. Jenkins, and P. Trayhurn, “Expression and secretion of inflammation-related adipokines by human adipocytes differentiated in culture: integrated response to TNF- α ,” *American Journal of Physiology Endocrinology and Metabolism*, vol. 288, no. 4, pp. E731–E740, 2005.
- [21] C.-K. Wu, J.-K. Lee, F.-T. Chiang et al., “Plasma levels of tumor necrosis factor- α and interleukin-6 are associated with diastolic heart failure through downregulation of sarcoplasmic reticulum Ca²⁺ ATPase,” *Critical Care Medicine*, vol. 39, no. 5, pp. 984–992, 2011.

- [22] C. M. Thaik, A. Calderone, N. Takahashi, and W. S. Colucci, "Interleukin-1 beta modulates the growth and phenotype of neonatal rat cardiac myocytes," *The Journal of Clinical Investigation*, vol. 96, no. 2, pp. 1093–1099, 1995.
- [23] T. Yokoyama, L. Vaca, R. D. Rossen, W. Durante, P. Hazarika, and D. L. Mann, "Cellular basis for the negative inotropic effects of tumor necrosis factor- α in the adult mammalian heart," *The Journal of Clinical Investigation*, vol. 92, no. 5, pp. 2303–2312, 1993.
- [24] S. Sedej, A. Schmidt, M. Denegri et al., "Subclinical abnormalities in sarcoplasmic reticulum Ca^{2+} release promote eccentric myocardial remodeling and pump failure death in response to pressure overload," *Journal of the American College of Cardiology*, vol. 63, no. 15, pp. 1569–1579, 2014.
- [25] J. Peng, D. Gurantz, V. Tran, R. T. Cowling, and B. H. Greenberg, "Tumor necrosis factor- α -induced AT_1 receptor upregulation enhances angiotensin II-mediated cardiac fibroblast responses that favor fibrosis," *Circulation Research*, vol. 91, no. 12, pp. 1119–1126, 2002.
- [26] D. Gurantz, R. T. Cowling, N. Varki, E. Frikovsky, C. D. Moore, and B. H. Greenberg, "IL-1 β and TNF- α upregulate angiotensin II type 1 (AT_1) receptors on cardiac fibroblasts and are associated with increased AT_1 density in the post-MI heart," *Journal of Molecular and Cellular Cardiology*, vol. 38, no. 3, pp. 505–515, 2005.
- [27] P. Libby, M. Nahrendorf, and F. K. Swirski, "Leukocytes link local and systemic inflammation in ischemic cardiovascular disease: an expanded "cardiovascular continuum"," *Journal of the American College of Cardiology*, vol. 67, no. 9, pp. 1091–1103, 2016.
- [28] P. Dutta, G. Courties, Y. Wei et al., "Myocardial infarction accelerates atherosclerosis," *Nature*, vol. 487, no. 7407, pp. 325–329, 2012.
- [29] K. R. Nilsson, B. D. Duscha, P. M. Hranitzky, and W. E. Kraus, "Chronic heart failure and exercise intolerance: the hemodynamic paradox," *Current Cardiology Reviews*, vol. 4, no. 2, pp. 92–100, 2008.
- [30] H. Tsutsui, T. Ide, S. Hayashidani et al., "Enhanced generation of reactive oxygen species in the limb skeletal muscles from a murine infarct model of heart failure," *Circulation*, vol. 104, no. 2, pp. 134–136, 2001.
- [31] Y. Nagatomo and W. H. Tang, "Intersections between microbiome and heart failure: revisiting the gut hypothesis," *Journal of Cardiac Failure*, vol. 21, no. 12, pp. 973–980, 2015.
- [32] A. Krack, B. M. Richartz, A. Gastmann et al., "Studies on intra-gastric PCO_2 at rest and during exercise as a marker of intestinal perfusion in patients with chronic heart failure," *European Journal of Heart Failure*, vol. 6, no. 4, pp. 403–407, 2004.
- [33] E. Pasini, R. Aquilani, C. Testa et al., "Pathogenic gut flora in patients with chronic heart failure," *JACC Heart Fail*, vol. 4, no. 3, pp. 220–227, 2016.
- [34] A. H. Banham, F. M. Powrie, and E. Suri-Payer, "FOXP3⁺ regulatory T cells: current controversies and future perspectives," *European Journal of Immunology*, vol. 36, no. 11, pp. 2832–2836, 2006.
- [35] V. O. Sokolov, T. L. Krasnikova, L. V. Prokofieva, N. B. Kukhtina, and T. I. Arefieva, "Expression of markers of regulatory $\text{CD4}^+\text{CD25}^+\text{foxp3}^+$ cells in atherosclerotic plaques of human coronary arteries," *Bulletin of Experimental Biology and Medicine*, vol. 147, no. 6, pp. 726–729, 2009.
- [36] T. T. Tang, J. Yuan, Z. F. Zhu et al., "Regulatory T cells ameliorate cardiac remodeling after myocardial infarction," *Basic Research in Cardiology*, vol. 107, no. 1, p. 232, 2012.
- [37] M. Dobaczewski, Y. Xia, M. Bujak, C. Gonzalez-Quesada, and N. G. Frangogiannis, "CCR5 signaling suppresses inflammation and reduces adverse remodeling of the infarcted heart, mediating recruitment of regulatory T cells," *The American Journal of Pathology*, vol. 176, no. 5, pp. 2177–2187, 2010.
- [38] Z. Mallat, A. Gojova, C. Marchiol-Fournigault et al., "Inhibition of transforming growth factor- β signaling accelerates atherosclerosis and induces an unstable plaque phenotype in mice," *Circulation Research*, vol. 89, no. 10, pp. 930–934, 2001.
- [39] A. K. Robertson, M. Rudling, X. Zhou, L. Gorelik, R. A. Flavell, and G. K. Hansson, "Disruption of TGF- β signaling in T cells accelerates atherosclerosis," *The Journal of Clinical Investigation*, vol. 112, no. 9, pp. 1342–1350, 2003.
- [40] J. Weirather, U. D. Hofmann, N. Beyersdorf et al., "Foxp3⁺ CD4^+ T cells improve healing after myocardial infarction by modulating monocyte/macrophage differentiation," *Circulation Research*, vol. 115, no. 1, pp. 55–67, 2014.
- [41] C. Zhang, L. Li, K. Feng, D. Fan, W. Xue, and J. Lu, "Repair' Treg cells in tissue injury," *Cellular Physiology and Biochemistry*, vol. 43, no. 6, pp. 2155–2169, 2017.
- [42] F. Abdolmaleki, S. M. Gheibi Hayat, V. Bianconi, T. P. Johnston, and A. Sahebkar, "Atherosclerosis and immunity: a perspective," *Trends in Cardiovascular Medicine*, vol. 29, no. 6, pp. 363–371, 2019.
- [43] M. A. Ismahil, T. Hamid, S. S. Bansal, B. Patel, J. R. Kingery, and S. D. Prabhu, "Remodeling of the mononuclear phagocyte network underlies chronic inflammation and disease progression in heart failure: critical importance of the cardiosplenic axis," *Circulation Research*, vol. 114, no. 2, pp. 266–282, 2014.
- [44] N. Li, H. Bian, J. Zhang, X. Li, X. Ji, and Y. Zhang, "The Th17/Treg imbalance exists in patients with heart failure with normal ejection fraction and heart failure with reduced ejection fraction," *Clinica Chimica Acta*, vol. 411, no. 23–24, pp. 1963–1968, 2010.
- [45] G. R. Lee, "The balance of Th17 versus Treg cells in autoimmunity," *International Journal of Molecular Sciences*, vol. 19, no. 3, p. 730, 2018.
- [46] L. Zhou, M. M. Chong, and D. R. Littman, "Plasticity of CD4^+ T cell lineage differentiation," *Immunity*, vol. 30, no. 5, pp. 646–655, 2009.
- [47] T. T. Tang, Y. J. Ding, Y. H. Liao et al., "Defective circulating $\text{CD4}^+\text{CD25}^+\text{Foxp3}^+\text{CD127}^{\text{low}}$ regulatory T-cells in patients with chronic heart failure," *Cellular Physiology and Biochemistry*, vol. 25, no. 4–5, pp. 451–458, 2010.
- [48] G. M. Felker, R. E. Thompson, J. M. Hare et al., "Underlying causes and long-term survival in patients with initially unexplained cardiomyopathy," *The New England Journal of Medicine*, vol. 342, no. 15, pp. 1077–1084, 2000.

Review Article

Ischemia/Reperfusion Injury: Pathophysiology, Current Clinical Management, and Potential Preventive Approaches

César Daniel Sánchez-Hernández,^{1,2} Lucero Aidé Torres-Alarcón,^{1,2}
Ariadna González-Cortés,^{1,2} and Alberto N. Peón ^{1,3}

¹Sociedad Española de Beneficencia (SEB), Pachuca, Hgo, Mexico

²Área Académica de Medicina, Universidad Autónoma del Estado de Hidalgo (UAEH), Mexico

³Laboratorio de Microbiología, Escuela Superior de Apan (ESAp), UAEH, Apan, Hgo, Mexico

Correspondence should be addressed to Alberto N. Peón; anpeon8@gmail.com

Received 30 August 2019; Revised 18 December 2019; Accepted 3 January 2020; Published 29 January 2020

Guest Editor: Alessio Rungtischer

Copyright © 2020 César Daniel Sánchez-Hernández et al. This is an open access article distributed under the Creative Commons Attribution License, which permits unrestricted use, distribution, and reproduction in any medium, provided the original work is properly cited.

Myocardial ischemia reperfusion syndrome is a complex entity where many inflammatory mediators play different roles, both to enhance myocardial infarction-derived damage and to heal injury. In such a setting, the establishment of an effective therapy to treat this condition has been elusive, perhaps because the experimental treatments have been conceived to block just one of the many pathogenic pathways of the disease, or because they thwart the tissue-repairing phase of the syndrome. Either way, we think that a discussion about the pathophysiology of the disease and the mechanisms of action of some drugs may shed some clarity on the topic.

1. Introduction

Myocardial infarction (MI) or acute myocardial infarction is a term used to refer to an event of heart attack. MI occurs when the cardiac muscle is injured by hypoxia, which happens when a coronary artery is blocked [1]. MI is classified as being either an ST-segment elevation myocardial infarction (STEMI) or a non-ST-segment elevation myocardial infarction (NSTEMI). Moreover, unstable angina (UA) is closely related to NSTEMI, and together, these entities are referred to as non-ST-segment elevation acute coronary syndromes (NSTEACS). Both STEMI and NSTEACS share an underlying pathophysiology: a superimposed thrombus caused by a disruption of an atherosclerotic plaque, which results in subtotal occlusion (NSTEACS) or total occlusion (STEMI) of a coronary artery [2], thus causing damage at the heart's muscle through hypoxia induction.

The principal symptoms of MI are chest pain, which travels to the left arm or left side of the neck, shortness of

breath, sweating, nausea, vomiting, abnormal heart beating, anxiety, and fatigue [3]. Risk factors include an advanced age, tobacco smoking, high blood pressure, diabetes, lack of physical activity, obesity, and chronic kidney disease [4]. Risk factors can be categorized into nonmodifiable and modifiable. Nonmodifiable risk factors include age of more than 45 years in men and more than 55 years in women, family history of early heart disease, and African-American race [5]. Modifiable risk factors include hypercholesterolemia, specifically related to elevation of low-density lipoprotein cholesterol (LDL-C), hypertension, tobacco abuse, diabetes mellitus, obesity, lack of physical activity, metabolic syndrome, and/or mental distress and depression [5]. The difference between both types of risk factors evidently lies in what can be prevented and what cannot.

There is an estimated five-million emergency department visits each year in the US for acute chest pain. Annually, over 800,000 people experience an MI, of which 27% die, mostly before reaching the hospital [6]. On the other hand, heart

disease is Mexico's leading cause of death [7], accounting for 18.8% of total deaths, of which 59% are attributable to myocardial infarction.

In several studies, reperfusion therapy (fibrinolysis and coronary angioplasty) has demonstrated to produce a decrease in the morbidity and mortality associated with myocardial infarction [8]. However, the process of myocardial reperfusion can, paradoxically, enhance myocardial injury through inflammation, finally contributing to 50% of the final MI size [9]. The precise role inflammation plays in the setting of MI has been debated since the 1980s with the infiltration of leukocytes now being recognized as inflammatory mediators, as opposed to the previous concept of them being bystanders of the damage [10].

Nonetheless, in the therapeutic setting, the requirement for best preserving myocardial structure and function upon MI is to restore coronary blood flow as early as possible, using thrombolytic therapy and/or angioplasty [11], but as soon as blood flow is restored, an inflammatory response arises in the damaged section of the heart. This immune response further expands the damage made by the occlusion, originating a phenomenon known as myocardial ischemia reperfusion injury, or myocardial ischemia reperfusion syndrome (MIRS). Actually, MIRS is a major challenge to the treatment of MI [12], because its characteristic local and systemic inflammatory response is able to greatly enhance MI-derived damage, worsening the patient's prognosis [13]. Moreover, current pharmacopeia lacks a specific treatment for such condition. The treatment has been elusive because the immune-muscular-vascular interplay that characterizes MIRS is very complex, and a midpoint between downregulating the inflammatory tissue-damaging response and allowing the leucocyte-orchestrated reparative phase must be achieved.

On the other hand, ischemia reperfusion injury (IRI) is not exclusive to MI, as it also happens as a consequence to brain, kidney, liver, testis, or lung ischemia [14]. In such a tonic, we think that some lessons can be learned from these separate entities that may be applicable in the setting of MIRS. Also, information about MIRS-specific tissue-damaging and tissue-remodeling mediators is currently very vast, so that it may be useful to analyze the current baggage of knowledge on the topic, with aims to pinpoint some of the pathogenic pathways that may help to restrain MIRS upon blockage, as well as some strategies that may be of use for that purpose.

2. Pathophysiology of Myocardial Ischemia Reperfusion Syndrome

In general terms, MIRS must be understood as a complex phenomenon that arises upon blood flow restoration, where reperfused leukocytes find many damage-associated molecular patterns (DAMPs), such as extracellular Ca^+ and ATP released by necrotic cells, which induce the activation of many TLR pathways to promote an inflammatory response. Thus, an acute Th1 response is rapidly induced to clean the necrotic debris, but such an immune response, unfortunately, expands MI-associated damage [9, 15]. Myocardial reperfu-

sion is unavoidable, as it occurs as a consequence to common MI treatments such as thrombolysis, angioplasty [16], and coronary bypass [17, 18]. At a later stage, the Th1-immune response subsides to a Th2-driven immunity, where leukocytes shift their phenotype in order to orchestrate tissue remodeling to avoid cardiac rupture [19]. A highly potent Th2 response, nonetheless, may induce pathological scarring, rendering the whole phenomenon as highly dependent on a very precise immune regulation. Thus, the mediators of this immunopathology must be precisely understood to find areas of opportunity for the development of a specific treatment (Figures 1 and 2).

2.1. Immunopathological Mechanisms of MIRS. The main trigger for MIRS is the vascular and cardiomyocyte cell death [11], which by the release of fragments of mitochondrial DNA, ATP, high mobility group box 1 protein (HMBGB1), and Ca^+ into the extracellular space acts as DAMPs [20], inducing the activation of the NLRP3-inflammasome [21] and TLR9 [22], which converge on the activation of the myeloid differentiation primary response gene 88 (MyD88) and nuclear factor- κ B (NF- κ B) pathways, thus inducing the release of a number of inflammatory mediators, including monocyte-chemoattractant protein 1 (MCP1), interleukin- 1β (IL- 1β), IL-6, tumor-necrosis factor- α (TNF- α), and IL-18 [23]. Inflammasome activation amplifies IL- 1β and IL-18 secretion by cardiac fibroblasts and induces the caspase-1-dependent death of nearby cardiomyocytes, termed pyroptosis—a highly inflammatory form of cell death, characterized by features that are typical of both apoptosis and necrosis [23].

Macrophage inflammatory protein-2 α (MIP-2 α), leukotriene B4 (LTB4), cytokine-induced neutrophil chemoattractant 1 (CINC-1), IL-8, CXCL8, and complement 5a massively recruit neutrophils [24] to infiltrate the MI-damaged area in the first few hours following onset of ischemia [25], peaking at days 1–3, and starting to decline at day 5. Neutrophils then generate high levels of reactive oxygen species (ROS), produce neutrophil-extracellular traps (NETs), and secrete granule components including myeloperoxidase and proteases, which exacerbate local vascular and tissue injury [26] with the purpose of removing necrotic cell debris from the affected zone [27] (Figure 1).

Along with neutrophils, complement proteins infiltrate the reperfused area. The complement is composed of 30 proteins and protein fragments, many of which are circulating as proenzymes and are activated by proteases in response to DAMPs. In this setting, all these proteins converge on two of the three common (terminal) complement pathways, which result in (a) inflammation to attract additional phagocytes (complements C3a, C4a, and C5a) and (b) activation of the cell-killing membrane attack complex (complement C5b-9 or MAC). Thus, the complement cascade amplifies MIRS-derived inflammation and damage [28] (Figure 1).

Both complement elements like C3a, C4a, and C5a and chemokines like MCP1 rapidly recruit monocytes [29] into the reperfused area. Such cells are produced in the bone marrow and are released into the blood in 2 waves, the first one being dominated by inflammatory Ly6C^{hi} monocytes (which

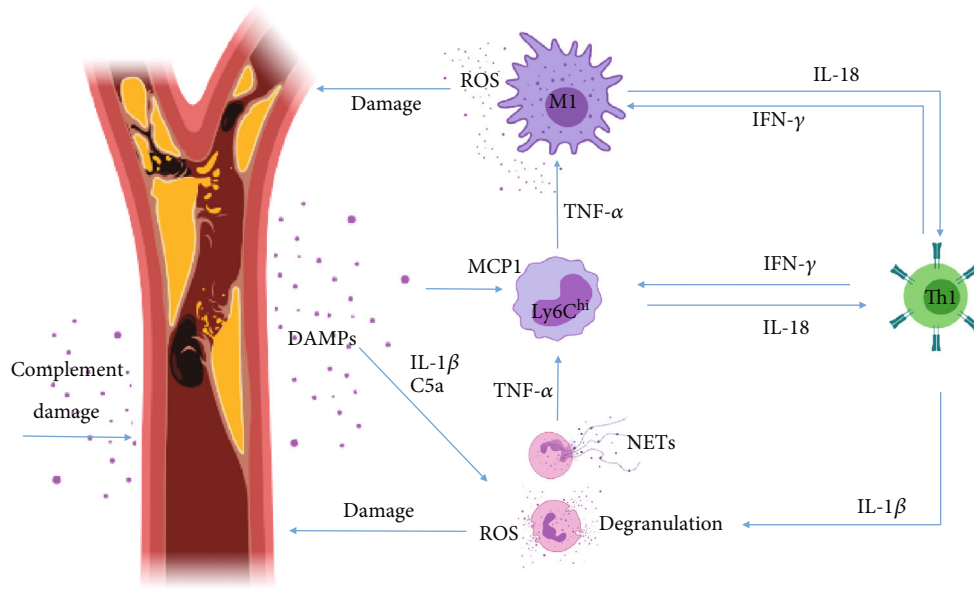


FIGURE 1: Inflammation during the Th1 tissue-damaging immune response of MIRS. Blood clots generate ischemia, which causes necrosis. Released DAMPs induce neutrophil and monocyte activation through TLR and inflammasome activation, which in turn potentiates Th1 polarization. Inflammatory monocytes mature and become M1 macrophages. Tissue damage amplification comes in the form of NETs, granule components, and ROS produced by innate cells and direct complement attack.

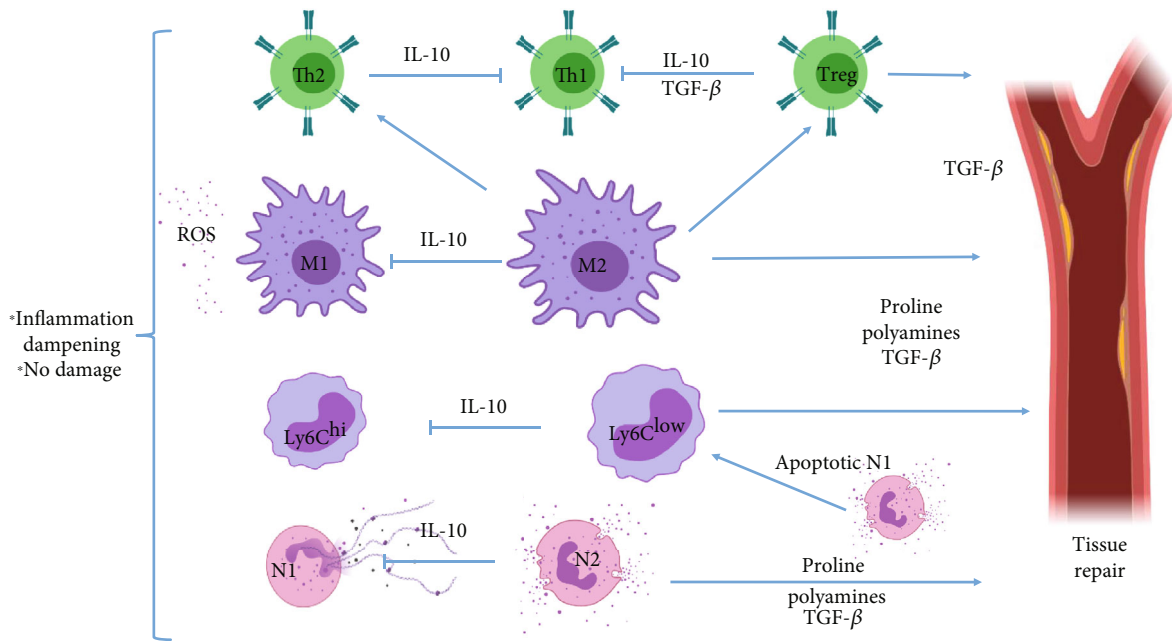


FIGURE 2: The Th2-mediated reparative phase of MIRS. N2 neutrophils and M2 macrophages both produce high levels of IL-10 to dampen N1, Ly6C^{hi}, and M1-mediated degradation of tissue integrity. Also, M2 macrophages induce Th2 and Treg differentiation, while both suppress Th1 development, and Tregs thwart Th2 cells. M2 differentiation is possible by phagocytosis of the neutrophil apoptotic bodies. M2 and Treg cells mediate tissue repair.

peak at days 3–4 post MI) and the second one by anti-inflammatory Ly6C^{low} monocytes (which peak at day 7 post-MI). The infiltrating Ly6C^{hi} cells contribute to debris clearing and vascular/muscular damage, mainly through phagocytosis (for the earlier function) and ROS production

(for the latter function) [30]. Monocytes then differentiate into M1-type macrophages, which have enhanced abilities to the phagocyte, produce ROS, and amplify inflammation through local antigen presentation and costimulation [31] (Figure 1). Subsequently, Ly6C^{low} monocytes start to infiltrate

the reperfused area, and M1 macrophages start to differentiate into M2-type cells (which suppress T-cell activation through negative costimulation and IL-10 production and orchestrate tissue remodeling and vascularization by the secretion of TGF- β), to orchestrate tissue remodeling (as it will be discussed in the following section). Nonetheless, high levels of Th1-inducing factors deter the shift from an M1-type of macrophages to an M2 phenotype, thereby reducing the healing potential of the chronic MIRS phase [32] (Figure 1).

The systemic release of diverse cytokines and chemokines induces the activation of CD4⁺ T-cells, which in the acute phase of MIRS differentiate into a Th1 phenotype, releasing chemokines like CCL7 and cytokines like interferon- γ (IFN- γ), IL-2, and TNF- α , which as a cluster reinforce Th1 differentiation; enhance N1, Ly6C^{hi}, and M1 cells' tissue-damaging abilities [33]; recruit CD8⁺ T-cells [34]; and enhance B cell activity [35]. Both CD8⁺ and B cells have been described to amplify inflammation during this stage and to produce damage on their own, by degranulation, in the case of T-cytotoxic cells [34], and antibody-mediated complement activation, in the case of B-lymphocytes [35] (Figure 1).

In this way, the immunopathology of MIRS can be succinctly described as the interplay between the innate and adaptive arms of the immune system, where a Th1-type immunity is critical for damage induction. In such a system, M1 macrophages and N1 neutrophils are key players on IRI induction, while the adaptive immunity component mainly amplifies the effector mechanisms of the aforementioned innate cells and complement.

2.2. The Th2-Mediated Reparative Phase of MIRS. On days 4-7 after MI, the Th1 tissue-destructive phase of MIRS enters a resolution stage, driven by a Th2 immune response induced by many changes in the cardiac microenvironment. This is regulated by the activation of endogenous inhibitory pathways that suppress the inflammatory phenotype in infiltrated leukocytes located in the MI zone [36].

After producing a high level of tissue damage, when most inflammatory debris have been cleared from the extracellular environment, neutrophils shift from their N1 phenotype to become N2-type cells. This change is accompanied by the production of high levels of IL-10, which aids in the suppression of the acute tissue-damaging Th1 response, by blocking the activation of CD4⁺, CD8⁺, B, N1, M1, and Ly6C^{hi} cells [37]. Moreover, they produce phosphatidylserine (PS), which facilitates ingestion of apoptotic neutrophils by macrophages, resulting in a phenotypic change for macrophages from the M1 to the M2 type, which secrete anti-inflammatory and profibrotic cytokines such as IL-10 and TGF- β , thus promoting tissue repair and vascularization, while aiding in the suppression of inflammation [38] (Figure 2).

Also, the polarization of monocytes and macrophages (M/M) from the tissue-damaging and proinflammatory Ly6C^{hi} and M1 phenotypes to the anti-inflammatory and tissue-repairing Ly6C^{low} and M2 phenotypes is critical to the reparative phase following MI [39], as these cells are able to produce an enzyme that is known as Arginase-1 (Arg-1). Such an enzyme catalyzes the conversion of L-arginine into L-ornithine, which is further metabolized into proline and

polyamines. Both metabolites drive collagen synthesis and bioenergetic pathways that are critical for cell proliferation, respectively, thus contributing to tissue repair. Also, Arg-1 competes for the same substrate, but with more affinity, with the inducible-nitric oxide synthase (iNOS) enzyme, which is responsible for NO production [40]. In this way, M2 macrophages block ROS production by M1, N1, and Ly6C^{hi} cells, thus limiting the extent of tissue damage by the remaining N1 and M1 cells (Figure 2).

The shift in M/M and neutrophil phenotype is mirrored by CD4⁺ T-cells, as Th1 cells subside to a vaster Th2 population that apparently amplifies the strength of the reparative actions of the M/M population [41]. This effect may be due to Th2-derived high levels of IL-4 and IL-13, which are able to induce M2 activation in macrophages [34]. Moreover, recent studies suggest that invariant natural killer (iNK) T-cells and $\gamma\delta$ T-cells have an important role in the settling of the Th1 acute inflammatory response through the secretion of anti-inflammatory cytokines such as TGF- β and IL-10, overall working with T-cells to dampen inflammation [42, 43]. Nonetheless, it has been observed that an enhanced Th2 response is able to induce pathological scarring with increased fibrosis in several settings [44, 45], in such a way that even the Th2 response must be controlled (Figure 2).

In the last decade, CD4⁺ CD25⁺ FoxP3⁺ T-regulatory (Tregs) cells have been recognized not only for their ability to dampen Th1 and Th2 lymphocyte activation and proliferation but also for their ability to downregulate innate immune cells' effector mechanisms [46, 47], while altering the cytokine milieu [48]. Tregs downregulate M1-macrophage activation and develop in parallel with M2 cells, presumably to control their level of activity [49]. In the setting of MIRS, Tregs have been shown to prevent cardiomyocyte apoptosis to limit further damage [48] and to downmodulate differentiation of fibroblasts into myofibroblasts, in order to avoid pathological scarring [50]. Their enhanced production of IL-10 has even been linked with a decrease in NKT cell activation [51]. In this way, they limit both the Th1- and Th2-mediated immunopathology [43] (Figure 2).

In a normal heart, there are a number of fibroblasts, which become activated during the reparative phase [52] mainly by the secretion of TGF- β [53], while the EDA-coated fibronectin produced by the newly transdifferentiated myofibroblasts induces extracellular matrix-protein (EMP) deposition [54]. Myofibroblast differentiation is also potentiated by the initial production of high levels of IL-1 β and interferon- γ -inducible protein- (IP-) 10 [55], so that the extent of scarring is also determined by the significance of the Th1 response.

Moreover, activated myofibroblasts then modify the extracellular matrix environment, by the expression of EMPs like fibronectin and nonfibrillar collagens [55, 56], all of which support myofibroblast migration and adherence in order for them to close the wound.

On the other hand, from a wound-healing perspective, three phases of the process are recognized: (1) the inflammatory, (2) the proliferative, and (3) the remodeling stages, the first one being dominated by a Th1 response, the second

one by Th2 immunity, and the third one being characterized by the reorganization, degradation, and resynthesis of the EM, in order to obtain maximum tensile strength. It is noteworthy that the latter process can last up to a year and only starts when Th2 cytokines have been downregulated, but also that in general, the strength and duration of each stage depends upon the strength and duration of the anterior phase [57]. In this way, Tregs have been linked to the transition from the Th1-mediated inflammatory stage to the Th2-mediated proliferative phase and finally to the remodeling phase, in such a way that these cells appear to promote the whole process of wound healing, while downregulating pathological scarring [58].

3. The Clinical Management of an MI Event

According to the European Society of Cardiology [59, 60], the best proceeding for the management of an MI is to obtain a 12-lead ECG as soon as possible, with the optimum proposed time lapse of 10 minutes in order to determine the precise location, extension, and kind of myocardial infarction for each patient, in order to personalize the surgical procedure. Pain relief should be practiced as soon as possible to avoid the increase of the heart's workload. It is usually done with the use of titrated opioids, although it is currently under debate if such drugs may interfere with the action of antiplatelet aggregation agents [61, 62]. Oxygen should also be administered in patients whose O₂ saturation is less than 90%, along with a mild tranquilizer in order to reduce stress. When the diagnosis of STEMI is made in a prehospital setting, immediate activation of the catheterization laboratory is encouraged, in order to reduce treatment delays and patient mortality [63]. Either way, after diagnosis, pain management, and oxygenation, the next step is an attempt to lyse the blood clot by the use of thrombolytic drugs [59, 60].

Two scenarios may happen after thrombolysis: (1) the heart may recover blood flow or (2) the heart's blood flow alterations may persist. In the first case, MIRS starts upon thrombolysis, while in the second, primary percutaneous coronary intervention (PCI) is the preferred strategy that should be applied to patients with confirmed STEMI diagnosis within the first 12 h of symptom onset. In this second scenario, MIRS will happen after surgical reperfusion.

3.1. Periprocedural Pharmacotherapy. Patients undergoing primary PCI should receive aspirin and a P2Y₁₂ inhibitor, in order to dampen platelet aggregation. The oral dose of aspirin should be administered without an enteric coat to ensure rapid action [59, 60].

Routine postprocedural anticoagulant therapy is not indicated after primary PCI, except when there is a separate indication for either full-dose anticoagulation or prophylactic doses for the prevention of venous thromboembolism in patients requiring prolonged bed rest, but ECG monitoring for arrhythmias and ST-segment deviations is recommended for at least 24 h after symptom onset in all STEMI patients. Afterwards, lifestyle changes are suggested to patients in order to prevent further risks [59, 60].

It should be noted that current medical guidelines do not mention any anti-inflammatory treatment to cope with MIRS, in such a way that the phenomenon still allows for an enhanced risk of post-MI injury progression [9].

4. Immunoregulation as a Modern Alternative to Immunosuppression

While the pathophysiological mechanisms of MIRS have been extensively studied, to the point where many inflammatory mediators, such as leukocytes and cytokines, and their role in the whole phenomenon are known, current pharmacopeia lacks a specific treatment to avoid MIRS. Despite this, much research has been done to attack the different pathways involved in postischemic injury progression, and it may be important to review these attempts in order to understand what has failed and what could be done.

As stated in the above sections, neutrophils have been identified as major targets in MIRS because of their ability to massively infiltrate the infarct area upon reperfusion [64], to locally produce high levels of tissue-damaging ROS, NETs [65], and granule components such as myeloperoxidase and proteases. As such, research using animal models has shown that the inhibition of their tissue-damaging mechanisms [66] and recruitment into the reperfusion site [67] may be a viable option to limit MIRS-associated damage. Nonetheless, clinical trials using α CD11/CD18 integrin blocking antibodies to avoid neutrophil recruitment during myocardial reperfusion have shown limited success in the reduction of MI size and the improvement of short-term (30 days after infarct) clinical outcome [68, 69].

Despite the inflammatory, tissue-damaging role that neutrophils have on the acute phase of MIRS, after ≈ 7 days, the inflammatory Ly6G⁺ CD206⁻ neutrophil population is replaced by a Ly6G⁺ CD206⁺ population that has been described to play an important role in the orchestration of the reparative phase, as reviewed in [70]. Also, apoptotic neutrophils induce an M2 phenotype in infiltrated macrophages upon their phagocytosis, which inhibits the macrophage proinflammatory tissue-damaging response and leads them to produce IL-10 and TGF- β [71, 72]. Importantly, IL-10 may serve to dampen both Th1 and Th2 inflammation, thus inhibiting MIRS-derived damage, as well as excessive tissue scarring during the reparative phase, while TGF- β may also play an important role in infarct revascularization (Figure 3).

Thus, blocking neutrophil recruitment may not be a good alternative to reduce reperfusion-derived damage. Rather, the inhibition of the pathogenic effects of such cells may have a beneficial effect on MIRS. For instance, glucocorticoids have been shown to inhibit NET formation [73] and ROS production [74], while enhancing neutrophil mobilization [75], which renders them as good candidates for the reduction of neutrophil-derived damage (Figure 3).

Moreover, upon activation and apoptosis, neutrophils release proinflammatory alarmins that recruit inflammatory Ly6C^{hi} monocytes [76], which are also important players in the acute production of ROS. In later stages (1-2 days after MI), these cells undergo differentiation (peaking at 3-4 days post MI) into the proinflammatory tissue-damaging

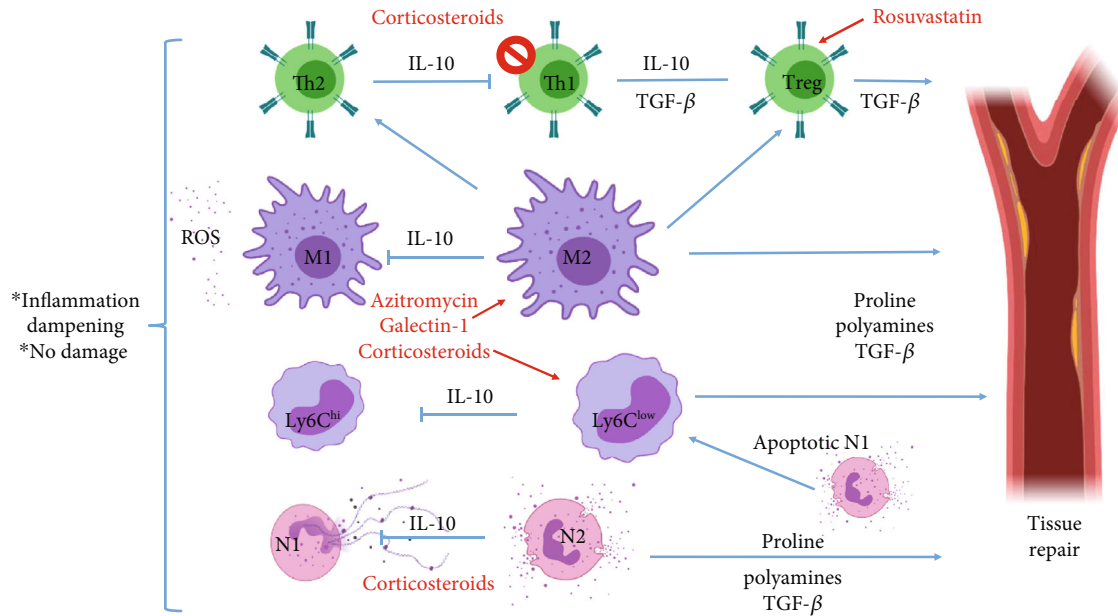


FIGURE 3: Immune-regulatory drugs could thwart destructive inflammation and promote tissue repair. Corticosteroids could enhance M2 differentiation while blocking NET, ROS, and granule-component deposition, thus blocking inflammatory damage. Also, azithromycin and rosuvastatin may induce cardioprotective leukocytes.

M1-type of macrophages [77]. Also, M1 macrophages can be directly recruited and activated through MCP1 early production by damaged endothelial cells and cardiomyocytes [78, 79]. Either way, increased Ly6C^{hi} cell counts after reperfusion have been associated with increased MIRS-derived damage [80, 81] as well as M1 macrophages, which further potentiate IRI [82]. At day 7 post MI, both the Ly6C^{hi} and the M1-macrophage populations subside to the inflammation-resolving tissue-remodeling Ly6C^{low} monocytes and M2 macrophages, which by Arg-1 expression deplete NO production and produce IL-10, TGF-β, polyamines, and proline, thus undermining the inflammatory tissue-damaging acute phase of the MIRS and promoting tissue repair and vascularization. Nonetheless, an excess of both M2 macrophages and Ly6C^{low} monocytes has also been associated with pathologic myocardial scarring [19, 83]. In this way, both the proinflammatory and the anti-inflammatory M/M fractions can have a pathogenic role in MIRS, so that they represent an important target to limit MIRS-associated damage as a whole (Figure 3).

Despite these evidences, blocking the inflammatory M/M recruitment into the MI zone might not be beneficial, as the adoptive transfer of M2 macrophages and Ly6C^{low} monocytes has shown to reduce MIRS-associated damage [84–86], so that the avoidance of M/M recruitment in the first place may limit the reparative phase of MIRS. On the other hand, M/M phenotype modulation to dampen such a cell's ability to produce oxidative and inflammatory stress may be a better strategy. Following this line of thought, IL-1β-blocking antibodies have been proposed as therapeutic alternatives to limit IRI, but results obtained from clinical trials have been contradictory, ranging from promising to discouraging [87–89]. Disregarding the results from clinical trials, animal models of this disease have shown a good

limitation of MIRS-associated damage in relation to the use of IL-1β-blocking antibodies administered to diabetic rats, which has more translational value because most MI patients are diabetic. Importantly, the MIRS blockage with this kind of antibody was effective to improve systolic function even when it was administered 80 days after reperfusion [90, 91] (Table 1).

Current data on the phenomenon does not allow an exact explanation of this phenomenon, but it can be speculated that the lack of effect in some cases may be due to a vast array of M1-inducing cytokines and Ly6C^{hi}-recruiting chemokines, other than IL-1β, being secreted at the MI zone upon reperfusion. Several cytokines and chemokines produced during MIRS, like TNF-α, IFN-γ, and MCP1, are known to have concomitant effects on the activation of inflammatory pathways like NF-κB [92, 93], PI3K/Akt [94], and JAK/STAT [95] in such a way that the inhibition of just one of the cytokines that signal through any of those pathways would not be able to have a consistent effect on the reduction of MIRS-associated damage (Figure 3).

In such line of thought, chemerin-15 [85] and netrin-1 [86] have been used in animal models to induce an M2 phenotype in macrophages during ischemia reperfusion, with the effect of reducing lesion size. Concordantly, glucocorticoid administration has shown to induce an alternative activation in macrophages, in such a way that they protect against inflammatory injury and are able to induce Treg expansion [96]. Such an effect may be attributable to the inhibition of the NF-κB pathway. Also, widely available drugs like azithromycin have shown to induce M2-type activation in macrophages to protect from ischemic stroke injury [97], in an effect associated with the inhibition of the PI3K/Akt pathway [98]. Moreover, the modulation of innate immunity using the C-type lectin, galectin-1, has also been proven to

TABLE 1: Main perspectives for the treatment of MIRS.

Clinical trial or animal model	Treatment	Proposed mechanisms of action	Findings	Reference
CT	α CD11/CD18	Reduction of neutrophil recruitment	No difference in baseline, angiographic of angioplasty characteristics	[68]
CT	α CD18	Reduction of neutrophil recruitment	No differences in coronary blood flow, infarct size, or ECG ST-segment elevation resolution	[69]
AM	Chemerin-15	Enhanced AAMs and IL-10; reduced ROS, neutrophils, IL-6, and TNF- α	Amelioration of MI	[85]
AM	Netrin-1	Reduction of neutrophil and macrophage recruitment, induction of AAMs	Decreased cardiomyocyte apoptosis	[86]
CT	α IL-1 β	Reduction of M/M inflammatory activation	Enhanced hemodynamics and left ventricular remodeling	[87]
CT	α IL-1 β	Reduction of CRP	No differences with the placebo-treated group	[88]
AM	α IL-1 β	n.a.	Reduces infarct size and improves left ventricle remodeling	[90]
AM	Azithromycin	Induction of AAMs, inhibition of the PI3K/Akt pathway	Neuroprotection on an animal model of stroke	[97]
AM	Rosuvastatin	Treg expansion, reduction of inflammatory infiltrates	Reduced cardiac troponin I, infarct size	[106]
CT	α C5	n.a.	No reduction of infarct size but improved survival	[108]
CT	α C5	n.a.	Enhanced survival	[109]
CT	α C5	n.a.	Reduction of troponin T and creatine kinase-MB	[110]
CT	C1-esterase inhibitor	C1, C3c, and C4 reduction	No difference in postoperative complications, hospital stay, or in-hospital mortality	[111]
CT	C1-esterase inhibitor	C3a and C4a reduction	Enhanced mean arterial pressure, cardiac index, and stroke volume. Lower levels of cardiac troponin	[112]
AM	Low dose of methylprednisolone	n.a.	Reduced infarction size and scar	[118]
CT	Alpha-1 antitrypsin (AAT)	Reduction of CRP	Lower creatine kinase myocardial levels	[116]
AM	Galectin-1	Reduction of macrophages, NK cells, and T lymphocytes. Increase in Tregs	Enhanced heart's contractility	[100]
AM	Intranasal troponin	Increased IL-10 and reduced IFN- γ	Reduction of infarct size	[104]
AM	Super-antagonistic α CD28 antibody	Treg and AAM induction	Increased collagen de novo expression, decreased rates of left ventricular ruptures	[49]

Abbreviations: CT: clinical trial; AM: animal model; α CD11/18: anticluster of differentiation 11/18; α C5: anti-C5 complement protein; AAM: alternatively activated macrophages; ROS: reactive oxygen species; M/M: monocyte/macrophages; CRP: C-reactive protein; Treg: T-regulatory cell, IL-1 β : interleukin-1 β ; IL-10: interleukin-10; ECG: electrocardiogram; n.a.: not available; MI: myocardial infarction.

effectively dampen inflammation, mainly through AAM induction [99]. Interestingly, galectin-1 knockout mice showed enhanced cardiac inflammation (characterized by increased numbers of macrophages, natural killer cells, and T-cells) and a reduced frequency of regulatory T-cells that are associated with impaired cardiac function and ventricular remodeling. In the same study, the authors treated infarcted mice with recombinant galectin-1, which led to attenuated cardiac damage [100] (Table 1).

Whether this strategy induces pathological scarring was not evaluated, but the possibility should not be ruled out. To our notice, no clinical trials have been made exploring any immunoregulatory drug that has a direct effect on the M/M phenotype, and it may be important to gather such data due to a wide variation between the characteristics of MI in animal models and the clinical reality in human patients [19] (Figure 3).

On the other hand, CD4⁺ T lymphocytes and B cells are recruited within the first 90 minutes after reperfusion and appear to play a pathogenic role during the acute stage of MIRS, presumably because of their ability to promote an inflammatory tissue-damaging phenotype in M/M cells [33, 101]. Furthermore, in the tissue-remodeling stage of MIRS CD4⁺ T-cells may also play a pathological role, as they have been described to induce excessive scarring [102]. Nonetheless, there is an increasingly clear role for Treg cells in the dampening of both the pathogenic Th1 and Th2 inflammation phenomena [103] that is supported by several data (Figure 3).

Firstly, the induction of IL-10 secreting Treg cells by intranasal troponin administration shortly after reperfusion has shown to reduce MIRS-associated damage by 50%, evaluated 1.5 months after reperfusion [104]. Moreover, pharmacologic activation/recruitment of CD4⁺ CD25⁺ FoxP3⁺ cells using a super-antagonistic α CD28 antibody has been linked to a change in the phenotype of macrophages from M1 to M2, which promotes an enhanced, but not pathogenic, healing through the local production of TGF- β [49]. The observed suppression of pathogenic scarring may be due to a direct effect for Treg cells in the modulation of a fibroblast phenotype, in such a way that the latter cells migrate less, thus limiting their ability to form bigger scars [50] (Figure 3) (Table 1).

Another potentially important strategy to limit MIRS may be the use of statins, as they have been rendered as potent cardioprotectors that have an interesting effect on T-cell activation [105]. For instance, rosuvastatin has been shown to limit MIRS through Treg expansion in a murine model [106], but the effect may not be exclusive to animal models, as a meta-analysis performed by Sorathia et al. shows a vast increase in Tregs in patients that use rosuvastatin [107] (Figure 3) (Table 1).

Another important early player in the field of MIRS is the complement cascade, where C1 and C5/C5a proteins have been targeted. While C5 has been targeted with limited success on limiting IRI size [108, 109], C1 inhibition with monoclonal antibodies was able to reduce injury on several clinical trials [110–112], so that complement-blocking antibodies, like Ceter or Berinert, may be used concomitantly

to reduce IRI extension. Additionally, corticosteroids have been used to regulate complement-gene expression and activation [113, 114] (Figure 3) (Table 1).

Finally, the potentiation of cardiomyocyte survival should be considered as a valuable alternative to be coopted in the treatment of MIRS. An interesting approach is the modulation of the low-density lipoprotein receptor-related protein 1 (LRP1), which is able to both downregulate the NF- κ B-related inflammation during MIRS and enhance cardiomyocyte survival through the activation of the PI3K/Akt and ERK1/2 pathways in such cells, as thoroughly reviewed in [115]. As an example of this approach, a clinical trial using plasma-derived alpha-1 antitrypsin, an agonist of the LRP1 receptor, showed shorter time-to-peak creatine kinase myocardial band (CK-MB) values [116] in relation to a significant reduction on CRP [117] (Table 1).

4.1. As Paracelsus Said: The Dose Makes the Potion. In the 70s, a word of caution was emitted against the use of corticosteroids to treat MIRS as it was observed that in some studies, it caused myocardial thinning and delayed healing [119–121]. Nonetheless, in all these studies, high doses of such hormones were administered and for prolonged times. In this way, even a decade later, this dosing was questioned by studies comparing MI size and healing pace between high and low corticosteroid dose groups [118], finding that as Paracelsus said, “the dose makes the potion.”

It can be speculated that the high doses used in such studies blocked the proliferative and remodeling stages of MIRS, along with the inflammatory phase that was initially the intended target. Nowadays, a protective role for corticosteroids in MIRS has been described in both experimental [122, 123] and clinical settings. Concordantly, a meta-analysis by Giugliano et al. [124] showed this cardioprotective effect for corticosteroids in MIRS in patients. On the other hand, corticosteroids have been successfully used to reduce IRI in kidneys [125], liver [126], and brain [127], with the added benefit of attenuating pathogenic fibrosis during the reparative phase [128].

In this way, the current understanding on the pathophysiology of MIRS and a brief review about the use of such drugs in MIRS-reduction allow us to think that a low dose of corticosteroids administered prior to reperfusion may help to reduce the inflammatory damage of such a syndrome, while allowing the healing phases of the syndrome.

5. Conclusions

MIRS is an unavoidable consequence of MI, with the potential to duplicate the damage made by the ischemic condition. As such, it represents a serious complication to one of the most prevalent diseases worldwide. Designing an effective therapy for such a condition has been challenging because the inflammatory phenomenon behind its pathophysiology is very complex. First, it involves a Th1 response that greatly contributes to tissue damage, which is relatively easy to dampen, but a chronic Th2-type immune response that contributes to the resolution of the inflammatory damage, and

tissue remodeling comes later, and its suppression has been associated with increased damage.

As such, a therapy that downregulates the acute Th1 tissue-damaging response, but promotes the later Th2 tissue-repairing phase of the disease, appears to be a good choice. Some well-known, widely used drugs, like rosuvastatin, azithromycin, corticosteroids, Cetor, or Berinert, have been purported as candidates to treat MIRS in the experimental setting, producing good results. Nonetheless, much research is needed in order to confirm such findings as they have not been used concomitantly, and a correct dose may be challenging to find, as too much Th1 undermining may result in a weak reparative stage, but too little may not properly limit the damage.

Innate immune cells, like M/M and neutrophils, appear to be good targets, because they are effector mediators of the damage and because they can regulate the adaptive immune response, both in potency and in profile, so that drugs like azithromycin, which can induce an M2 phenotype in macrophages, or corticosteroids that can reduce ROS production in both cell types could have a positive effect on MIRS management. Also, rosuvastatin may be cardioprotective beyond its effects on dyslipidemia, as it can recruit Treg cells at the injured heart. Such lymphocyte population has been associated to the resolution of both the Th1- and Th2-type responses, thus allowing a healthy scar maturation.

Another point to be considered is the rational use for corticosteroids, as they can limit the extent of MIRI and induce protective leukocyte populations, but overdoses with such a drug have produced myocardial thinning and delayed healing.

Finally, complement-blocking antibodies have been used successfully in the clinical setting, so that they may be coopted with the aforementioned drugs to design a more complete treatment.

Conflicts of Interest

The authors declare that no potential conflicts of interest exist both in the writing and in the publication of this paper.

Acknowledgments

All the authors wish to thank Sociedad Española de Beneficencia (Pachuca, Hidalgo) for funding the publication of this article. Moreover, César Daniel Sánchez-Hernández, Lucero Torres-Alarcón, and Ariadna González-Cortés wish to give their thanks for the scholarship they receive from such institution.

References

- [1] M. Kosuge, K. Kimura, T. Ishikawa et al., “Differences between men and women in terms of clinical features of ST-segment elevation acute myocardial infarction,” *Circulation Journal*, vol. 70, no. 3, pp. 222–226, 2006.
- [2] E. M. Antman, D. T. Anbe, P. W. Armstrong et al., “ACC/AHA Guidelines for the Management of Patients With ST-Elevation Myocardial Infarction: A Report of the American College of Cardiology/American Heart Association

- Task Force on Practice Guidelines (Committee to Revise the 1999 Guidelines for the Management of Patients With Acute Myocardial Infarction),” *Journal of the American College of Cardiology*, vol. 44, no. 3, pp. E1–E211, 2004.
- [3] P. Valensi, L. Lorgis, and Y. Cottin, “Prevalence, incidence, predictive factors and prognosis of silent myocardial infarction: A review of the literature,” *Archives of Cardiovascular Diseases*, vol. 104, no. 3, pp. 178–188, 2011.
- [4] I. Graham, D. Atar, K. Borch-Johnsen et al., “European guidelines on cardiovascular disease prevention in clinical practice: executive summary,” *Atherosclerosis*, vol. 194, no. 1, pp. 1–45, 2007.
- [5] D. H. Harrington, F. Stueben, and C. M. Lenahan, “ST-elevation myocardial infarction and non-ST-elevation myocardial infarction: medical and surgical interventions,” *Critical Care Nursing Clinics of North America*, vol. 31, no. 1, pp. 49–64, 2019.
- [6] J. L. Anderson, L. A. Karagounis, and R. M. Califf, “Metaanalysis of five reported studies on the relation of early coronary patency grades with mortality and outcomes after acute myocardial infarction,” *The American Journal of Cardiology*, vol. 78, no. 1, pp. 1–8, 1996.
- [7] C. Martinez-Sanchez, A. Arias-Mendoza, H. Gonzalez-Pacheco et al., “Reperfusion therapy of myocardial infarction in Mexico: a challenge for modern cardiology,” *Archivos de Cardiología de México*, vol. 87, no. 2, pp. 144–150, 2017.
- [8] J. P. Seeger, N. M. Benda, N. P. Riksen et al., “Heart failure is associated with exaggerated endothelial ischaemia-reperfusion injury and attenuated effect of ischaemic preconditioning,” *European Journal of Preventive Cardiology*, vol. 23, no. 1, pp. 33–40, 2016.
- [9] D. M. Yellon and D. J. Hausenloy, “Myocardial reperfusion injury,” *The New England Journal of Medicine*, vol. 357, no. 11, pp. 1121–1135, 2007.
- [10] R. L. Engler, M. D. Dahlgren, D. D. Morris, M. A. Peterson, and G. W. Schmid-Schonbein, “Role of leukocytes in response to acute myocardial ischemia and reflow in dogs,” *The American Journal of Physiology*, vol. 251, pp. H314–H323, 1986.
- [11] J. P. Monassier, “Reperfusion injury in acute myocardial infarction. From bench to cath lab. Part I: basic considerations,” *Archives of Cardiovascular Diseases*, vol. 101, no. 7-8, pp. 491–500, 2008.
- [12] V. Gurewich, “Thrombolysis: a critical first-line therapy with an unfulfilled potential,” *The American Journal of Medicine*, vol. 129, no. 6, pp. 573–575, 2016.
- [13] N. G. Frangogiannis, “The inflammatory response in myocardial injury, repair, and remodelling,” *Nature Reviews. Cardiology*, vol. 11, no. 5, pp. 255–265, 2014.
- [14] L. Minutoli, D. Puzzolo, M. Rinaldi et al., “ROS-mediated NLRP3 inflammasome activation in brain, heart, kidney, and testis ischemia/reperfusion injury,” *Oxidative Medicine and Cellular Longevity*, vol. 2016, Article ID 2183026, 10 pages, 2016.
- [15] F. Van de Werf, J. Bax, A. Betriu et al., “Management of acute myocardial infarction in patients presenting with persistent ST-segment elevation,” *European Heart Journal*, vol. 29, no. 23, pp. 2909–2945, 2008.
- [16] R. Zahn, A. Koch, J. Rustige et al., “Primary angioplasty versus thrombolysis in the treatment of acute myocardial

- infarction," *The American Journal of Cardiology*, vol. 79, no. 3, pp. 264–269, 1997.
- [17] N. S. Dhalla, A. B. Elmoselhi, T. Hata, and N. Makino, "Status of myocardial antioxidants in ischemia-reperfusion injury," *Cardiovascular Research*, vol. 47, no. 3, pp. 446–456, 2000.
- [18] D. Brevoord, P. Kranke, M. Kuijpers, N. Weber, M. Hollmann, and B. Preckel, "Remote ischemic conditioning to protect against ischemia-reperfusion injury: a systematic review and meta-analysis," *PLoS One*, vol. 7, no. 7, article e42179, 2012.
- [19] S. B. Ong, S. Hernandez-Resendiz, G. E. Crespo-Avilan et al., "Inflammation following acute myocardial infarction: multiple players, dynamic roles, and novel therapeutic opportunities," *Pharmacology & Therapeutics*, vol. 186, pp. 73–87, 2018.
- [20] X. M. Yang, L. Cui, J. White et al., "Mitochondrially targeted endonuclease III has a powerful anti-infarct effect in an in vivo rat model of myocardial ischemia/reperfusion," *Basic Research in Cardiology*, vol. 110, no. 2, p. 3, 2015.
- [21] S. Mariathasan, D. S. Weiss, K. Newton et al., "Cryopyrin activates the inflammasome in response to toxins and ATP," *Nature*, vol. 440, no. 7081, pp. 228–232, 2006.
- [22] H. A. Cabrera-Fuentes, M. Ruiz-Meana, S. Simsekylmaz et al., "RNase1 prevents the damaging interplay between extracellular RNA and tumour necrosis factor- α in cardiac ischaemia/reperfusion injury," *Thrombosis and Haemostasis*, vol. 112, no. 6, pp. 1110–1119, 2014.
- [23] G. P. van Hout, F. Arslan, G. Pasterkamp, and I. E. Hoefer, "Targeting danger-associated molecular patterns after myocardial infarction," *Expert Opinion on Therapeutic Targets*, vol. 20, no. 2, pp. 223–239, 2016.
- [24] Y. Ma, A. Yabluchanskiy, R. P. Iyer et al., "Temporal neutrophil polarization following myocardial infarction," *Cardiovascular Research*, vol. 110, no. 1, pp. 51–61, 2016.
- [25] E. Kolaczowska and P. Kuberski, "Neutrophil recruitment and function in health and inflammation," *Nature Reviews Immunology*, vol. 13, no. 3, pp. 159–175, 2013.
- [26] Y. Ma, A. Yabluchanskiy, and M. L. Lindsey, "Neutrophil roles in left ventricular remodeling following myocardial infarction," *Fibrogenesis & Tissue Repair*, vol. 6, no. 1, p. 11, 2013.
- [27] Z. Q. Zhao, D. A. Velez, N. P. Wang et al., "Progressively developed myocardial apoptotic cell death during late phase of reperfusion," *Apoptosis*, vol. 6, no. 4, pp. 279–290, 2001.
- [28] L. Timmers, G. Pasterkamp, V. C. de Hoog, F. Arslan, Y. Appelman, and D. P. de Kleijn, "The innate immune response in reperfused myocardium," *Cardiovascular Research*, vol. 94, no. 2, pp. 276–283, 2012.
- [29] O. Dewald, P. Zymek, K. Winkelmann et al., "CCL2/monocyte chemoattractant protein-1 regulates inflammatory responses critical to healing myocardial infarcts," *Circulation Research*, vol. 96, no. 8, pp. 881–889, 2005.
- [30] P. Song, J. Zhang, Y. Zhang et al., "Hepatic recruitment of CD11b+Ly6C+ inflammatory monocytes promotes hepatic ischemia/reperfusion injury," *International Journal of Molecular Medicine*, vol. 41, no. 2, pp. 935–945, 2018.
- [31] P. Italiani and D. Boraschi, "From Monocytes to M1/M2 Macrophages: Phenotypical vs. Functional Differentiation," *Frontiers in Immunology*, vol. 5, p. 514, 2014.
- [32] E. N. ter Horst, N. Hakimzadeh, A. M. van der Laan, P. A. Krijnen, H. W. Niessen, and J. J. Piek, "Modulators of macrophage polarization influence healing of the infarcted myocardium," *International Journal of Molecular Sciences*, vol. 16, no. 12, pp. 29583–29591, 2015.
- [33] Y. Zougari, H. Ait-Oufella, P. Bonnin et al., "B lymphocytes trigger monocyte mobilization and impair heart function after acute myocardial infarction," *Nature Medicine*, vol. 19, no. 10, pp. 1273–1280, 2013.
- [34] J. Rao, L. Lu, and Y. Zhai, "T cells in organ ischemia reperfusion injury," *Current Opinion in Organ Transplantation*, vol. 19, no. 2, pp. 115–120, 2014.
- [35] J. Chen, J. C. Crispin, T. F. Tedder, J. Dalle Lucca, and G. C. Tsokos, "B cells contribute to ischemia/reperfusion-mediated tissue injury," *Journal of Autoimmunity*, vol. 32, no. 3–4, pp. 195–200, 2009.
- [36] O. Dewald, G. Ren, G. D. Duerr et al., "Of mice and dogs: species-specific differences in the inflammatory response following myocardial infarction," *The American Journal of Pathology*, vol. 164, no. 2, pp. 665–677, 2004.
- [37] P. Yang, Y. Li, Y. Xie, and Y. Liu, "Different faces for different places: heterogeneity of neutrophil phenotype and function," *Journal of Immunology Research*, vol. 2019, Article ID 8016254, 18 pages, 2019.
- [38] A. Ortega-Gomez, M. Perretti, and O. Soehnlein, "Resolution of inflammation: an integrated view," *EMBO Molecular Medicine*, vol. 5, no. 5, pp. 661–674, 2013.
- [39] M. Nahrendorf, M. J. Pittet, and F. K. Swirski, "Monocytes: protagonists of infarct inflammation and repair after myocardial infarction," *Circulation*, vol. 121, no. 22, pp. 2437–2445, 2010.
- [40] L. Zhu, Q. Zhao, T. Yang, W. Ding, and Y. Zhao, "Cellular metabolism and macrophage functional polarization," *International Reviews of Immunology*, vol. 34, no. 1, pp. 82–100, 2015.
- [41] H. Liu, W. Gao, J. Yuan et al., "Exosomes derived from dendritic cells improve cardiac function via activation of CD4⁺ T lymphocytes after myocardial infarction," *Journal of Molecular and Cellular Cardiology*, vol. 91, pp. 123–133, 2016.
- [42] N. Marek-Trzonkowska, M. Mysliwiec, A. Dobyszyk et al., "Therapy of type 1 diabetes with CD4(+)/CD25 (high)/CD127-regulatory T cells prolongs survival of pancreatic islets - results of one year follow-up," *Clinical Immunology*, vol. 153, no. 1, pp. 23–30, 2014.
- [43] U. Hofmann, N. Beyersdorf, J. Weirather et al., "Activation of CD4⁺ T lymphocytes improves wound healing and survival after experimental myocardial infarction in mice," *Circulation*, vol. 125, no. 13, pp. 1652–1663, 2012.
- [44] L. Barron and T. A. Wynn, "Fibrosis is regulated by Th2 and Th17 responses and by dynamic interactions between fibroblasts and macrophages," *American Journal of Physiology-Gastrointestinal and Liver Physiology*, vol. 300, no. 5, pp. G723–G728, 2011.
- [45] R. L. Gieseck 3rd, M. S. Wilson, and T. A. Wynn, "Type 2 immunity in tissue repair and fibrosis," *Nature Reviews Immunology*, vol. 18, no. 1, pp. 62–76, 2018.
- [46] S. T. Rashid and G. J. Alexander, "Induced pluripotent stem cells: from Nobel prizes to clinical applications," *Journal of Hepatology*, vol. 58, no. 3, pp. 625–629, 2013.
- [47] D. R. Littman and A. Y. Rudensky, "Th17 and regulatory T cells in mediating and restraining inflammation," *Cell*, vol. 140, no. 6, pp. 845–858, 2010.

- [48] Q. Tang and K. Lee, "Regulatory T-cell therapy for transplantation: how many cells do we need?," *Current Opinion in Organ Transplantation*, vol. 17, no. 4, pp. 349–354, 2012.
- [49] J. Weirather, U. D. Hofmann, N. Beyersdorf et al., "Foxp3+ CD4+ T cells improve healing after myocardial infarction by modulating monocyte/macrophage differentiation," *Circulation Research*, vol. 115, no. 1, pp. 55–67, 2014.
- [50] A. Saxena, M. Dobaczewski, V. Rai et al., "Regulatory T cells are recruited in the infarcted mouse myocardium and may modulate fibroblast phenotype and function," *American Journal of Physiology. Heart and Circulatory Physiology*, vol. 307, no. 8, pp. H1233–H1242, 2014.
- [51] T. Homma, S. Kinugawa, M. Takahashi et al., "Activation of invariant natural killer T cells by α -galactosylceramide ameliorates myocardial ischemia/reperfusion injury in mice," *Journal of Molecular and Cellular Cardiology*, vol. 62, pp. 179–188, 2013.
- [52] N. G. Frangogiannis, L. H. Michael, and M. L. Entman, "Myofibroblasts in reperfused myocardial infarcts express the embryonic form of smooth muscle myosin heavy chain (SMemb)," *Cardiovascular Research*, vol. 48, no. 1, pp. 89–100, 2000.
- [53] A. Ruiz-Villalba, A. M. Simon, C. Pogontke et al., "Interacting resident epicardium-derived fibroblasts and recruited bone marrow cells form myocardial infarction scar," *Journal of the American College of Cardiology*, vol. 65, no. 19, pp. 2057–2066, 2015.
- [54] M. Kohan, A. F. Muro, E. S. White, and N. Berkman, "EDA-containing cellular fibronectin induces fibroblast differentiation through binding to alpha4beta7 integrin receptor and MAPK/Erk 1/2-dependent signaling," *The FASEB Journal*, vol. 24, no. 11, pp. 4503–4512, 2010.
- [55] A. V. Shinde and N. G. Frangogiannis, "Fibroblasts in myocardial infarction: a role in inflammation and repair," *Journal of Molecular and Cellular Cardiology*, vol. 70, pp. 74–82, 2014.
- [56] J. J. Santiago, A. L. Dangerfield, S. G. Rattan et al., "Cardiac fibroblast to myofibroblast differentiation in vivo and in vitro: expression of focal adhesion components in neonatal and adult rat ventricular myofibroblasts," *Developmental Dynamics*, vol. 239, no. 6, pp. 1573–1584, 2010.
- [57] A. C. Gonzalez, T. F. Costa, Z. A. Andrade, and A. R. Medrado, "Wound healing - a literature review," *Anais Brasileiros de Dermatologia*, vol. 91, no. 5, pp. 614–620, 2016.
- [58] S. A. Eming, P. Martin, and M. Tomic-Canic, "Wound repair and regeneration: mechanisms, signaling, and translation," *Science Translational Medicine*, vol. 6, no. 265, p. 265sr6, 2014.
- [59] S. Savonitto, M. Azzarone, R. Salsi, and G. Tortorella, "The new ESC guidelines for non-ST-elevation acute coronary syndromes: one direction, many ways, clinical wisdom," *Giornale Italiano Di Cardiologia*, vol. 13, no. 3, pp. 157–168, 2012.
- [60] Task Force on the management of ST-segment elevation, P. G. Steg, S. K. James et al., "ESC guidelines for the management of acute myocardial infarction in patients presenting with ST-segment elevation," *European Heart Journal*, vol. 33, pp. 2569–2619, 2012.
- [61] E. L. Hobl, T. Stimpfl, J. Ebner et al., "Morphine decreases clopidogrel concentrations and effects: a randomized, double-blind, placebo-controlled trial," *Journal of the American College of Cardiology*, vol. 63, no. 7, pp. 630–635, 2014.
- [62] E. L. Hobl, B. Reiter, C. Schoergenhofer et al., "Morphine decreases ticagrelor concentrations but not its antiplatelet effects: a randomized trial in healthy volunteers," *European Journal of Clinical Investigation*, vol. 46, no. 1, pp. 7–14, 2016.
- [63] C. Barstow, M. Rice, and J. D. McDivitt, "Acute coronary syndrome: diagnostic evaluation," *American Family Physician*, vol. 95, no. 3, pp. 170–177, 2017.
- [64] R. Fernandez-Jimenez, J. Garcia-Prieto, J. Sanchez-Gonzalez et al., "Pathophysiology underlying the bimodal edema phenomenon after myocardial ischemia/reperfusion," *Journal of the American College of Cardiology*, vol. 66, no. 7, pp. 816–828, 2015.
- [65] L. Ge, X. Zhou, W. J. Ji et al., "Neutrophil extracellular traps in ischemia-reperfusion injury-induced myocardial no-reflow: therapeutic potential of DNase-based reperfusion strategy," *American Journal of Physiology. Heart and Circulatory Physiology*, vol. 308, no. 5, pp. H500–H509, 2015.
- [66] M. Wallert, M. Ziegler, X. Wang et al., " α -Tocopherol preserves cardiac function by reducing oxidative stress and inflammation in ischemia/reperfusion injury," *Redox Biology*, vol. 26, article 101292, 2019.
- [67] M. Arai, D. J. Lefer, T. So, A. DiPaula, T. Aversano, and L. C. Becker, "An anti-CD18 antibody limits infarct size and preserves left ventricular function in dogs with ischemia and 48-hour reperfusion," *Journal of the American College of Cardiology*, vol. 27, no. 5, pp. 1278–1285, 1996.
- [68] D. P. Faxon, R. J. Gibbons, N. A. Chronos, P. A. Gurbel, F. Sheehan, and Investigators H-M, "The effect of blockade of the CD11/CD18 integrin receptor on infarct size in patients with acute myocardial infarction treated with direct angioplasty: the results of the HALT-MI study," *Journal of the American College of Cardiology*, vol. 40, no. 7, pp. 1199–1204, 2002.
- [69] K. W. Baran, M. Nguyen, G. R. McKendall et al., "Double-blind, randomized trial of an anti-CD18 antibody in conjunction with recombinant tissue plasminogen activator for acute myocardial infarction: limitation of myocardial infarction following thrombolysis in acute myocardial infarction (LIMIT AMI) study," *Circulation*, vol. 104, no. 23, pp. 2778–2783, 2001.
- [70] S. L. Puhl and S. Steffens, "Neutrophils in post-myocardial infarction inflammation: damage vs. resolution?," *Frontiers in Cardiovascular Medicine*, vol. 6, p. 25, 2019.
- [71] N. G. Frangogiannis, "Regulation of the inflammatory response in cardiac repair," *Circulation Research*, vol. 110, no. 1, pp. 159–173, 2012.
- [72] M. Horckmans, L. Ring, J. Duchene et al., "Neutrophils orchestrate post-myocardial infarction healing by polarizing macrophages towards a reparative phenotype," *European Heart Journal*, vol. 38, no. 3, pp. 187–197, 2017.
- [73] F. Fan, X. Huang, K. Yuan et al., "Glucocorticoids may exacerbate fungal keratitis by increasing fungal aggressivity and inhibiting the formation of neutrophil extracellular traps," *Current Eye Research*, vol. 45, no. 2, pp. 124–133, 2020.
- [74] R. Dey and B. Bishayi, "Dexamethasone exhibits its anti-inflammatory effects in S. aureus induced microglial inflammation via modulating TLR-2 and glucocorticoid receptor expression," *International Immunopharmacology*, vol. 75, article 105806, 2019.
- [75] I. H. Hiemstra, J. L. van Hamme, M. H. Janssen, T. K. van den Berg, and T. W. Kuijpers, "Dexamethasone promotes granulocyte mobilization by prolonging the half-life of

- granulocyte-colony-stimulating factor in healthy donors for granulocyte transfusions,” *Transfusion*, vol. 57, no. 3, pp. 674–684, 2017.
- [76] G. Marinkovic, H. Grauen Larsen, T. Yndigeegn et al., “Inhibition of pro-inflammatory myeloid cell responses by short-term S100A9 blockade improves cardiac function after myocardial infarction,” *European Heart Journal*, vol. 40, no. 32, pp. 2713–2723, 2019.
- [77] I. Hilgendorf, L. M. Gerhardt, T. C. Tan et al., “Ly-6Chi monocytes depend on Nr4a1 to balance both inflammatory and reparative phases in the infarcted myocardium,” *Circulation Research*, vol. 114, no. 10, pp. 1611–1622, 2014.
- [78] A. G. Kumar, C. M. Ballantyne, L. H. Michael et al., “Induction of monocyte chemoattractant protein-1 in the small veins of the ischemic and reperfused canine myocardium,” *Circulation*, vol. 95, no. 3, pp. 693–700, 1997.
- [79] S. T. Tarzami, R. Cheng, W. Miao, R. N. Kitsis, and J. W. Berman, “Chemokine expression in myocardial ischemia: MIP-2 dependent MCP-1 expression protects cardiomyocytes from cell death,” *Journal of Molecular and Cellular Cardiology*, vol. 34, no. 2, pp. 209–221, 2002.
- [80] Y. Maekawa, T. Anzai, T. Yoshikawa et al., “Prognostic significance of peripheral monocytosis after reperfused acute myocardial infarction: a possible role for left ventricular remodeling,” *Journal of the American College of Cardiology*, vol. 39, no. 2, pp. 241–246, 2002.
- [81] M. Mariani, R. Fetiveau, E. Rossetti et al., “Significance of total and differential leucocyte count in patients with acute myocardial infarction treated with primary coronary angioplasty,” *European Heart Journal*, vol. 27, no. 21, pp. 2511–2515, 2006.
- [82] F. K. Swirski, P. Libby, E. Aikawa et al., “Ly-6Chi monocytes dominate hypercholesterolemia-associated monocytosis and give rise to macrophages in atheromata,” *The Journal of Clinical Investigation*, vol. 117, no. 1, pp. 195–205, 2007.
- [83] I. Andreadou, H. A. Cabrera-Fuentes, Y. Devaux et al., “Immune cells as targets for cardioprotection: new players and novel therapeutic opportunities,” *Cardiovascular Research*, vol. 115, no. 7, pp. 1117–1130, 2019.
- [84] Y. Yue, X. Yang, K. Feng et al., “M2b macrophages reduce early reperfusion injury after myocardial ischemia in mice: a predominant role of inhibiting apoptosis via A20,” *International Journal of Cardiology*, vol. 245, pp. 228–235, 2017.
- [85] C. Chang, Q. Ji, B. Wu et al., “Chemerin15-Ameliorated Cardiac Ischemia-Reperfusion Injury Is Associated with the Induction of Alternatively Activated Macrophages,” *Mediators of Inflammation*, vol. 2015, Article ID 563951, 9 pages, 2015.
- [86] X. Mao, H. Xing, A. Mao et al., “Netrin-1 attenuates cardiac ischemia reperfusion injury and generates alternatively activated macrophages,” *Inflammation*, vol. 37, no. 2, pp. 573–580, 2014.
- [87] A. Abbate, M. C. Kontos, J. D. Grizzard et al., “Interleukin-1 blockade with anakinra to prevent adverse cardiac remodeling after acute myocardial infarction (Virginia Commonwealth University Anakinra Remodeling Trial [VCU-ART] pilot study),” *The American Journal of Cardiology*, vol. 105, no. 10, pp. 1371–1377.e1, 2010.
- [88] A. Abbate, B. W. Van Tassel, G. Biondi-Zoccai et al., “Effects of interleukin-1 blockade with anakinra on adverse cardiac remodeling and heart failure after acute myocardial infarction [from the Virginia Commonwealth University-Anakinra Remodeling Trial (2) (VCU-ART2) pilot study],” *The American Journal of Cardiology*, vol. 111, no. 10, pp. 1394–1400, 2013.
- [89] A. C. Morton, A. M. Rothman, J. P. Greenwood et al., “The effect of interleukin-1 receptor antagonist therapy on markers of inflammation in non-ST elevation acute coronary syndromes: the MRC-ILA Heart Study,” *European Heart Journal*, vol. 36, no. 6, pp. 377–384, 2015.
- [90] S. Toldo, B. W. Van Tassel, and A. Abbate, “Interleukin-1 blockade in acute myocardial infarction and heart failure: getting closer and closer,” *JACC: Basic to Translational Science*, vol. 2, no. 4, pp. 431–433, 2017.
- [91] N. Harouki, L. Nicol, I. Remy-Jouet et al., “The IL-1 β Antibody Gevokizumab Limits Cardiac Remodeling and Coronary Dysfunction in Rats With Heart Failure,” *JACC: Basic to Translational Science*, vol. 2, no. 4, pp. 418–430, 2017.
- [92] S. C. Sun, “The non-canonical NF- κ B pathway in immunity and inflammation,” *Nature Reviews Immunology*, vol. 17, no. 9, pp. 545–558, 2017.
- [93] J. Napetschnig and H. Wu, “Molecular basis of NF- κ B signaling,” *Annual Review of Biophysics*, vol. 42, pp. 443–468, 2013.
- [94] M. C. Jimenez-Sainz, B. Fast, F. Mayor Jr., and A. M. Aragay, “Signaling pathways for monocyte chemoattractant protein 1-mediated extracellular signal-regulated kinase activation,” *Molecular Pharmacology*, vol. 64, no. 3, pp. 773–782, 2003.
- [95] J. J. O’Shea, D. M. Schwartz, A. V. Villarino, M. Gadina, I. B. McInnes, and A. Laurence, “The JAK-STAT pathway: impact on human disease and therapeutic intervention,” *Annual Review of Medicine*, vol. 66, pp. 311–328, 2015.
- [96] G. W. Tu, Y. Shi, Y. J. Zheng et al., “Glucocorticoid attenuates acute lung injury through induction of type 2 macrophage,” *Journal of Translational Medicine*, vol. 15, no. 1, p. 181, 2017.
- [97] D. Amantea, M. Certo, F. Petrelli et al., “Azithromycin protects mice against ischemic stroke injury by promoting macrophage transition towards M2 phenotype,” *Experimental Neurology*, vol. 275, Part 1, pp. 116–125, 2016.
- [98] J. Wang, L. Xie, S. Wang, J. Lin, J. Liang, and J. Xu, “Azithromycin promotes alternatively activated macrophage phenotype in systematic lupus erythematosus via PI3K/Akt signaling pathway,” *Cell Death & Disease*, vol. 9, no. 11, p. 1080, 2018.
- [99] I. M. Seropian, G. E. Gonzalez, S. M. Maller, D. H. Berrocal, A. Abbate, and G. A. Rabinovich, “Galectin-1 as an emerging mediator of cardiovascular inflammation: mechanisms and therapeutic opportunities,” *Mediators of Inflammation*, vol. 2018, Article ID 8696543, 11 pages, 2018.
- [100] I. M. Seropian, J. P. Cerliani, S. Toldo et al., “Galectin-1 controls cardiac inflammation and ventricular remodeling during acute myocardial infarction,” *The American Journal of Pathology*, vol. 182, no. 1, pp. 29–40, 2013.
- [101] S. E. Boag, R. Das, E. V. Shmeleva et al., “T lymphocytes and fractalkine contribute to myocardial ischemia/reperfusion injury in patients,” *The Journal of Clinical Investigation*, vol. 125, no. 8, pp. 3063–3076, 2015.
- [102] A. Azouz, M. S. Razzaque, M. El-Hallak, and T. Taguchi, “Immunoinflammatory responses and fibrogenesis,” *Medical Electron Microscopy*, vol. 37, no. 3, pp. 141–148, 2004.
- [103] R. Sharif, J. Semo, S. Shimoni et al., “Experimental myocardial infarction induces altered regulatory T cell homeostasis, and adoptive transfer attenuates subsequent remodeling,” *PLoS One*, vol. 9, no. 12, article e113653, 2014.

- [104] D. Frenkel, A. S. Pachori, L. Zhang et al., "Nasal vaccination with troponin reduces troponin specific T-cell responses and improves heart function in myocardial ischemia-reperfusion injury," *International Immunology*, vol. 21, no. 7, pp. 817–829, 2009.
- [105] D. A. Forero-Pena and F. R. Gutierrez, "Statins as modulators of regulatory T-cell biology," *Mediators of Inflammation*, vol. 2013, Article ID 167086, 10 pages, 2013.
- [106] D. Ke, J. Fang, L. Fan, Z. Chen, and L. Chen, "Regulatory T cells contribute to rosuvastatin-induced cardioprotection against ischemia-reperfusion injury," *Coronary Artery Disease*, vol. 24, no. 4, pp. 334–341, 2013.
- [107] N. Sorathia, H. Al-Rubaye, and B. Zal, "The effect of statins on the functionality of CD4+CD25+FOXP3+ regulatory T-cells in acute coronary syndrome: a systematic review and meta-analysis of randomised controlled trials in Asian populations," *European Cardiology Review*, vol. 14, no. 2, pp. 123–129, 2019.
- [108] C. B. Granger, K. W. Mahaffey, W. D. Weaver et al., "Pexelizumab, an anti-C5 complement antibody, as adjunctive therapy to primary percutaneous coronary intervention in acute myocardial infarction," *Circulation*, vol. 108, no. 10, pp. 1184–1190, 2003.
- [109] E. D. Verrier, S. K. Shernan, K. M. Taylor et al., "Terminal complement blockade with pexelizumab during coronary artery bypass graft surgery requiring cardiopulmonary bypass: a randomized trial," *JAMA*, vol. 291, no. 19, pp. 2319–2327, 2004.
- [110] C. de Zwaan, A. H. Kleine, J. H. Diris et al., "Continuous 48-h C1-inhibitor treatment, following reperfusion therapy, in patients with acute myocardial infarction," *European Heart Journal*, vol. 23, no. 21, pp. 1670–1677, 2002.
- [111] M. Thielmann, G. Marggraf, M. Neuhauser et al., "Administration of C1-esterase inhibitor during emergency coronary artery bypass surgery in acute ST-elevation myocardial infarction," *European Journal of Cardio-Thoracic Surgery*, vol. 30, no. 2, pp. 285–293, 2006.
- [112] K. Fattouch, G. Bianco, G. Speziale et al., "Beneficial effects of C1 esterase inhibitor in ST-elevation myocardial infarction in patients who underwent surgical reperfusion: a randomised double-blind study," *European Journal of Cardio-Thoracic Surgery*, vol. 32, no. 2, pp. 326–332, 2007.
- [113] B. D. Packard and J. M. Weiler, "Steroids inhibit activation of the alternative-amplification pathway of complement," *Infection and Immunity*, vol. 40, no. 3, pp. 1011–1014, 1983.
- [114] D. F. Lappin and K. Whaley, "Modulation of complement gene expression by glucocorticoids," *The Biochemical Journal*, vol. 280, no. 1, Part 1, pp. 117–123, 1991.
- [115] N. Potere, M. G. Del Buono, G. Niccoli, F. Crea, S. Toldo, and A. Abbate, "Developing LRP1 agonists into a therapeutic strategy in acute myocardial infarction," *International Journal of Molecular Sciences*, vol. 20, no. 3, p. 544, 2019.
- [116] N. A. Abouzaki, S. Christopher, C. Trankle et al., "Inhibiting the inflammatory injury after myocardial ischemia reperfusion with plasma-derived alpha-1 antitrypsin: a post hoc analysis of the VCU- α 1RT study," *Journal of Cardiovascular Pharmacology*, vol. 71, no. 6, pp. 375–379, 2018.
- [117] A. Abbate, B. W. Van Tassel, S. Christopher et al., "Effects of prolastin C (plasma-derived alpha-1 antitrypsin) on the acute inflammatory response in patients with ST-segment elevation myocardial infarction (from the VCU-alpha 1-RT pilot study)," *The American Journal of Cardiology*, vol. 115, no. 1, pp. 8–12, 2015.
- [118] H. Hammerman, R. A. Kloner, S. Hale, F. J. Schoen, and E. Braunwald, "Dose-dependent effects of short-term methylprednisolone on myocardial infarct extent, scar formation, and ventricular function," *Circulation*, vol. 68, no. 2, pp. 446–452, 1983.
- [119] R. A. Kloner, M. C. Fishbein, H. Lew, P. R. Maroko, and E. Braunwald, "Mummification of the infarcted myocardium by high dose corticosteroids," *Circulation*, vol. 57, no. 1, pp. 56–63, 1978.
- [120] B. H. Bulkley and W. C. Roberts, "Steroid therapy during acute myocardial infarction: A cause of delayed healing and of ventricular aneurysm," *The American Journal of Medicine*, vol. 56, no. 2, pp. 244–250, 1974.
- [121] R. Roberts, V. DeMello, and B. E. Sobel, "Deleterious effects of methylprednisolone in patients with myocardial infarction," *Circulation*, vol. 53, pp. I204–I206, 1976.
- [122] P. Paulus, J. Holfeld, A. Urbschat et al., "Prednisolone as preservation additive prevents from ischemia reperfusion injury in a rat model of orthotopic lung transplantation," *PLoS One*, vol. 8, no. 8, article e73298, 2013.
- [123] S. Tokudome, M. Sano, K. Shinmura et al., "Glucocorticoid protects rodent hearts from ischemia/reperfusion injury by activating lipocalin-type prostaglandin D synthase-derived PGD2 biosynthesis," *The Journal of Clinical Investigation*, vol. 119, no. 6, pp. 1477–1488, 2009.
- [124] G. R. Giugliano, R. P. Giugliano, C. M. Gibson, and R. E. Kuntz, "Meta-analysis of corticosteroid treatment in acute myocardial infarction," *The American Journal of Cardiology*, vol. 91, no. 9, pp. 1055–1059, 2003.
- [125] J. Zhang, Y. Yao, F. Xiao et al., "Administration of dexamethasone protects mice against ischemia/reperfusion induced renal injury by suppressing PI3K/AKT signaling," *International Journal of Clinical and Experimental Pathology*, vol. 6, no. 11, pp. 2366–2375, 2013.
- [126] M. Taghizadieh, B. Hajipour, N. A. Asl, A. Khodadadi, M. H. Somi, and M. Bane'i, "Combination effect of melatonin and dexamethasone on liver ischemia/reperfusion injury," *Bratislavské Lekárske Listy*, vol. 117, no. 1, pp. 47–53, 2016.
- [127] W. H. Sun, F. He, N. N. Zhang, Z. A. Zhao, and H. S. Chen, "Time dependent neuroprotection of dexamethasone in experimental focal cerebral ischemia: the involvement of NF- κ B pathways," *Brain Research*, vol. 1701, pp. 237–245, 2018.
- [128] L. Moonen, H. Geryl, P. C. D'Haese, and B. A. Vervaeet, "Short-term dexamethasone treatment transiently, but not permanently, attenuates fibrosis after acute-to-chronic kidney injury," *BMC Nephrology*, vol. 19, no. 1, p. 343, 2018.

Research Article

Analysis of Myocardial Ischemia Parameters after Coronary Artery Bypass Grafting with Minimal Extracorporeal Circulation and a Novel Microplegia versus Off-Pump Coronary Artery Bypass Grafting

Luca Koechlin , Urs Zenklusen, Thomas Doebele, Bejtush Rrahmani, Brigitta Gahl, Thibault Schaeffer, Denis Berdajs, Friedrich S. Eckstein, and Oliver Reuthebuch 

Department of Cardiac Surgery, University Hospital Basel, Basel, Switzerland

Correspondence should be addressed to Oliver Reuthebuch; oliver.reuthebuch@usb.ch

Received 29 August 2019; Revised 7 December 2019; Accepted 17 December 2019; Published 25 January 2020

Guest Editor: Bruno Podesser

Copyright © 2020 Luca Koechlin et al. This is an open access article distributed under the Creative Commons Attribution License, which permits unrestricted use, distribution, and reproduction in any medium, provided the original work is properly cited.

Background. To compare the performance of our institutionally refined microplegia protocol in conjunction with minimal extracorporeal circulation system (MiECC) with off-pump coronary artery bypass grafting (OPCAB). **Methods.** We conducted a single center study including patients undergoing isolated CABG surgery performed either off-pump or on-pump using our refined microplegia protocol in conjunction with MiECC. We used propensity modelling to calculate the inverse probability of treatment weights (IPTW). Primary endpoints were peak values of high-sensitivity cardiac troponin T (hs-cTnT) during hospitalization, and respective first values on the first postoperative day. Endpoint analysis was adjusted for intraoperative variables. **Results.** After IPTW, we could include 278 patients into our analyses, 153 of which had received OPCAB and 125 of which had received microplegia. Standardized differences indicated that treatment groups were comparable after IPTW. The multivariable quantile regression yielded a nonsignificant median increase of first hs-cTnT by 39 ng/L (95% CI -8 to 87 ng/L, $p=0.11$), and of peak hs-cTnT by 35 ng/L (CI -13 to 84, $p=0.16$), when microplegia was used, as compared to OPCAB. Major adverse cardiac and cerebrovascular events (MACCE) occurred with equal frequency in both groups (7.8% vs. 5.0%; $p=0.51$), and length of stay in the intensive care unit (ICU) was significantly shorter after the use of microplegia (geometric mean 1.6 days versus 1.3 days; $p=0.01$). **Conclusion.** The use of our institutionally refined microplegia in conjunction with MiECC was associated with similar results with regard to ischemic injury, expressed in hs-cTnT compared to OPCAB. MACCE was seen equally frequent. ICU discharge was earlier if microplegia was used.

1. Introduction

Despite a Ib recommendation for off-pump coronary artery bypass grafting (OPCAB) in patients with significant atherosclerotic aortic disease and a IIa recommendation for OPCAB for high-risk patients, OPCAB is not consistently applied [1, 2]. This is most probably due to the missing proof of long-term benefits of the OPCAB procedure since large randomized controlled trials failed to show a clear benefit for OPCAB procedures [3–7].

To reduce the potential negative side effects of the extracorporeal circulation systems (ECC), such as systemic

inflammatory response syndrome or postoperative renal insufficiency, the minimal extracorporeal circulation system (MiECC) was introduced [8–10]. The use of the MiECC in coronary artery bypass grafting (CABG) was shown to be associated with excellent outcomes [11, 12]. Moreover, with regard to perioperative myocardial damage, the use of MiECC was shown to be comparable to OPCAB [11]. However, it is unknown to which extent the perioperative myocardial damage is dependent on the applied cardioplegic protocol. To further optimize MiECC in CABG surgery, we introduced the Myocardial Protection System (MPS®) in our clinic to deliver a novel microplegia solution [13]. This

strategy, also referred to as Basel Microplegia Protocol (BMP), was shown to be beneficial regarding perioperative myocardial damage and length of stay on the intensive care unit (ICU) [14].

However, in comparison to OPCAB, the clinical role of the Basel Microplegia Protocol is undetermined. To better address this issue, we used observational data and performed a propensity modelling to calculate inverse probability of treatment weights (IPTW). These data were adjusted for possible confounding factors by indication.

2. Material and Methods

2.1. Ethical Approval. The local ethical committee (EKNZ BASEC Req-2018-00923) approved the study protocol, which is in accordance with the principles of the Declaration of Helsinki. The ethical committee has waived the need to obtain informed consent.

The trial was registered at ClinicalTrials.gov (ID NCT03609723). The authors designed the study, gathered and analyzed the data, vouched for the data and analysis, wrote the paper, and decided to publish.

2.2. Patients and Study Design (Figure 1). The preferred revascularization strategies for isolated CABG surgery in our clinic were either OPCAB or MiECC-assisted surgery. In May 2017, we started to deliver our institutionally refined microplegia (Basel Microplegia Protocol) using the MPS® as an adjunct to the MiECC [13]. Since it performed excellently, this combination became a routine in isolated CABG with MiECC in our clinic [13, 14].

OPCAB is preferably used in patients with a high thromboembolic risk when manipulation of the aorta has to be minimized, in patients with severe renal insufficiency, and in patients with impaired myocardial function. Conventional ECC is only applied in emergency operations or concomitant non-CABG surgeries.

To investigate the effect of the two operation techniques (microplegia versus OPCAB) on the basis of our own observational data, we performed a propensity modelling to calculate inverse probability of treatment weights (IPTW) to adjust for possible confounding by indication.

Using a prospectively maintained institutional registry (Intellect 1.7, Dendrite Clinical Systems, Henley-on-Thames, UK), we identified all patients who underwent isolated CABG in our institution from February 2010 on. All clinical data were exported from this registry, where data are regularly controlled for completeness and accuracy [13, 14]. Intraoperative data were collected prospectively with a standardized protocol, and serological parameters were assessed according to the standard clinical algorithm in our hospital, beginning on the first postoperative day (POD) at 06:00 a.m. and continued during the following days until a normalization of the values was achieved. According to previous studies, we recorded the first postoperative value and the peak value of high-sensitivity cardiac troponin T (hs-cTnT) as well as creatine kinase (CK) and CK-MB as indicators for myocardial damage [13, 14]. As a safety endpoint, major adverse cardiac and cerebrovascular events (MACCE) were

assessed, defined as a composite of myocardial infarction, stroke, or all-cause mortality. Moreover, we recorded the duration of ICU stay, in-hospital mortality, postoperative atrial fibrillation, and intraoperative parameters such as aortic cross-clamping time and number of distal anastomoses. Perioperative acute myocardial infarction was assessed by the treating clinicians (mainly on the intensive care unit) according to the recent guidelines [15–17].

Patients with nonstandard cardioplegic strategy, concomitant ablation, or previous myocardial infarction within 7 days before the operation, as well as patients undergoing minimally invasive direct coronary artery bypass grafting (MIDCAB), were excluded from this analysis (Figure 1).

2.3. Technical Aspects and Surgical Technique. Our techniques for OPCAB and isolated CABG using our novel microplegia protocol were previously described in detail [11, 13, 14]. All operations were performed through median sternotomy. When using the MiECC, the ascending aorta and the right atrium were cannulated after full heparinisation. Cardioplegic arrest was induced using microplegia after cross-clamping, as previously described [13, 14]. In brief, the microplegia (composed of patient's blood with potassium (K), magnesium (Mg), and lidocaine, thus normovolemic) is applied under pressure and flow control via the aortic root. The targeted flow is approximately 300 mL/min, and for safety reasons, the pressure is limited to 250 mmHg (measured directly in the MPS® console). The microplegia protocol consists of a 4-minute induction time (with reduced dosage of K after 2 minutes) and repetitive administration of 2 minutes every 20 minutes. Before declamping, a hot shot is given for 1 minute [13, 14].

The internal mammary artery (IMA), the radial artery, or the great saphenous vein were used as graft material. The vast majority of OPCAB procedures was performed by two experienced off-pump surgeons.

2.4. Statistical Analysis. We conducted an inverse probability of treatment (IPTW) analysis and included age, body mass index, ejection fraction (EF), diabetes, three-vessel coronary artery disease, peripheral artery disease, preoperative stroke, preoperative renal failure, prior myocardial infarction (MI), hypertension, hypercholesterolemia, NYHA class 3 or 4, current smoking status, and EuroSCORE 2 as covariates into the propensity model. We trimmed the tails of the propensity score distribution according to Figure 1S (supplemental Figure 1S). Differences between the treatment groups (microplegia and OPCAB) before and after IPTW were expressed as standardized differences to assess comparability independently of the number of observations; the standardized differences are displayed in Figure 2S (supplemental Figure 2S). Standardized differences of ≤ 0.1 are considered sufficiently small to indicate no relevant differences. To investigate the impact of treatment on hs-cTnT, CK-MB, and CK, we used IPT-weighted median regression, given the skewed distribution of these cardiac markers. We included the number of distal anastomoses, duration of operation, main stem stenosis, and the use of both internal mammary arteries (BIMA) as

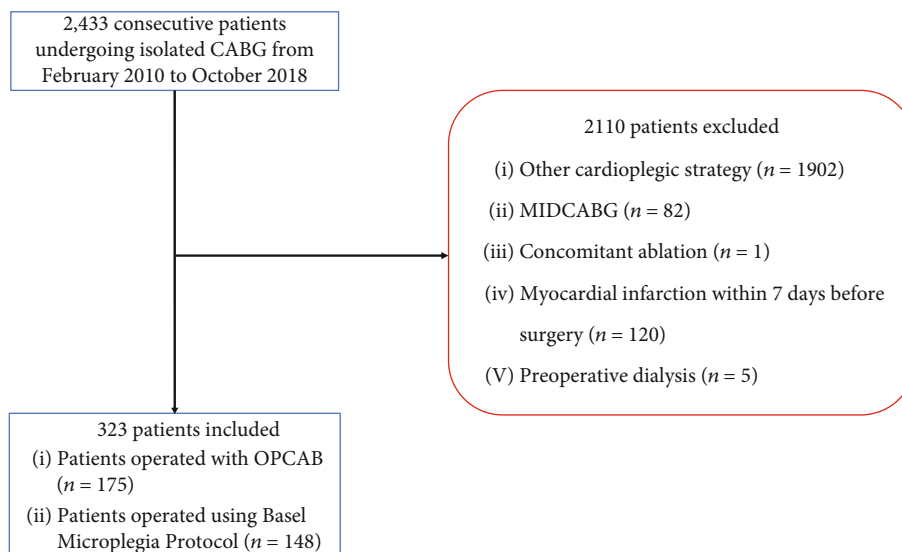


FIGURE 1: Patient flow chart.

TABLE 1: Patient characteristics.

	Before IPTW				After IPTW			
	OPCAB (n = 175)	Microplegia (n = 148)	Diff.	<i>p</i>	OPCAB (n = 153)	Microplegia (n = 125)	Diff.	<i>p</i>
Age in years, m (SD)	69.3 (10.2)	68.0 (8.7)	-0.143	0.205	68.1 (10.4)	68.2 (9.7)	0.005	0.969
BMI in kg/m ² , m (SD)	26.8 (4.0)	27.9 (4.7)	0.253	0.023	27.0 (4.3)	26.9 (5.1)	-0.017	0.890
Ejection fraction in %, m (SD)	53.0 (11.2)	56.3 (10.2)	0.306	0.007	54.4 (10.4)	54.2 (15.4)	-0.016	0.899
EuroSCORE 2, m (SD)	2.3 (2.0)	1.6 (1.6)	-0.383	0.001	1.9 (1.3)	1.8 (3.3)	-0.010	0.938
Female, <i>n</i> (%)	33 (18.9)	28 (18.9)	-0.002	0.989	27 (17.9)	23 (18.4)	-0.014	0.914
Diabetes, <i>n</i> (%)	57 (32.6)	60 (40.5)	-0.166	0.138	52 (33.9)	42 (33.5)	0.009	0.948
Peripheral artery disease, <i>n</i> (%)	45 (25.7)	22 (14.9)	0.272	0.018	32 (21.2)	25 (19.9)	0.033	0.811
Preoperative stroke, <i>n</i> (%)	24 (13.7)	11 (7.4)	0.205	0.074	17 (11.4)	11 (8.5)	0.096	0.460
Renal disease, <i>n</i> (%)	8 (4.6)	3 (2.0)	0.143	0.221	4 (2.4)	3 (2.3)	0.002	0.987
COPD, <i>n</i> (%)	18 (10.3)	17 (11.5)	-0.039	0.730	15 (9.7)	15 (12.1)	-0.077	0.546
Prior myocardial infarction, <i>n</i> (%)	75 (42.9)	44 (29.7)	0.276	0.015	60 (39.1)	49 (39.4)	-0.007	0.961
Hypertension, <i>n</i> (%)	158 (90.3)	126 (85.1)	0.157	0.160	135 (88.4)	110 (88.2)	0.006	0.964
Hypercholesterolemia, <i>n</i> (%)	141 (80.6)	113 (76.4)	0.103	0.357	120 (78.3)	100 (80.0)	-0.043	0.739
NYHA III or IV, <i>n</i> (%)	36 (20.6)	23 (15.5)	0.131	0.245	27 (17.9)	22 (17.7)	0.006	0.965
Preoperative atrial fibrillation, <i>n</i> (%)	9 (5.1)	9 (6.1)	-0.041	0.714	7 (4.5)	5 (4.4)	0.005	0.969
Current smoker, <i>n</i> (%)	31 (17.7)	29 (19.6)	-0.048	0.665	30 (19.8)	28 (22.1)	-0.056	0.689

Diff.: standardized differences. Data are presented as mean and standard deviation or as numbers (%). OPCAB: off-pump coronary artery bypass grafting; COPD: chronic obstructive pulmonary disease; IPTW: inverse probability of treatment weighting.

covariates into median regression, as we expect the association between treatment and endpoint to be confounded by these intraoperative variables. We also show crude values before IPTW as median and interquartile range with a Kruskal-Wallis test for differences.

All other continuous data are reported as mean \pm standard deviation comparisons being made using linear

regression. However, length of stay on the ICU and hospital stay are shown as geometric means with confidence intervals that were back-transformed from the logarithmic scale (due to skewed distribution). Categorical data are reported as numbers with percentage and compared using logistic regression. Confidence intervals and *p* values are two-sided; a *p* value below 0.05 is considered significant. All analyses

TABLE 2: Intraoperative data.

	Before IPTW				After IPTW			
	OPCAB (n = 175)	Microplegia (n = 148)	Diff.	p	OPCAB (n = 153)	Microplegia (n = 125)	Diff.	p
Number of distal anastomoses, m (SD)	3.2 (1.2)	3.8 (0.9)	0.613	0.000	3.3 (1.1)	3.7 (1.1)	0.370	0.002
Duration of operation in minutes, m (SD)	191.6 (42.9)	222.9 (50.2)	0.670	0.000	194.3 (42.7)	217.0 (63.4)	0.420	0.001
Three vessel coronary artery disease, n (%)	132 (75.4)	137 (92.6)	-0.481	0.000	132 (86.0)	105 (84.0)	0.057	0.696
Presence of main stem stenosis, n (%)	21 (12.0)	42 (28.4)	-0.417	0.000	19 (12.6)	37 (29.9)	-0.434	0.001
Total arterial revascularization, n (%)	45 (25.7)	34 (23.0)	0.064	0.568	34 (22.0)	30 (23.8)	-0.044	0.740
LIMA, n (%)	164 (93.7)	146 (98.6)	-0.260	0.041	145 (94.6)	123 (98.2)	-0.194	0.295
RIMA, n (%)	40 (22.9)	26 (17.6)	0.132	0.241	37 (24.4)	22 (17.8)	0.163	0.223
BIMA, n (%)	38 (21.7)	26 (17.6)	0.105	0.352	36 (23.4)	22 (17.8)	0.139	0.295
Use of the radial artery, n (%)	15 (8.6)	43 (29.1)	-0.543	0.000	15 (9.9)	33 (26.7)	-0.444	0.001
IV inotropes at end of operation, n (%)	32 (18.4)	27 (18.5)	-0.003	0.981	28 (18.1)	29 (23.0)	-0.121	0.383

Data are presented as mean and standard deviation or as numbers (%). Diff.: standardized differences; OPCAB: off-pump coronary artery bypass grafting; LIMA: left internal mammary artery; RIMA: right internal mammary artery; BIMA: both internal mammary arteries; IV: intravenous; IPTW: inverse probability of treatment weighting.

were performed by a biostatistician (BG) using Stata 15 (StataCorp, Texas).

3. Results

3.1. Preoperative Data (Table 1). From February 2010 until October 2018, 2433 patients underwent isolated CABG surgery in our institution. 323 met the inclusion criteria and thus represent the cohort of this study (Figure 1). Before IPTW, patients undergoing OPCAB had significantly lower ejection fraction (EF), higher EuroSCORE 2, more peripheral artery disease, and more previous MIs. After IPTW, groups were comparable in regard to pretreatment characteristics.

After IPTW, 278 patients were analyzed, 153 of which had received OPCAB and 125 of which had received microplegia. Absolute standardized differences between treatment groups dropped below 0.1 for all baseline characteristics, indicating no relevant difference (Table 1).

3.2. Intraoperative Data (Table 2). Before IPTW, patients undergoing CABG using microplegia were more likely to have three-vessel coronary artery disease and main stem stenosis, and they had longer operation times compared to patients undergoing OPCAB. Moreover, patients undergoing on-pump CABG had more distal anastomoses; the radial artery was more frequently used.

These differences maintained even after IPTW, indicating that they relate to the treatment itself rather than to patient characteristics. This supports the concept of including these variables as covariates. Intraoperative data are provided in Table 2.

3.3. Postoperative Data (Table 3). No differences regarding in-hospital mortality, postoperative MI, postoperative stroke, or atrial fibrillation at discharge remained after IPTW. However, length of stay on the ICU was significantly shorter in patients operated using microplegia. Postoperative results are depicted in Table 3.

3.4. Endpoint Analysis (Table 4, Figures 2–4). After IPTW, both median (IQR) POD1 and peak hs-cTnT values were numerically higher in the microplegia group than in the OPCAB group, but this difference did not reach statistical significance (POD1: 174 ng/L (73–274 ng/L) in the OPCAB group versus 213 ng/L (117–308 ng/L) in the microplegia group, $p = 0.105$; peak: 178 ng/L (68–289 ng/L) in the OPCAB group versus 213 ng/L (109–318 ng/L) in the microplegia group, $p = 0.155$). Median (IQR) CK-MB was significantly lower in patients undergoing OPCAB than in patients receiving microplegia (POD1: 6.7 $\mu\text{g/L}$ (1.3–12.1 $\mu\text{g/L}$) versus 11.6 $\mu\text{g/L}$ (6.7–16.4 $\mu\text{g/L}$); $p < 0.001$; peak: 8.0 $\mu\text{g/L}$ (2.7–13.4 $\mu\text{g/L}$) versus 12.0 $\mu\text{g/L}$ (7.2–16.8 $\mu\text{g/L}$), $p = 0.002$). Median (IQR) CK on POD1 was significantly higher in the microplegia group than in the OPCAB group (174 U/L (0–376 U/L) versus 295 U/L (113–478 U/L), $p = 0.012$), whereas median (IQR) peak CK values were higher in the OPCAB group than in the microplegia group; this difference, however, was not statistically significant (404 U/L (166–642 U/L) versus 371 U/L (156–585 U/L), $p = 0.522$).

4. Discussion

The aim of this study was to compare our institutionally refined microplegia, applied with the MPS® (Basel Microplegia Protocol), in patients undergoing isolated CABG surgery using the MiECC, with mere OPCAB revascularization. We report five major findings.

First, OPCAB as well as CABG using the Basel Microplegia Protocol is safe and feasible in isolated CABG surgery, with low in hospital mortality and low MACCE rates in both groups. Second, the number of distal anastomoses was significantly lower among patients undergoing OPCAB procedure than in patients operated on-pump. Third, cardiac markers were extraordinarily low in both groups. While there were no significant differences regarding POD1 and peak hs-cTnT, POD1 values of CK-MB and CK as well as peak values of CK-MB were significantly lower in the OPCAB group.

TABLE 3: Postoperative data.

	Before IPTW				After IPTW			
	OPCAB (<i>n</i> = 175)	Microplegia (<i>n</i> = 148)	Diff.	<i>p</i>	OPCAB (<i>n</i> = 153)	Microplegia (<i>n</i> = 125)	Diff.	<i>p</i>
Operative mortality, <i>n</i> (%)	6 (3.4)	0 (0.0)	0.266	0.033	4 (2.5)	0 (0.0)	0.228	0.130
MACCE, <i>n</i> (%)	14 (8.0)	6 (4.1)	0.166	0.150	12 (7.8)	6 (5.0)	0.113	0.507
Postoperative MI, <i>n</i> (%)	4 (2.3)	1 (0.7)	0.134	0.272	5 (3.0)	0 (0.0)	0.249	0.130
Postoperative stroke, <i>n</i> (%)	5 (2.9)	5 (3.4)	-0.030	0.788	5 (3.2)	6 (5.0)	-0.089	0.568
Pulmonary infection, <i>n</i> (%)	12 (6.9)	5 (3.4)	0.158	0.171	11 (6.9)	4 (3.3)	0.168	0.193
Postoperative renal failure, <i>n</i> (%)	15 (8.6)	5 (3.4)	0.220	0.062	13 (8.6)	3 (2.7)	0.255	0.077
AF at discharge, <i>n</i> (%)	34 (19.4)	35 (23.6)	-0.103	0.357	25 (16.5)	27 (21.9)	-0.136	0.281
Reoperation for bleeding, <i>n</i> (%)	3 (1.7)	5 (3.4)	-0.106	0.347	3 (1.7)	7 (5.8)	-0.218	0.157
Intubation > 72 h, <i>n</i> (%)	2 (1.1)	0 (0.0)	0.152	0.502	2 (1.1)	0 (0.0)	0.149	0.503
Length of ICU stay in days, geometric mean (CI)	1.7 (1.5-1.9)	1.3 (1.2-1.4)	0.423	0.003	1.6 (1.5-1.8)	1.3 (1.2-1.4)	0.419	0.014
Length of stay in days, geometric mean (CI)	8.5 (7.9-9.2)	8.7 (8.3-9.2)	0.658	0.399	8.7 (8.0-9.4)	8.8 (8.3-9.4)	0.646	0.395

Data are presented as geometric mean and standard deviation back-transformed from the log scale or as numbers (%). Diff.: standardized differences; OPCAB: off-pump coronary artery bypass grafting; MACCE: major adverse cardiac and cerebrovascular events; ICU: intensive care unit; MI: myocardial infarction; IPTW: inverse probability of treatment weighting.

TABLE 4: Cardiac markers.

	Crude nonparametric analysis, before IPTW			Adjusted, after IPTW			
	OPCAB (<i>n</i> = 175)	Microplegia (<i>n</i> = 148)	<i>p</i>	OPCAB (<i>n</i> = 153)	Microplegia (<i>n</i> = 125)	Effect on median	<i>p</i>
hs-cTnT, POD1 in ng/L, median (IQR)	176 (106-258)	225 (159-372)	<0.001	174 (73-274)	213 (117-308)	39 (-8-87)	0.105
Peak hs-cTnT in ng/L, median (IQR)	187 (112-318)	237 (167-380)	0.001	178 (68-289)	213 (109-318)	35 (-13-84)	0.155
CK-MB POD1 in $\mu\text{g/L}$, median (IQR)	8.6 (5.3-13.9)	13.4 (9.3-19.7)	<0.001	6.7 (1.3-12.1)	11.6 (6.7-16.4)	4.9 (2.3-7.4)	0.000
Peak CK-MB in $\mu\text{g/L}$, median (IQR)	9.4 (5.6-14.6)	13.4 (9.3-19.9)	<0.001	8.0 (2.7-13.4)	12.0 (7.2-16.8)	4.0 (1.4-6.5)	0.002
CK POD1 in U/L, median (IQR)	357 (233-542)	503 (322-691)	<0.001	174 (0-376)	295 (113-478)	121 (27-216)	0.012
Peak CK in U/L, median (IQR)	508 (339-783)	577 (401-768)	0.296	404 (166-642)	371 (156-585)	-34 (-137-70)	0.522

Note that average cardiac markers on the right hand side are estimated from median regression at the average of the covariates (main stem stenosis, use of BIMA, duration of operation, and number of distal anastomoses) after IPTW. Data are presented as median with an interquartile range. OPCAB: off-pump coronary artery bypass grafting; hs-cTnT: high-sensitivity cardiac troponin T; CK: creatine kinase; CK-MB: creatine kinase-myocardial type; POD: postoperative day; IPTW: inverse probability of treatment weighting.

Fourth, we found no significant differences regarding postoperative atrial fibrillation between the two groups. Fifth, length of stay on the ICU was significantly lower in patients undergoing MiECC assisted CABG surgery using the microplegia than in OPCAB patients.

These data corroborate our promising first results that we have achieved after having introduced our institutionally refined dose/volume-dependent microplegia applied with the MPS® in isolated CABG surgery using the MiECC [13, 14].

The question of whether to perform OPCAB or on-pump surgery has been the subject of controversy for decades. While OPCAB provides advantages due to the missing contact between blood and foreign material or air as well as due to the absence of aortic cannulation potentially causing embolisms, there are also concerns regarding the long-term patency rates and completeness of revascularization in OPCAB procedures [3, 8, 9, 18, 19]. Large randomized controlled trials failed to show a clear benefit for OPCAB procedures [3–6]. Moreover, after worse composite outcomes and

poorer graft patency rates after one year in the Randomized On/Off Bypass (ROOBY) study, the ROOBY-FS study showed a higher prevalence of death from any cause and of the composite outcome consisting of death from any cause, repeat revascularization, and nonfatal myocardial infarction after 5 years in patients undergoing OPCAB [3, 7]. However, OPCAB may still be the preferred technique for experienced surgeons in selected patient cohorts, such as elderly, calcified, or high-risk patients [20–22].

Regarding our results, a few points merit consideration: First, the number of distal anastomoses was significantly lower in patients undergoing OPCAB, but still higher compared to other studies (Shroyer et al.: 2.9 ± 0.9 ; Parmeshwar et al.: 2.79 ± 0.8) [3, 23]. Lower numbers of anastomoses among patients undergoing OPCAB are a common finding; yet, it questions the completeness of revascularization [3]. However, there is also literature indicating that completeness of revascularization is dependent not only on the number of grafts performed but also on the number of grafts needed [24]. Second, we found no significant difference regarding

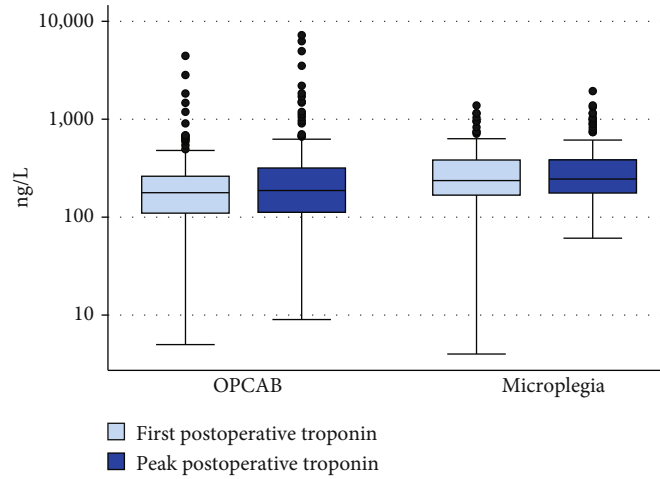


FIGURE 2: Boxplots hs-cTnT.

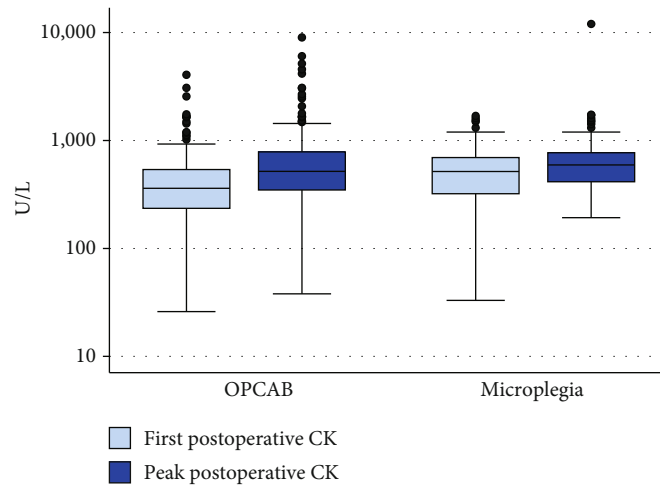


FIGURE 3: Boxplots CK.

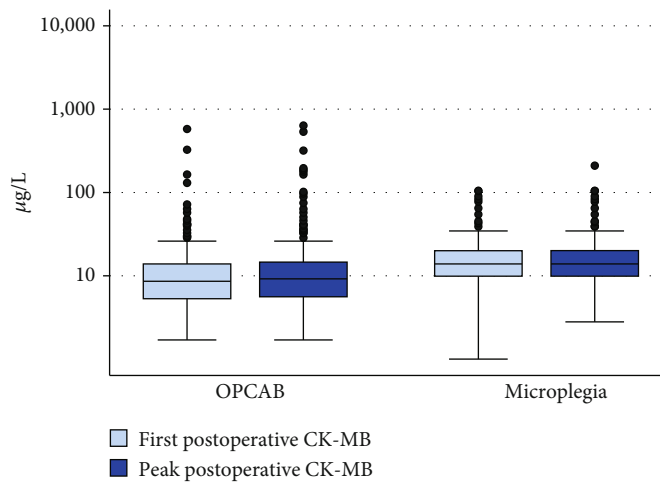


FIGURE 4: Boxplots CK-MB.

postoperative hs-cTnT values between the groups, and the values were on a remarkably low level [13, 14]. Moreover, there were no differences regarding in-hospital mortality or MACCE. However, there is evidence for an association between high postoperative hs-cTnT values and adverse outcomes after on-pump cardiac surgery including CABG [25–27]. Therefore, we believe that optimizing cardioplegic solutions, reflected by low postoperative cardiac markers, is a crucial cornerstone in CABG surgery to provide the best possible outcomes. The low levels of cardiac markers are especially important when considering that OPCAB surgery in our clinic is only performed by two experienced off-pump surgeons, while on-pump CABG is an important part of the education of younger and unexperienced cardiac surgeons. The remarkably low values of cardiac markers achieved with our microplegia protocol allow for a good cardiac protection, even during longer operations with multiple anastomoses. Third, patients operated using microplegia were significantly shorter on the ICU than patients operated off-pump. This supports previous findings regarding shorter length of stay on the ICU after the use of microplegia [14, 28].

While hs-cTnT levels were similar in both groups, levels of CK-MB and CK on POD1 were significantly lower in the OPCAB group, indicating a possible increased myocardial damage in the microplegia group. Whether these differences are based on different pathophysiological mechanisms remains speculative.

Comparing these results to standard on-pump CABG surgery is difficult since various factors influence levels of cardiac markers. First, it was shown that the use of MiECC was associated with lower cTnI values compared to the use of ECC [29]. Moreover, also the use of the cardioplegia solution influences postoperative values of cardiac markers [14].

Some limitations warrant consideration when interpreting the findings of this study. First, it was an observational single-center study, which may compromise the external validity of our findings. Second, due to the propensity modelling method, the final study population is relatively small, which increases the risk of results being attributable to chance. Further studies with larger sample sizes will be more beneficial to enlighten the topic. On the other hand, the standardized differences after propensity modelling indicate that the treatment groups are very similar with respect to patient characteristics. Thus, differences observed during the postoperative course are likely related to the treatment, particularly because records that were suspicious for residual confounding have been trimmed. Third, the ingredients that were used as arrest agents (K, Mg, and lidocaine) have the drug approval and are licensed to be used in humans. A possible off-label use is to be considered [13].

5. Conclusion

The use of our institutionally refined microplegia in conjunction with the MiECC was associated with comparable results to OPCAB revascularization in regard to hs-cTnT while

values of CK-MB and CK on POD1 were lower in the OPCAB group. MACCE were seen equally frequent in both patient groups, and patients could be discharged from the ICU earlier when microplegia was used than when OPCAB was applied.

Data Availability

The data used to support the findings of this study have not been made available because of the local ethical regulations.

Conflicts of Interest

The authors declare that they have no conflicts of interest.

Supplementary Materials

Figure 1S: distribution of the propensity score in the two treatment groups. The red lines indicate the cut-off points beyond which observations were dropped before analysis. Figure 2S: standardized differences. (*Supplementary Materials*)

References

- [1] M. Sousa-Uva, F. J. Neumann, A. Ahlsson et al., “2018 ESC/EACTS guidelines on myocardial revascularization,” *European Journal of Cardio-Thoracic Surgery*, vol. 55, no. 1, pp. 4–90, 2019.
- [2] F. G. Bakaen, A. L. W. Shroyer, J. S. Gammie et al., “Trends in use of off-pump coronary artery bypass grafting: results from the Society of Thoracic Surgeons Adult Cardiac Surgery Database,” *Journal of Thoracic and Cardiovascular Surgery*, vol. 148, no. 3, pp. 856–864.e1, 2014.
- [3] A. L. Shroyer, F. L. Grover, B. Hattler et al., “On-pump versus off-pump coronary-artery bypass surgery,” *The New England Journal of Medicine*, vol. 361, no. 19, pp. 1827–1837, 2009.
- [4] A. Lamy, P. J. Devereaux, D. Prabhakaran et al., “Effects of off-pump and on-pump coronary-artery bypass grafting at 1 year,” *New England Journal of Medicine*, vol. 368, no. 13, pp. 1179–1188, 2013.
- [5] A. Diegeler, J. Börgermann, U. Kappert et al., “Off-pump versus on-pump coronary-artery bypass grafting in elderly patients,” *The New England Journal of Medicine*, vol. 368, no. 13, pp. 1189–1198, 2013.
- [6] A. Lamy, P. J. Devereaux, D. Prabhakaran et al., “Five-year outcomes after off-pump or on-pump coronary-artery bypass grafting,” *The New England Journal of Medicine*, vol. 375, no. 24, pp. 2359–2368, 2016.
- [7] A. L. Shroyer, B. Hattler, T. H. Wagner et al., “Five-year outcomes after on-pump and off-pump coronary-artery bypass,” *The New England Journal of Medicine*, vol. 377, no. 7, pp. 623–632, 2017.
- [8] A. Lamy, P. J. Devereaux, D. Prabhakaran et al., “Off-pump or on-pump coronary-artery bypass grafting at 30 days,” *The New England Journal of Medicine*, vol. 366, no. 16, pp. 1489–1497, 2012.
- [9] T. Puehler, A. Haneya, A. Philipp et al., “Minimal extracorporeal circulation: an alternative for on-pump and off-pump coronary revascularization,” *The Annals of Thoracic Surgery*, vol. 87, no. 3, pp. 766–772, 2009.

- [10] W. van Boven, W. Gerritsen, F. Waanders, F. Haas, and L. Aarts, "Mini extracorporeal circuit for coronary artery bypass grafting: initial clinical and biochemical results: a comparison with conventional and off-pump coronary artery bypass grafts concerning global oxidative stress and alveolar function," *Perfusion*, vol. 19, no. 4, pp. 239–246, 2004.
- [11] O. Reuthebuch, L. Koechlin, B. Gahl et al., "Off-pump compared to minimal extracorporeal circulation surgery in coronary artery bypass grafting," *Swiss Medical Weekly*, vol. 144, 2014.
- [12] B. Winkler, P. P. Heinisch, G. Zuk et al., "Minimally invasive extracorporeal circulation: excellent outcome and life expectancy after coronary artery bypass grafting surgery," *Swiss Medical Weekly*, vol. 147, no. 2728, 2017.
- [13] L. Koechlin, U. Zenklusen, T. Doebele et al., "Clinical implementation of a novel myocardial protection pathway in coronary artery bypass surgery with minimal extracorporeal circulation," *Perfusion*, vol. 34, no. 4, pp. 277–284, 2018.
- [14] L. Koechlin, B. Rrahmani, B. Gahl et al., "Microplegia versus Cardioplexol® in coronary artery bypass surgery with minimal extracorporeal circulation: comparison of two cardioplegia concepts," *The Thoracic and Cardiovascular Surgeon*, 2019.
- [15] K. Thygesen, J. S. Alpert, H. D. White, and Joint ESC/ACC/AHA/WHF Task Force for the Redefinition of Myocardial Infarction, "Universal definition of myocardial infarction," *Journal of the American College of Cardiology*, vol. 50, no. 22, pp. 2173–2195, 2007.
- [16] K. Thygesen, J. S. Alpert, A. S. Jaffe et al., "Third universal definition of myocardial infarction," *European Heart Journal*, vol. 33, no. 20, pp. 2551–2567, 2012.
- [17] K. Thygesen, J. S. Alpert, A. S. Jaffe et al., "Fourth universal definition of myocardial infarction (2018)," *Journal of the American College of Cardiology*, vol. 72, no. 18, pp. 2231–2264, 2018.
- [18] G. F. V. Panday, S. Fischer, A. Bauer et al., "Minimal extracorporeal circulation and off-pump compared to conventional cardiopulmonary bypass in coronary surgery☆," *Interactive Cardiovascular and Thoracic Surgery*, vol. 9, no. 5, pp. 832–836, 2009.
- [19] T. Puehler, A. Haneya, A. Philipp et al., "Minimized extracorporeal circulation system in coronary artery bypass surgery: a 10-year single-center experience with 2243 patients," *European Journal of Cardio-Thoracic Surgery*, vol. 39, no. 4, pp. 459–464, 2011.
- [20] J. D. Puskas, V. H. Thourani, P. Kilgo et al., "Off-pump coronary artery bypass disproportionately benefits high-risk patients," *The Annals of Thoracic Surgery*, vol. 88, no. 4, pp. 1142–1147, 2009.
- [21] K. G. Tarakji, Sabik JF 3rd, S. K. Bhudia, L. H. Batizy, and E. H. Blackstone, "Temporal onset, risk factors, and outcomes associated with stroke after coronary artery bypass grafting," *Journal of the American Medical Association*, vol. 305, no. 4, pp. 381–390, 2011.
- [22] E. H. Blackstone and J. F. Sabik III, "Changing the discussion about on-pump versus off-pump CABG," *The New England Journal of Medicine*, vol. 377, no. 7, pp. 692–693, 2017.
- [23] N. Parmeshwar, K. E. Fero, G. Manecke, and J. M. Coletta, "Off-pump versus on-pump: long-term outcomes after coronary artery bypass in a veteran population," *Journal of Cardiothoracic and Vascular Anesthesia*, vol. 33, no. 5, pp. 1187–1194, 2019.
- [24] M. J. Magee, E. Hebert, M. A. Herbert et al., "Fewer grafts performed in off-pump bypass surgery: patient selection or incomplete revascularization?," *The Annals of Thoracic Surgery*, vol. 87, no. 4, pp. 1113–1118, 2009.
- [25] B. Gahl, V. Göber, A. Odutayo et al., "Prognostic value of early postoperative troponin T in patients undergoing coronary artery bypass grafting," *Journal of the American Heart Association*, vol. 7, no. 5, 2018.
- [26] E. Mauer mann, D. Bolliger, J. Fassl et al., "Association of troponin trends and cardiac morbidity and mortality after on-pump cardiac surgery," *The Annals of Thoracic Surgery*, vol. 104, no. 4, pp. 1289–1297, 2017.
- [27] E. Mauer mann, D. Bolliger, J. Fassl et al., "Postoperative high-sensitivity troponin and its association with 30-day and 12-month, all-cause mortality in patients undergoing on-pump cardiac surgery," *Anesthesia and Analgesia*, vol. 125, no. 4, pp. 1110–1117, 2017.
- [28] M. W. Gerdisch, S. Robinson, G. David, S. Makepeace, M. P. Ryan, and C. Gunnarsson, "Clinical and economic benefits of advanced microplegia delivery system in cardiac surgery: evidence from 250 hospitals," *Journal of Comparative Effectiveness Research*, vol. 7, no. 7, pp. 673–683, 2018.
- [29] F. F. Immer, A. Ackermann, E. Gyax et al., "Minimal extracorporeal circulation is a promising technique for coronary artery bypass grafting," *The Annals of Thoracic Surgery*, vol. 84, no. 5, pp. 1515–1521, 2007.

Research Article

Bretschneider (Custodiol®) and St. Thomas 2 Cardioplegia Solution in Mitral Valve Repair via Anterolateral Right Thoracotomy: A Propensity-Modelled Comparison

Constantin Mork , Luca Koechlin , Thibault Schaeffer, Lena Schoemig, Urs Zenklusen, Brigitta Gahl, Oliver Reuthebuch, Friedrich S. Eckstein, and Martin T. R. Grapow 

Department of Cardiac Surgery, University Hospital Basel, Basel, Switzerland

Correspondence should be addressed to Martin T. R. Grapow; martin.grapow@usb.ch

Received 30 August 2019; Accepted 12 November 2019; Published 4 December 2019

Guest Editor: Bruno Podesser

Copyright © 2019 Constantin Mork et al. This is an open access article distributed under the Creative Commons Attribution License, which permits unrestricted use, distribution, and reproduction in any medium, provided the original work is properly cited.

Background. Single-dose cardioplegia is preferred in minimal invasive mitral valve surgery to maintain the adjustment of the operative site without change of preset visualization. The aim of our study was to compare two widely used crystalloid cardioplegias Bretschneider (Custodiol®) versus St. Thomas 2 in patients who underwent mitral valve repair via small anterolateral right thoracotomy. **Material and Methods.** From May 2012 until February 2019, 184 isolated mitral valve procedures for mitral valve repair via anterolateral right thoracotomy were performed using Bretschneider (Custodiol®) cardioplegia ($n = 123$) or St. Thomas ($n = 61$). Primary efficacy endpoint was peak postoperative high-sensitivity cardiac troponin (hs-cTnT) during hospitalization. Secondary endpoints were peak creatine kinase-muscle brain type (CK-MB) and creatine kinase (CK) as well as safety outcomes. We used inverse probability of treatment weighting (IPTW) in order to adjust for confounding by indication. **Results.** Peak hs-cTnT was higher after use of Bretschneider (Custodiol®) (geometric mean 716 mg/L, 95% confidence interval (CI) 605-847 mg/L) vs. St. Thomas 2 (561 mg/L, CI 467-674 mg/L, $p = 0.047$). Peak CK-MB (geometric mean after Bretschneider (Custodiol®): 40 $\mu\text{g/L}$, CI 35-46, St. Thomas 2: 33 $\mu\text{g/L}$, CI 27-41, $p = 0.295$) and CK (geometric mean after Bretschneider (Custodiol®): 1370 U/L, CI 1222-1536, St. Thomas 2: 1152 U/L, CI 972-1366, $p = 0.037$) showed the same pattern. We did not see any difference with respect to postoperative complications between treatment groups after IPTW. **Conclusion.** Use of St. Thomas 2 cardioplegia was associated with lower postoperative peak levels of all cardiac markers that reflect cardiac ischemia such as hs-cTnT, CK, and CK-MB as compared to Bretschneider (Custodiol®) in propensity-weighted treatment groups.

1. Introduction

Mitral regurgitation is the second most common valve disease and a common indication for valve surgery in Europe. Therefore, mitral valve repair is the gold standard for the correction of severe mitral regurgitation and recommended (class I) by current ESC/EACTS guidelines for the management of valvular heart disease [1]. Minimal invasive mitral valve surgery via a minithoracotomy has become a preferred surgical approach to treat mitral valve pathologies. This procedure is less invasive; hence, it has a lower risk of severe wound complications and is cosmetically more attractive to

patients, while being technically more demanding for the cardiac surgeon. Several studies have shown the benefit of minimal invasive cardiac surgery due to decreased blood loss and shorter ICU stay [2]. Anesthesia management has improved along with postoperative care and as a consequence has the surgical outcome. Due to the increasing complexity of patients and limited surgical access, myocardial protection strategies became the focus of surgical attention. During the procedure of mitral valve repair, there is no doubt that optimal myocardial protection plays a key role in achieving a successful outcome and in minimizing myocardial damage. However, there is an ongoing discussion about the optimal

cardioplegic solution for myocardial preservation. Several smaller studies have shown the benefit of using crystalloid cardioplegia in cardiac surgery [3–9]. The striking advantage of crystalloid solutions is the longevity of duration of a single dose with avoidance of several adjustments of the operative site, which is necessary in other cardioplegic formulas with repetitive administrations. To assess possible differences among crystalloid cardioplegia solutions, we included patients in whom single-dose antegrade crystalloid cardioplegia with either Bretschneider (Custodiol®) or St. Thomas 2 was used. Both are very appealing for minimally invasive cardiac surgery due to their single-dose application and secure cardioprotective arrest for up to two hours.

The aim of our study was to investigate whether St. Thomas 2 provides superior myocardial protection and decreases myocardial damage compared to Bretschneider (Custodiol®) in patients undergoing full endoscopic minimal invasive anterolateral right minithoracotomy.

2. Methods

2.1. Ethical Approval. The local ethical committee (EKNZ BASEC Req-2019-00070) approved the study protocol, which is in accordance with the principles of the declaration of Helsinki. The ethical committee has waived the need to obtain informed consent.

The trial was registered at the ClinicalTrials.gov (ID NCT03818113). The authors designed the study, gathered and analyzed the data, vouched for the data and analysis, wrote the paper, and decided to publish.

2.2. Study Population. We included patients who underwent isolated mitral valve surgery using an anterolateral minithoracotomy with femoral installation of extracorporeal circulation (ECC) in the department of cardiac surgery at the University Hospital Basel from May 2012 until February 2019. Patients received either St. Thomas 2 or Bretschneider (Custodiol®) cardioplegia as a single dose. Standard protocol for Bretschneider (Custodiol®) included antegrade delivery of 20 mL/kg and for St. Thomas 2 30 mL/kg within 6 minutes at 4°C perfusion temperature. We excluded patients who had known coronary artery disease, mitral valve replacement, second cross-clamping, and combined cardiac procedures.

A group of 123 patients, who received Bretschneider (Custodiol®) cardioplegia, was compared to 61 patients with St. Thomas 2 cardioplegia. Given the observational origin of the data, we used IPTW to adjust for confounding by indication, including age, female gender, logistic EuroSCORE, and hypertension as covariates into the propensity model. We trimmed the tails of the propensity score, as the corresponding records are suspicious of residual confounding, and calculated standardized differences to assess comparability of treatment groups after IPTW.

2.3. Surgical Technique. In brief, minimally invasive mitral valve repair is performed through a right anterolateral thoracotomy with a periareolar incision, usually entering the thoracic cavity through the fourth intercostal space. Usually, the left groin is used for venous and arterial femoral cannulation

for the cardiopulmonary bypass. For the first two years, we used the Chitwood clamp; later, we switched to the Glauber clamp for aortic cross-clamping. Either St. Thomas 2 or Bretschneider (Custodiol®) cardioplegia as a single dose is administered. In all our cases, mitral valve repair with leaflet resection and/or implantation of artificial chordae in combination with ring annuloplasty is exclusively performed. Every patient is monitored by transesophageal echocardiography, which is used perioperatively to evaluate the surgical results.

2.4. Outcomes. Primary efficacy outcome was the highest postoperative hs-cTnT level measured before discharge; secondary outcomes were peak CK-MB and CK and the first postoperative hs-cTnT, CK-MB, and CK, which have been measured at the first day after surgery at 6 am. Safety outcomes were postoperative complications such as myocardial infarction, MACCE, and need for defibrillation at the end of surgery. Operative mortality was defined as death during surgery. Postoperative stroke was defined as a new, permanent neurological disability or deficit. Atrial fibrillation was defined as a new and permanent postoperative atrial fibrillation during hospitalization. Length of hospital stay was defined as one day prior to the procedure until discharge.

2.5. Statistical Analysis. We conducted an IPTW analysis and included age, female gender, EuroSCORE 2, hypertension, last preoperative creatinine, ejection fraction (EF), prior myocardial infarction (MI), and preoperative stroke as covariates into the propensity model. We trimmed the tails of the propensity score distribution. Differences between the treatment groups (Bretschneider (Custodiol®) and St. Thomas cardioplegia 2) after IPTW were expressed as standardized differences to assess the difference independent of the number of observations. We considered an absolute standardized difference above 0.1 to be indicative for a possibly meaningful difference. Given the skewed distribution of hs-cTnT, CK-MB, and CK, these variables were analyzed as geometric mean with confidence interval which was back transformed from the logarithmic scale. To investigate the impact of cardioplegic solution on these cardiac markers, we used IPT-weighted Poisson regression with robust standard errors. We included size of ring for annuloplasty as covariate into the model as a first sensitivity analysis. As a second sensitivity analysis, we included year of surgery as fractional polynomial covariate into the model to adjust for the impact of changes in surgical details that might have happened within 7 years of patients' enrolment.

Normally distributed continuous data were reported as mean \pm standard deviation, and comparisons were made using linear regression. Nonnormally distributed continuous variables were analyzed the same way as cardiac markers. Categorical data are reported as numbers with percentage and compared using logistic regression. Confidence intervals and *p* values are two-sided; a *p* value below 0.05 is considered significant. All analyses were done by a biostatistician (BG) using Stata 15 (StataCorp, Texas).

TABLE 1: Patient characteristics.

	Before IPTW				After IPTW			
	Bretschneider (n = 123)	St. Thomas (n = 61)	Diff	p	Bretschneider (n = 113)	St. Thomas (n = 55)	Diff	p
Age (years)	63.0 ± 11.5	64.2 ± 9.8	0.114	0.480	63.3 ± 11.8	64.0 ± 10.2	0.063	0.696
Female	44 (35.8%)	22 (36.1%)	-0.006	0.969	39 (34.3%)	19 (34.0%)	0.007	0.965
Diabetes	3 (2.4%)	1 (1.6%)	0.057	0.728	3 (2.4%)	1 (2.2%)	0.015	0.933
Hypertension	78 (63.4%)	27 (44.3%)	0.391	0.014	66 (58.7%)	31 (56.4%)	0.045	0.791
Hypercholesterolemia	24 (19.5%)	14 (23.0%)	-0.084	0.588	21 (18.7%)	12 (22.7%)	-0.099	0.561
Current smoker	13 (10.6%)	6 (9.8%)	0.024	0.878	11 (9.4%)	5 (9.9%)	-0.016	0.921
BMI	25.3 ± 4.6	25.2 ± 3.8	-0.024	0.884	25.1 ± 3.8	25.5 ± 4.0	0.108	0.519
Preoperative stroke	9 (7.3%)	2 (3.3%)	0.181	0.289	5 (4.6%)	3 (5.4%)	-0.035	0.851
Renal disease	1 (0.8%)	1 (1.6%)	-0.075	0.618	1 (1.0%)	0 (0.0%)	0.141	0.484
Last preoperative creatinine (μ mmol/L)	80.5 ± 17.9	84.8 ± 20.7	0.225	0.143	82.0 ± 17.8	80.6 ± 16.1	-0.080	0.622
COPD	3 (2.4%)	3 (4.9%)	-0.132	0.382	3 (2.8%)	1 (2.7%)	0.005	0.977
NYHA III or IV	27 (22.0%)	14 (23.0%)	-0.024	0.878	24 (21.1%)	12 (22.0%)	-0.022	0.896
AF preoperative	24 (19.5%)	12 (19.7%)	-0.004	0.979	23 (20.3%)	12 (21.1%)	-0.019	0.910
Ejection fraction	60.6 ± 7.9	62.0 ± 8.9	0.167	0.277	60.9 ± 7.8	61.4 ± 9.0	0.061	0.717
EuroSCORE 2	1.2 ± 0.8	1.3 ± 0.9	0.054	0.727	1.2 ± 0.8	1.2 ± 0.7	-0.064	0.690
Additive EuroSCORE	3.5 (3.3 to 3.9)	3.8 (3.4 to 4.2)	0.670	0.550	3.5 (3.2 to 3.8)	3.7 (3.3 to 4.2)	0.659	0.589
Logistic EuroSCORE	2.7 (2.4 to 3.0)	2.8 (2.5 to 3.3)	0.586	0.825	2.7 (2.4 to 3.0)	2.8 (2.4 to 3.3)	0.572	0.889

BMI: body mass index; COPD: chronic obstructive pulmonary disease; NYHA: New York Heart Association; AF: atrial fibrillation.

3. Results

3.1. Baseline Characteristics. From January 2009 to February 2019, 871 patients underwent 904 mitral valve operations at our hospital. In 695 patients who received mitral valve repair, anterolateral thoracotomy was chosen as surgical access in 269 patients. 184 of which met the inclusion criteria of this study.

The median age of the patients in the group of Bretschneider (Custodiol®) was 63 years (SD = \pm 11.8) and in the group of St. Thomas 2 64 years (SD = \pm 10.2), respectively (p = 0.48). Male gender was predominant in both groups (Bretschneider (Custodiol®) n = 64% vs. St. Thomas 2 n = 66%). Before IPTW, groups were comparable with respect to hemodynamic profiles and all other baseline characteristics except hypertension which was more frequent in patients treated with Bretschneider (Custodiol®). After IPTW, treatment groups were similar with respect to patient characteristics and mitral valve pathology (Tables 1 and 2).

3.2. Surgical Results. Duration of operation and aortic clamping time were similar in both groups (208 min vs. 207 min and 90 min vs. 88 min, respectively). There was no statistical difference in perfusion time. Defibrillation was more frequently used in patients receiving Bretschneider (Custodiol®) cardioplegia (50%) vs. St. Thomas 2 (36%). Both cardioplegias were given as a single-shot antegrade. Neither of the two groups received a second injection of Bretschneider (Custodiol®) or St. Thomas 2 cardioplegia. The hemody-

namic profiles of the matched patients were comparable in both groups. Both groups had predominantly a valve annuloplasty.

3.3. Postoperative Data. The in-hospital outcomes and complications are summarized in Table 3 after IPTW. In terms of in-hospital mortality, there was no significant difference between the two groups (Bretschneider (Custodiol®) n = 1 (0.7%) vs. St. Thomas 2 n = 0 (0%); p = 0.484). Although there were three cases (n = 2.4%) of myocardial infarction in the group of Bretschneider (Custodiol®), these were without statistical significance in comparison with the group of St. Thomas 2 (n = 0%, p = 0.22). Moreover, we did not find any statistically significant difference in the stay of the hospital length in days and for atrial fibrillation at discharge (Bretschneider (Custodiol®) n = 32 (28.5%) vs. St. Thomas n = 15 (27.7%); p = 0.918).

3.4. Efficacy Outcome. Postoperative biomarkers including creatine, CRP, GFR, potassium, hemoglobin, leucocytes, sodium, hs-cTnT, CK, and CK-MB are shown in Table 4.

After IPTW, our primary outcome peak hs-cTnT was higher after use of Bretschneider (median = 716 ng/L) as compared to St. Thomas 2 (median = 561 ng/L; p = 0.0047). The first hs-cTnT and CK showed the same pattern.

There was a statically significant difference in the first CRP (Bretschneider (Custodiol®) mean = 51.1 mg/L vs. St. Thomas 2 mean = 64.2 mg/L; p = 0.005). Additionally, the first potassium was significantly lower in the group of Bretschneider (Custodiol®) (p = 0.017) but in the normal

TABLE 2: Perioperative variables.

Indication	Before IPTW				After IPTW			
	Bretschneider (<i>n</i> = 123)	St. Thomas (<i>n</i> = 61)	Diff	<i>p</i>	Bretschneider (<i>n</i> = 113)	St. Thomas (<i>n</i> = 55)	Diff	<i>p</i>
Active endocarditis	3 (2.4%)	1 (1.6%)	0.057	0.728	3 (2.2%)	1 (2.2%)	0.003	0.985
Previous endocarditis	5 (4.1%)	1 (1.6%)	0.146	0.399	4 (3.7%)	0 (0.0%)	0.278	0.158
Degenerative	103 (83.7%)	51 (83.6%)	0.004	0.982	97 (85.7%)	44 (80.6%)	0.137	0.437
Calcification	10 (8.1%)	5 (8.2%)	-0.002	0.988	8 (6.7%)	5 (9.1%)	-0.091	0.586
Function	9 (7.3%)	6 (9.8%)	-0.090	0.558	7 (6.1%)	7 (13.1%)	-0.241	0.166
Rheuma	1 (0.8%)	0 (0.0%)	0.128	0.480	1 (0.9%)	0 (0.0%)	0.136	0.484
Ischemia	1 (0.8%)	0 (0.0%)	0.128	0.480	1 (0.8%)	0 (0.0%)	0.126	0.484
Dilatation of annulus	11 (8.9%)	23 (37.7%)	-0.723	0.000	9 (7.6%)	21 (37.6%)	-0.768	0.000
Barlow	15 (12.2%)	16 (26.2%)	-0.362	0.019	13 (11.1%)	14 (25.3%)	-0.374	0.026
Annuloplasty	121 (98.4%)	56 (91.8%)	0.308	0.048	111 (98.6%)	50 (91.1%)	0.345	0.037
Neochordae	95 (77.2%)	48 (78.7%)	-0.035	0.824	89 (78.8%)	42 (76.6%)	0.053	0.763
Resection	4 (3.3%)	1 (1.6%)	0.105	0.534	4 (3.7%)	1 (1.5%)	0.141	0.412
Procedure								
Duration of operation (min)	209.6 ± 35.1	208.0 ± 31.9	-0.048	0.764	207.9 ± 35.0	207.1 ± 31.1	-0.025	0.879
Aortic clamping time (min)	91.2 ± 19.3	89.2 ± 16.0	-0.110	0.495	90.6 ± 19.3	88.4 ± 16.0	-0.124	0.439
Perfusion time (min)	147.8 ± 29.1	143.6 ± 28.4	-0.145	0.356	147.0 ± 29.0	141.8 ± 27.0	-0.188	0.250
Valve size	34.0 ± 3.7	36.8 ± 2.9	0.854	0.000	34.1 ± 3.6	36.6 ± 3.0	0.754	0.000
Severe insufficiency	117 (95.1%)	60 (98.4%)	-0.183	0.303	108 (95.7%)	54 (97.8%)	-0.121	0.526

TABLE 3: Postoperative outcomes: clinical outcomes.

	Bretschneider (<i>n</i> = 113)	After IPTW St. Thomas 2 (<i>n</i> = 55)	Diff	<i>p</i>
30 days mortality	1 (0.7%)	0 (0.0%)	0.118	0.484
Postoperative stroke	0 (0.0%)	1 (1.2%)	-0.155	0.151
MACCE	3 (3.1%)	1 (1.2%)	0.130	0.415
Postoperative MI	3 (2.4%)	0 (0.0%)	0.220	0.321
Postoperative renal failure	0 (0.0%)	1 (1.3%)	-0.164	0.151
Pulmonary infection	4 (3.3%)	0 (0.0%)	0.260	0.223
Sternal infection	1 (0.8%)	0 (0.0%)	0.129	0.484
Intubation > 72 h	1 (1.2%)	0 (0.0%)	0.157	0.484
Reoperation for bleeding	3 (2.7%)	0 (0.0%)	0.235	0.223
Permanent pacemaker	1 (0.7%)	0 (0.0%)	0.118	0.484
AF at discharge	32 (28.5%)	15 (27.7%)	0.018	0.915
Ejection fraction (%)*	50.3 ± 10.3	49.1 ± 14.2	-0.097	0.580
Length of stay (day)	8.5 (8.1 to 8.9)	9.0 (8 to 10)	0.734	0.186

MACCE: major adverse cardiac and cerebrovascular events; MI: myocardial infarction; AF: atrial fibrillation.

TABLE 4: Postoperative biomarkers.

	Bretschneider (<i>n</i> = 113)	After IPTW St. Thomas 2 (<i>n</i> = 55)	Diff	<i>p</i>
First creatinine ($\mu\text{mmol/L}$)	71.0 ± 19.8	73.8 ± 19.3	0.144	0.381
Max. creatinine ($\mu\text{mmol/L}$)	86.1 ± 27.5	89.9 ± 27.0	0.138	0.403
First CRP (mg/L)	51.1 ± 26.7	64.2 ± 28.1	0.477	0.005
Max. CRP (mg/L)	163.6 ± 68.0	145.0 ± 81.3	-0.248	0.147
First GFR (mL/min/1.7)	91.5 ± 20.1	88.9 ± 22.8	-0.120	0.479
Max. GFR (mL/min/1.7)	97.1 ± 15.8	92.7 ± 21.4	-0.237	0.173
First potassium (mmol/L)	4.4 ± 0.4	4.6 ± 0.5	0.412	0.017
Max. potassium (mmol/L)	4.6 ± 0.4	4.7 ± 0.5	0.160	0.356
First hemoglobin (g/L)	104.3 ± 16.3	104.1 ± 13.5	-0.011	0.943
Max. hemoglobin (g/L)	118.2 ± 13.9	118.6 ± 16.6	0.028	0.871
First leucocytes ($\times 10^9/\text{L}$)	14.1 ± 5.4	13.8 ± 5.8	-0.055	0.744
Max. leucocytes ($\times 10^9/\text{L}$)	15.4 ± 5.1	14.7 ± 5.1	-0.142	0.391
First sodium (mmol/L)	139.0 ± 3.5	138.6 ± 2.9	-0.124	0.441
Max. sodium (mmol/L)	141.6 ± 3.9	141.4 ± 2.2	-0.047	0.754
First hs-cTnT (ng/L)	604 (482 to 756)	512 (426 to 616)	0.317	0.052
Max. troponin hs-cTnT (ng/L)	716 (605 to 847)	561 (467 to 674)	0.350	0.047
First CK (U/L)	1186 (1042 to 1351)	1023 (837 to 1250)	0.417	0.103
Max. CK (U/L)	1370 (1222 to 1536)	1152 (972 to 1366)	0.449	0.037
First CKMB ($\mu\text{g/L}$)	36.5 (32.3 to 41.3)	31.2 (26.6 to 36.7)	0.454	0.059
Max. CKMB ($\mu\text{g/L}$)	40.0 (35.1 to 45.6)	33.4 (27.3 to 40.8)	0.400	0.295

CRP: C-reactive protein; GFR: glomerular filtration rate; hs-cTnT: high-sensitivity cardiac troponin; CK: creatine kinase; CK-MB: creatine kinase-muscle brain type.

range of lab analysis. All cardiac markers measured in blood were higher in the group of Bretschneider (Custodiol®). These results were robust after further adjustment for size of ring ($p = 0.027$) but less pronounced after adjustment for year of enrolment ($p = 0.054$).

4. Discussion

This study has shown the benefit of St. Thomas 2 cardioplegia regarding the postoperative cardiac markers in minimally invasive mitral valve repair.

The purpose of cardioplegia is to cause myocardial arrest, to support normal physiology during ischemia, and to decrease the metabolism. Bretschneider (Custodiol®) and St. Thomas 2 are appealing cardioplegic agents for minimal invasive cardiac surgery. Both are given as a single dose and offer myocardial protection for up to 2 hours. On the one hand, Bretschneider (Custodiol®) cardioplegia is an intracellular crystalloid cardioplegic solution with low concentration of calcium and sodium. On the other hand, St. Thomas 2 cardioplegia is an extracellular cardioplegic solution, which is based on potassium and magnesium. Few studies compare the effect of either Bretschneider (Custodiol®) or St. Thomas 2 with other established cardioplegic solutions, but they have never been compared directly [10–13].

This retrospective analysis focused on patients with a minimally invasive mitral valve repair via an anterolateral right thoracotomy. Patients receiving a single dose of Bretschneider (Custodiol®) were compared with patients receiving St. Thomas 2 cardioplegia regarding the postoperative cardiac markers such as hs-cTnT, CK, and CK-MB. Our primary endpoint was the hs-cTnT postoperatively, and the secondary endpoints were the CK, CK-MB, and safety outcomes. The patients' characteristics were similar in both groups.

We measured significantly lower cardiac markers postoperatively in patients receiving St. Thomas 2 cardioplegia in mitral valve repair via an anterolateral thoracotomy. Since the surgeons had the same experience, the duration of the operation, the cross-clamping time, and the perfusion time were statistically not significant. The number of perioperative defibrillation was statistically not significant, but there is a tendency in the group of St. Thomas 2, which needed fewer defibrillations ($n = 20$ (37%) as compared to Bretschneider (Custodiol®) $n = 56$ (50%); $p = 0.130$). There were no statistically significant differences in the postoperative outcomes. However, all postoperative cardiac markers were elevated in the group of Bretschneider (Custodiol®). In particular, the maximum values of hs-cTnT and CK were significantly increased compared to the group with St. Thomas 2 cardioplegia (hs-cTnT: median 716 ng/L vs. 561 ng/L; $p = 0.047$; CK: median 1370 U/L vs. 1152 U/L; $p = 0.037$).

There are some limitations in our study: First, this is a single-center observational study. The sample size is relatively small, and there is a mismatch in the number of patients in these two groups. After IPTW, 113 patients were treated with Bretschneider (Custodiol®) as cardioplegic solution versus 55 patients who were given St. Thomas 2 cardioplegic solution for myocardial protection during cardiac surgery. Second, measurement of the postoperative biomarkers was not according to a specific time. Time frame for the first postoperative hs-cTnT, CK, and CK-MB was within the first 36 hours after the cardiac surgery. The maximum values of high-sensitive troponin, creatine kinase, and creatine kinase-myocardial type were defined/measured as maximum during hospitalization. Additionally, in comparison to hs-cTnT and CK-MB, CK has a low specificity as a biomarker for myocardial damage. Concerning St. Thomas 2, it seems unusual to use it as a single shot, but we never had to reperfuse St. Thomas 2 cardioplegia due to cardiac activity while performing mitral valve repair.

5. Conclusion

It is important to understand that such a complex operation like mitral valve repair with Bretschneider (Custodiol®) or St. Thomas 2 cardioplegia should be done without having interruption or complex changes in the position of the heart. Single-dose antegrade cold Bretschneider (Custodiol®) and St. Thomas 2 in elective valve surgery are both effective in protecting the myocardium. Both cardioplegia strategies had a similar cross-clamp time. All postoperative cardiac markers were higher in the group of Bretschneider (Custodiol®) cardioplegia. In addition to that, there was a statistically significant difference in the maximum values of hs-cTnT and CK.

In summary, St. Thomas 2 cardioplegic solution was associated with significant lower levels of postoperative cardiac biomarkers compared to Bretschneider (Custodiol®) cardioplegic solution and therefore should be recommended in patients undergoing minimal invasive mitral valve repair.

Abbreviations

AF:	Atrial fibrillation
BMI:	Body mass index
CK:	Creatine kinase
CK-MB:	Creatine kinase-muscle brain type
COPD:	Chronic obstructive pulmonary disease
CRP:	C-reactive protein
ECC:	Extracorporeal circulation
EF:	Ejection fraction
GFR:	Glomerular filtration rate
hs-cTnT:	High-sensitivity cardiac troponin
ICU:	Intensive care unit
IPTW:	Inverse probability of treatment weighting
MACCE:	Major adverse cardiac and cerebrovascular events
MI:	Myocardial infarction
NYHA:	New York Heart Association.

Data Availability

The data used to support the findings of this study have not been made available because of local ethical guidelines.

Disclosure

Preliminary results were presented at the Joint Annual Meeting 2019 of the Swiss Society of Cardiology and the Swiss Society of Cardiac Surgery. Constantin Mork and Luca Koechlin should be considered co-first authors.

Conflicts of Interest

The authors declare that they have no competing interests.

Authors' Contributions

Constantin Mork and Luca Koechlin contributed equally to this manuscript.

References

- [1] H. Baumgartner, V. Falk, J. J. Bax et al., “2017 ESC/EACTS guidelines for the management of valvular heart disease,” *European Heart Journal*, vol. 38, no. 36, pp. 2739–2791, 2017.
- [2] S. W. Grant, G. L. Hickey, P. Modi, S. Hunter, E. Akowuah, and J. Zacharias, “Propensity-matched analysis of minimally invasive approach versus sternotomy for mitral valve surgery,” *Heart*, vol. 105, no. 10, pp. 783–789, 2019.
- [3] M. Schaefer, M.-M. Gebhard, and W. Gross, “The efficiency of heart protection with HTK or HTK-N depending on the type of ischemia,” *Bioelectrochemistry*, vol. 125, pp. 58–69, 2019.
- [4] G. D. Buckberg and C. L. Athanasuleas, “Cardioplegia: solutions or strategies?,” *European Journal of Cardio-Thoracic Surgery*, vol. 50, no. 5, pp. 787–791, 2016.
- [5] Z.-H. Wang, Y. An, M. C. du et al., “Clinical assessment of histidine-tryptophan-ketoglutarate solution and modified St. Thomas’ solution in pediatric cardiac surgery of tetralogy of Fallot,” *Artificial Organs*, vol. 41, no. 5, pp. 470–475, 2017.
- [6] R. Giordano, L. Arcieri, M. Cantinotti et al., “Custodiol solution and cold blood cardioplegia in arterial switch operation: retrospective analysis in a single center,” *The Thoracic and Cardiovascular Surgeon*, vol. 64, no. 1, pp. 053–058, 2016.
- [7] B. W. Hummel, R. W. Buss, P. L. DiGiorgi et al., “Myocardial protection and financial considerations of custodiol cardioplegia in minimally invasive and open valve surgery,” *Innovations: Technology and Techniques in Cardiothoracic and Vascular Surgery*, vol. 11, no. 6, pp. 420–424, 2016.
- [8] S. Mkalaluh, M. Szczechowicz, B. Dib et al., “Early and long-term results of minimally invasive mitral valve surgery through a right mini-thoracotomy approach: a retrospective propensity-score matched analysis,” *PeerJ*, vol. 6, article e4810, 2018.
- [9] S. J. Matzelle, M. J. Murphy, W. M. Weightman, N. M. Gibbs, J. J. B. Edelman, and J. Passage, “Minimally invasive mitral valve surgery using single dose antegrade custodiol cardioplegia,” *Heart Lung and Circulation*, vol. 23, no. 9, pp. 863–868, 2014.
- [10] D. J. Chambers, K. Haire, N. Morley et al., “St. Thomas’ hospital cardioplegia: enhanced protection with exogenous creatine phosphate,” *The Annals of Thoracic Surgery*, vol. 61, no. 1, pp. 67–75, 1996.
- [11] H. Bretschneider, “Myocardial protection,” *The Thoracic and Cardiovascular Surgeon*, vol. 28, no. 5, pp. 295–302, 1980.
- [12] M. Gebhard, C. Preusse, P. Schnabel, and H. Bretschneider, “Different effects of cardioplegic solution HTK during single or intermittent administration,” *The Thoracic and Cardiovascular Surgeon*, vol. 32, no. 5, pp. 271–276, 1984.
- [13] R. Gallandat Huet, G. Karliczek, J. Homan van der Heide et al., “Clinical effect of Bretschneider-HTK and St. Thomas cardioplegia on hemodynamic performance after bypass measured using an automatic datalogging database system,” *The Thoracic and Cardiovascular Surgeon*, vol. 36, no. 3, pp. 151–156, 1988.

Research Article

Post-TTM Rebound Pyrexia after Ischemia-Reperfusion Injury Results in Sterile Inflammation and Apoptosis in Cardiomyocytes

Giang Tong ¹, Nalina N. A. von Garlen,¹ Sylvia J. Wowro,¹ Phuong D. Lam,¹ Jana Krech,¹ Felix Berger,^{1,2} and Katharina R. L. Schmitt¹

¹Department of Congenital Heart Disease/Pediatric Cardiology, Universitäres Herzzentrum Berlin-Medical Heart Center of Charité and German Heart Institute Berlin, Augustenburger Platz 1, 13353 Berlin, Germany

²Department of Pediatric Cardiology, Charité-Universitätsmedizin Berlin, Corporate Member of Freie Universität Berlin, Humboldt-Universität zu Berlin and Berlin Institute of Health, Berlin, Germany

Correspondence should be addressed to Giang Tong; giang.tong@charite.de

Received 16 August 2019; Accepted 4 November 2019; Published 21 November 2019

Guest Editor: Alessio Rungtischer

Copyright © 2019 Giang Tong et al. This is an open access article distributed under the Creative Commons Attribution License, which permits unrestricted use, distribution, and reproduction in any medium, provided the original work is properly cited.

Introduction. Fever is frequently observed after acute ischemic events and is associated with poor outcome and higher mortality. Targeted temperature management (TTM) is recommended for neuroprotection in comatose cardiac arrest survivors, but pyrexia after rewarming is proven to be detrimental in clinical trials. However, the cellular mechanisms and kinetics of post-TTM rebound pyrexia remain to be elucidated. Therefore, we investigated the effects of cooling and post-TTM pyrexia on the inflammatory response and apoptosis in a cardiomyocyte ischemia-reperfusion (IR) injury model. **Methods.** HL-1 cardiomyocytes were divided into the following groups to investigate the effect of oxygen-glucose deprivation/reperfusion (OGD/R), hypothermia (33.5°C), and pyrexia (40°C): normoxia controls maintained at 37°C and warmed to 40°C, OGD/R groups maintained at 37°C and cooled to 33.5°C for 24 h with rewarming to 37°C, and OGD/R pyrexia groups further warmed from 37 to 40°C. Caspase-3 and RBM3 were assessed by Western blot and TNF- α , IL-6, IL-1 β , SOCS3, iNOS, and RBM3 transcriptions by RT-qPCR. **Results.** OGD-induced oxidative stress (iNOS) in cardiomyocytes was attenuated post-TTM by cooling. Cytokine transcriptions were suppressed by OGD, while reperfusion induced significant TNF- α transcription that was exacerbated by cooling. Significant inductions of TNF- α , IL-6, IL-1 β , and SOCS3 were observed in noncooled, but not in cooled and rewarmed, OGD/R-injured cardiomyocytes. Further warming to pyrexia induced a sterile inflammatory response in OGD/R-injured groups that was attenuated by previous cooling, but no inflammation was observed in pyrexia normoxia groups. Moreover, cytoprotective RBM3 expression was induced by cooling but suppressed by pyrexia, correlating with apoptotic caspase-3 activation. **Conclusion.** Our findings show that maintaining a period of post-TTM “therapeutic normothermia” is effective in preventing secondary apoptosis-driven myocardial cell death, thus minimizing the infarct area and further release of mediators of the innate sterile inflammatory response after acute IR injury.

1. Introduction

Therapeutic hypothermia (TH) is the standard of care for neuroprotection in selected term newborns with hypoxic-ischemic encephalopathy (HIE) and is most effective when applied at 33.5°C for 72 hours [1]. Currently, a targeted temperature management (TTM) of 32–36°C for 24–48 hours is the recommended guideline for mitigating neurological injury in comatose adults with out-of-hospital cardiac arrest [2, 3]. However, the development of fever after rewarming

from TTM, termed rebound pyrexia, has been observed in 41% of surviving patients in a multicenter cohort study [4]. They defined pyrexia as a temperature $\geq 38^\circ\text{C}$ within 24 h following rewarming from postarrest TTM, and pyrexia temperature $> 38.7^\circ\text{C}$ was associated with worse neurological outcome but not overall lower survival at discharge. Recent randomized TTM control trials even suggest that the prevention of fever or temperature variability by actively maintaining the patient’s temperature at 36°C may be just as effective for long-term neurological outcomes as applying mild TH to

approximately 33°C [5, 6]. Moreover, Rungtatscher et al. observed that postoperative hyperthermia (>37°C) after rewarming from deep hypothermic circulatory arrest was associated with increased morbidity and mortality [7]. While the adverse effects of experimentally induced fever on neuronal damage after global ischemia have been observed [8], the effects of post-TTM rebound pyrexia on ischemia-reperfusion- (IR-) injured cardiomyocytes remain to be elucidated.

Acute myocardial infarction (AMI) has been shown to result in increased expression of proinflammatory cytokines, including tumor necrosis factor- (TNF-) α , interleukin- (IL-) 6, and IL-1 β [9], that can lead to cardiac cell death and dysfunction, as well as ventricular remodeling [10]. Moreover, elevated blood concentrations of IL-6 and TNF- α have been reported as independent predictors of mortality in this cohort [11, 12]. Although the majority of proinflammatory cytokines and chemokines are derived from infiltrating monocytes/macrophages to the infarct site after AMI, they are also expressed and secreted by resident cardiac cells [13]. Cardiomyocytes make up 25% of cells in the normal heart and play an active role in mediating innate inflammatory responses, which can result in acute inflammation after IR injury [14]. Therefore, controlling cytokine release from resident cardiomyocytes is a plausible strategy for preventing further tissue damage following prolonged ischemia-reperfusion injury.

We previously demonstrated that IR injury simulated by exposure to oxygen-glucose deprivation (OGD) and subsequent reperfusion (OGD/R) resulted in reduced ATP production, leading to myocardial cell death [15]. Moreover, intra-OGD therapeutic hypothermia (IOTH) attenuated mitochondrial impairment, restored cellular metabolic activity, attenuated cardiomyocyte cell death, and induced RNA binding motif protein 3 (RBM3) expression, a cold shock protein with cytoprotective properties that is expressed in response to hypothermia and various other mild stresses [15, 16]. However, the effect of hypothermia and subsequent rewarming to normothermia or pyrexia on the sterile inflammatory response in an OGD/R cardiomyocyte injury model remains to be elucidated. Therefore, we investigated the efficacy of moderate therapeutic hypothermia (33.5°C) to attenuate the ischemia/reperfusion injury-mediated sterile inflammatory response and the adverse effects of rebound pyrexia in a murine cardiomyocyte model. Additionally, we also investigated the effect of rebound pyrexia on RBM3 expression and further myocardial cell death after an acute ischemia-reperfusion injury.

2. Materials and Methods

2.1. HL-1 Cell Culture. HL-1 cardiomyocytes are derived from the murine atrial AT-1 tumor cell lineage and were obtained from William C. Claycomb, Ph.D. (LSU Health Sciences Center, New Orleans, LA, USA). They are reported to show spontaneous contractions and a phenotype comparable to adult cardiomyocytes [17] and were cultured following the methods of Krech et al. [16]. Briefly, culture flasks and Petri dishes were precoated with 0.2 $\mu\text{g}/\text{cm}^2$ fibronectin in 0.02% gelatine for 1 h at 37°C. Cardiomyocytes were cultured at

21% O₂ and 5% CO₂ in Claycomb Medium (Sigma-Aldrich), supplemented with 10% FBS (Sigma-Aldrich), 50 $\mu\text{g}/\text{ml}$ Primocin (InvivoGen), 2 mM L-glutamine (Merck Millipore), and 0.1 mM norepinephrine (Sigma-Aldrich). Cells were passaged upon reaching 90% confluency at 1:2 to 1:5 using trypsin/EDTA (0.05/0.02%, respectively; Biochrom). HL-1 cardiomyocytes were divided into the following groups to investigate the effect of OGD/R, hypothermia (33.5°C), and pyrexia (40°C): normoxia control groups maintained at 37°C and warmed to 40°C, OGD/R groups maintained at 37°C and cooled to 33.5°C for 24 hours with subsequent rewarming to 37°C, and OGD/R pyrexia groups further warmed from 37 to 40°C.

2.2. Oxygen-Glucose Deprivation/Reperfusion (OGD/R). Ischemia-reperfusion injury was simulated *in vitro* by exposure to OGD/R, as previously established in our laboratory [16]. Briefly, HL-1 cardiomyocytes were deprived of oxygen and glucose for 6 hours in glucose/serum-free DMEM (Biochrom) at 0.2% O₂ and 5% CO₂ in a CO₂ incubator (Binder) [15]. Control groups were kept at normoxia (21% O₂) in DMEM containing glucose (Biochrom) and 10% FBS (Biochrom). After 6 h of OGD, reperfusion was simulated by restoration of nutrients in complete Claycomb Medium (Sigma-Aldrich) and 21% O₂ in all the groups. All experimental media were supplemented with 50 $\mu\text{g}/\text{ml}$ Primocin (InvivoGen) and 2 mM L-glutamine (Merck Millipore).

2.3. Targeted Temperature Management (TTM). We previously established a time-temperature protocol for intraischemic cooling (33.5°C) for the HL-1 cardiomyocytes, based on the guidelines from the European Resuscitation Council for cardiac arrest survivors (see Figure 1) [15, 18]. Briefly, normothermic OGD/R-injured groups were maintained at 37°C for the duration of the experiment, while TTM groups were cooled to 33.5°C after 3-hour exposure to OGD and maintained during simulated reperfusion for 24 hours. All experimental cooled groups were then rewarmed to and maintained at 37°C. Cooled pyrexia groups were maintained at 37°C for only 2 hours, then along with normothermic pyrexia groups further warmed to 40°C at 29 h after experimental start and maintained for an additional 24 hours. Samples were analyzed directly after OGD (6 h), 2 hours into the early reperfusion phase (8 h), the end of the cooling phase (27 h), 2 hours after rewarming to normothermia (29 h), and 2, 12, and 24 hours after initiation of pyrexia (31, 41, and 53 h after experimental start, respectively) in order to thoroughly investigate the effects of OGD/R, TTM, and pyrexia on the cardiomyocytes.

2.4. Protein Extraction and Western Blot Analysis. Caspase-3 activation and RBM3 expression were assessed by Western blot following the methods of Krech et al. [16]. Briefly, HL-1 cardiomyocytes were seeded onto 22 cm² cell culture dishes at a density of 5×10^5 cells per dish 48 h before conducting the experiments as described above. Attached cells were mechanically scratched off the plate surface and lysed using a modified RIPA buffer (50 mM Tris-HCl, pH 7.5), 150 mM sodium chloride, 1% Triton X-100, 0.1% sodium dodecyl

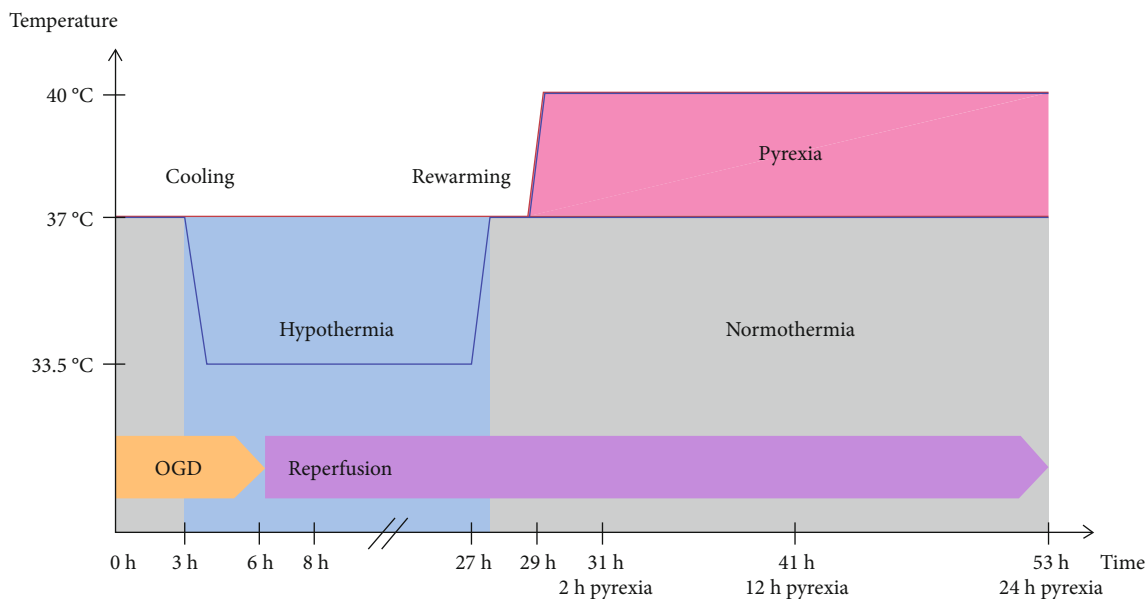


FIGURE 1: Experimental time-temperature protocol. Normothermic OGD/R-injured groups were maintained at 37°C for the duration of the experiment, while TTM groups were cooled to 33.5°C after 3-hour exposure to OGD and maintained during simulated reperfusion for 24 hours. All experimental cooled groups were then rewarmed to and maintained at 37°C. Cooled pyrexia groups were maintained at 37°C for only 2 hours and then along with normothermic pyrexia groups further warmed to 40°C at 29 h after experimental start and maintained for an additional 24 hours. Samples were analyzed directly after OGD (6 h), 2 hours into the early reperfusion phase (8 h), the end of the cooling phase (27 h), 2 hours after rewarming to normothermia (29 h), and then 2, 12, and 24 hours after initiation of pyrexia (31, 41, and 53 h after experimental start, respectively).

sulfate, 0.5% Na-deoxycholate, 2 mM ethylenediaminetetraacetic acid, 1 mM phenylmethylsulfonyl fluoride, sodium fluoride, and protease inhibitor cocktail 3 (all from Sigma-Aldrich) and quantified using a BCA-Protein Assay Kit (Pierce Biotechnology). Protein extracts (30 μ g) were electrophoresed on 15% SDS polyacrylamide gels and transferred to PVDF membranes. Membranes were blocked with 5% nonfat dried milk powder in Tris-buffered saline+0.1% Tween-20 and incubated with anti-caspase-3 (1:500) and anti-RBM3 (1:1000) or blocked with 5% BSA for incubation with anti- β -actin (1:15,000) at 4°C overnight. All primary antibodies were rabbit polyclonals purchased from Cell Signaling Technology. An HRP-conjugated donkey anti-rabbit secondary antibody (Dianova) was incubated for 1 h and detected with SuperSignal™ West Dura Chemiluminescent Substrate (Pierce Biotechnology). Densitometry quantification of the Western blots was performed using Image Lab (Bio-Rad Laboratories) and normalized to β -actin for equal protein loading.

2.5. RNA Isolation and RT-qPCR. Sterile inflammatory response was assessed by real-time quantitative PCR (RT-qPCR). Total RNA from HL-1 cardiomyocytes was isolated using the GeneMatrix Universal RNA Purification Kit (Roboklon) according to the manufacturer's instructions. RNA concentration and purity were determined by spectrophotometric measurements at 260 and 280 nm using NanoDrop 2000 (NanoDrop) and agarose gel electrophoresis. cDNA was transcribed from 1.5 μ g total RNA using a High-Capacity cDNA Reverse Transcription Kit (Applied Biosystems) using a PTC200 Thermal Cycler (MJ Research).

TABLE 1: TaqMan® Gene Expression Assays.

Gene	Assay ID
GAPDH	99999915_g1
IL-1 β	00434228_m1
IL-6	00446190_m1
iNOS	00440502_m1
RBM3	01609819_g1
SOCS3	00545913_s1
TNF- α	00443260_g1

Expression of target genes and the endogenous control glyceraldehyde 3-phosphate dehydrogenase (GAPDH) was assessed by real-time qPCR using the TaqMan® Gene Expression Assays (see Table 1) and StepOnePlus™ Real-Time PCR System (Applied Biosystems) according to the manufacturer's recommendations. Reactions with no reverse transcripts and templates were included as negative controls. Relative quantification of gene expression was normalized to the housekeeping gene GAPDH, using the $2^{-\Delta\Delta Ct}$ method, and illustrated as fold change [15].

2.6. Statistical Analysis. Data were analyzed and graphed using GraphPad Prism 5 (GraphPad Software). Results were expressed as means \pm standard deviations. Experiments were independently repeated at least three times. One-way ANOVA followed by Tukey's posttest was used for multiple group comparison, and $p < 0.05$ was considered statistically significant.

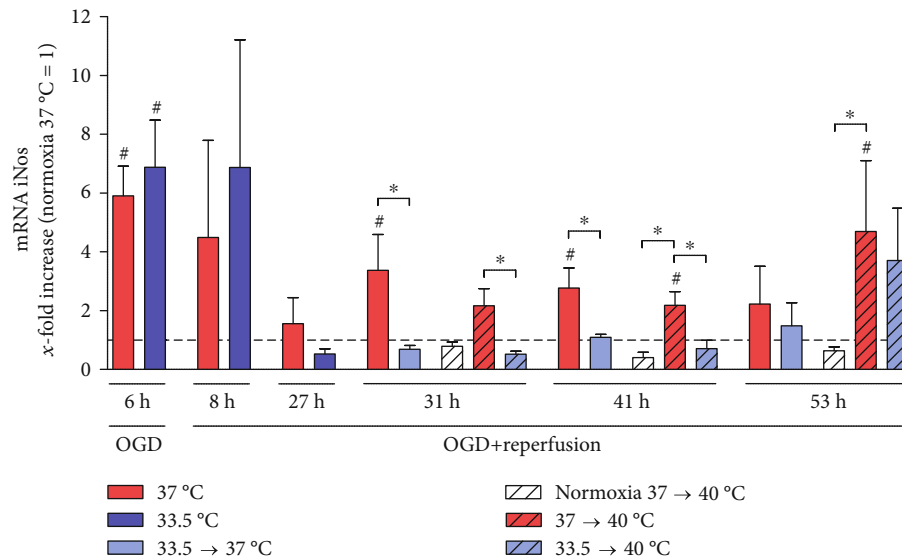


FIGURE 2: Hypothermia attenuated OGD/R- and pyrexia-induced iNOS expression in the HL-1 cardiomyocytes in the late reperfusion and pyrexia phase (31–53 h). Data from 3 to 5 independent experiments is presented as mean \pm SD. * $p \leq 0.05$ and # $p \leq 0.05$ as compared to normoxia control at 37°C (normalized to 1).

3. Results

3.1. OGD/R Induces Oxidative Stress in HL-1 Cardiomyocytes.

We investigated the effect of exposure to OGD/R, hypothermia, and pyrexia on the inducible NO synthase (iNOS) expression in the HL-1 cardiomyocytes (see Figure 2) and observed a significant increase in iNOS expression relative to normoxia control after exposure to OGD that was not attenuated by the brief period of hypothermia (6 h), but no significant increases were observed in the reperfusion phase (8–27 h). Even after posthypothermia rewarming to 37°C, iNOS transcription stayed significantly attenuated by cooling compared to noncooled OGD/R groups (29–41 h). Further warming to pyrexia also resulted in a significant increase in iNOS expression (31–53 h) that was attenuated by cooling in the early pyrexia phase (31–41 h), but not after 24 hours (53 h). Interestingly, exposure to pyrexia alone did not induce increased iNOS transcription in the undamaged control cardiomyocytes that were warmed to pyrexia.

3.2. OGD/R-Induced Sterile Inflammatory Response Is Exacerbated by Pyrexia.

We investigated the effect of hypothermia and subsequent warming to pyrexia on OGD/R-induced TNF- α (see Figure 3(a)), IL-6 (see Figure 3(b)), and IL-1 β (see Figure 3(c)) expression, as well as the negative regulator of cytokine signaling, SOCS-3 (see Figure 3(d)), in the HL-1 cardiomyocytes. A significant decrease in TNF- α transcription relative to normoxia control was observed after exposure to OGD (6 h) that was followed by a significant spike in the early reperfusion phase, which was augmented by cooling (8 h). TNF- α transcription eventually diminished to normoxia control levels in the cooled groups (27–53 h), but stayed significantly higher in the noncooled groups at the later reperfusion time points (31–41 h). Warming OGD/R-injured cardiomyocytes to pyrexia also resulted in significantly higher TNF- α transcription relative to normoxia

controls at 37°C as well as normoxia groups warmed to pyrexia (31–53 h), but not to the OGD/R-injured groups that were either maintained at or rewarmed to 37°C (31–41 h). Additionally, no significant attenuations by cooling were observed in the OGD/R-injured groups after 24-hour exposure to pyrexia (53 h).

Similar to TNF- α , IL-6 transcription was also significantly suppressed relative to normoxia control by exposure to OGD (6 h). Unlike TNF- α , IL-6 transcription did not peak in the reperfusion phase (8–29 h). A brief increase in IL-6 transcription was observed in the noncooled OGD/R group, but not in the cooled OGD/R group in the late reperfusion phase (31 h). Further warming to pyrexia resulted in the greatest increases in IL-6 transcriptions in both cooled and noncooled OGD/R groups relative to both normoxia control and OGD/R groups maintained at or rewarmed to 37°C (41 and 53 h). Even though previous cooling attenuated this increase in IL-6 after 12-hour exposure to pyrexia (41 h) in the cooled OGD/R group compared to the noncooled OGD/R group, this protective effect was no longer observed after 24-hour exposure to pyrexia (53 h). Pyrexia alone however did not induce IL-6 expression in the undamaged normoxia control cardiomyocytes.

The expression of IL-1 β was observed to be comparable to IL-6 expressions in all experimental groups during the OGD/R phase and was not significantly induced by hypothermia. However, a significantly lower IL-1 β transcription was observed in the cooled OGD/R group rewarmed to 37°C relative to the noncooled OGD/R-injured group (31 h). Moreover, warming to pyrexia resulted in a significant increase in IL-1 β transcription in the noncooled OGD/R-injured group (53 h).

Suppressor of cytokine signaling 3 (SOCS-3) gene expression was significantly decreased by OGD (6 h) relative to normoxia control, recovered to normoxia level in the reperfusion phase, and was significantly induced in the noncooled

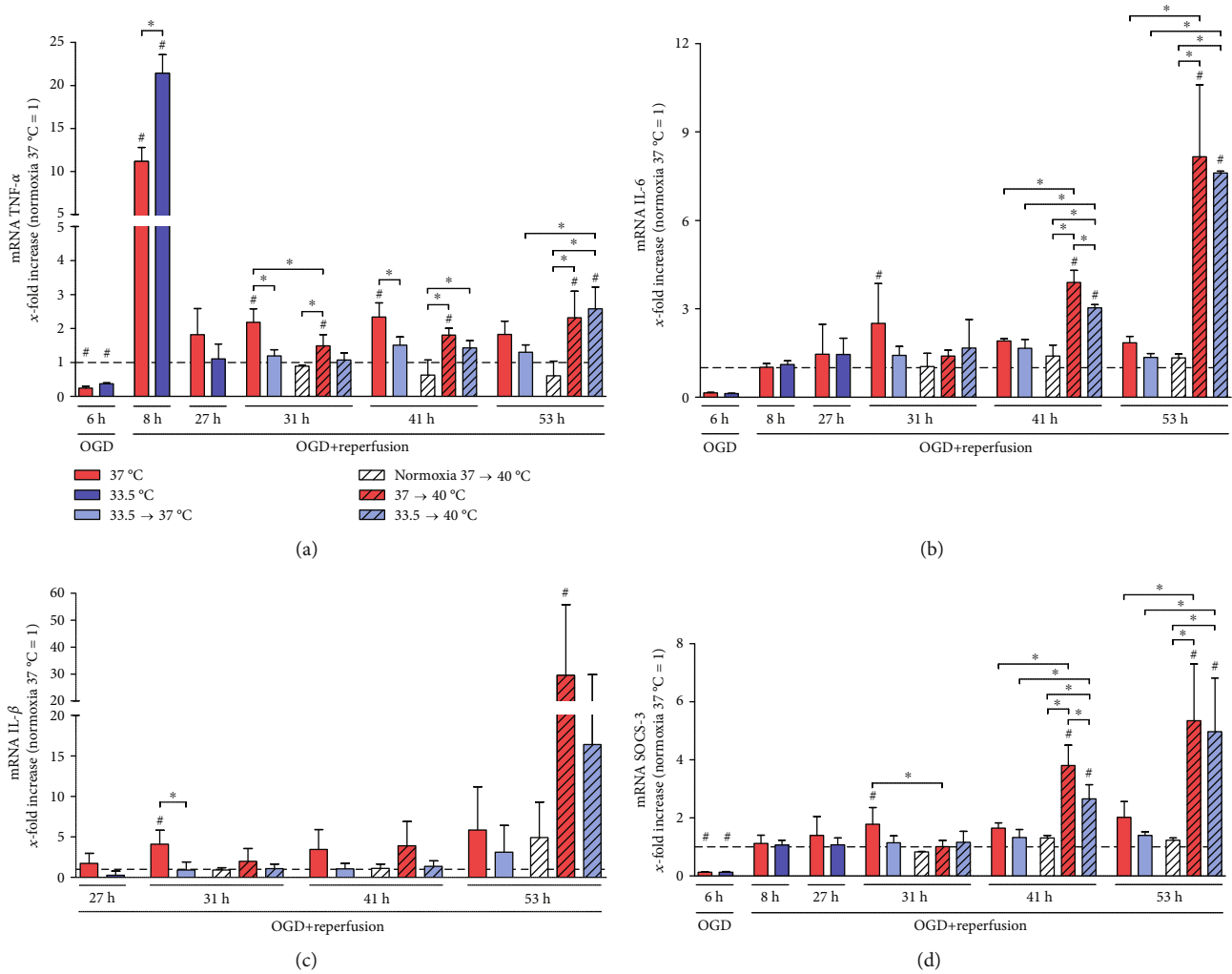


FIGURE 3: (a) TNF- α expression was suppressed by OGD (6 h). OGD/R-induced damage leads to a significant increase in TNF- α expression relative to normoxia control in the early reperfusion phase (8 h), which was significantly higher in the cooled than in the noncooled group. During late reperfusion (31 and 41 h), however, the noncooled OGD/R-injured group stayed significantly elevated, whereas the cooled group showed no such effect. Further warming to pyrexia induced TNF- α expression in OGD/R-injured groups irrespective of previous temperature management. (b) IL-6 expression was suppressed by OGD (6 h), and hypothermia temporarily attenuated pyrexia-induced IL-6 expression in OGD/R-injured cardiomyocytes (41 h). (c) Pyrexia increased IL-1 β expression in noncooled OGD/R-injured cardiomyocytes that was not attenuated by hypothermia (53 h). (d) SOCS-3 expression was significantly inhibited by OGD (6 h) and increased during late reperfusion (31 h) in the noncooled OGD/R-injured groups. Warming to pyrexia significantly induced SOCS-3 expression in both cooled and noncooled OGD/R-injured cardiomyocytes and was briefly attenuated by hypothermia (41 h). Data from 3 to 5 independent experiments is presented as mean \pm SD. * $p \leq 0.05$ and # $p \leq 0.05$ as compared to normoxia control at 37°C (normalized to 1).

OGD/R-injured group but not in the cooled groups (29 and 31 h). Rewarming to pyrexia, however, induced significant increases in SOCS-3 transcription in the OGD/R-injured cardiomyocytes compared to both normoxia control and corresponding OGD/R-injured groups maintained at or rewarmed to 37°C (41 and 53 h), which was briefly attenuated by previous cooling after 12-hour exposure to pyrexia (41 h). Interestingly, no significant increased SOCS-3 expression was observed in the undamaged normoxia control cardiomyocytes warmed to 40°C.

3.3. Cold Shock RBM3 Is Induced by Hypothermia and Suppressed by Pyrexia. Exposure to moderate hypothermia for 24 hours significantly induced both RBM3 mRNA and

protein expressions in the HL-1 cardiomyocytes (27 h) (see Figure 4). Induced RBM3 expression was observable up to 14 hours after rewarming to normothermia (37°C at 29, 31, and 41 h), 2 hours after further warming to pyrexia (31 h), and gradually returned to baseline levels after 24 hours. However, prolonged exposure to pyrexia for 24 hours resulted in a significant suppression of RBM3 expression in all groups at the mRNA and protein levels (53 h).

3.4. Pyrexia Induces Apoptosis in OGD/R-Injured Cardiomyocytes. Further warming to fever induced a secondary cell death mechanism in the cardiomyocytes exposed to OGD/R. We observed significant increases in caspase-3 activation, a hallmark of the apoptosis programmed cell death

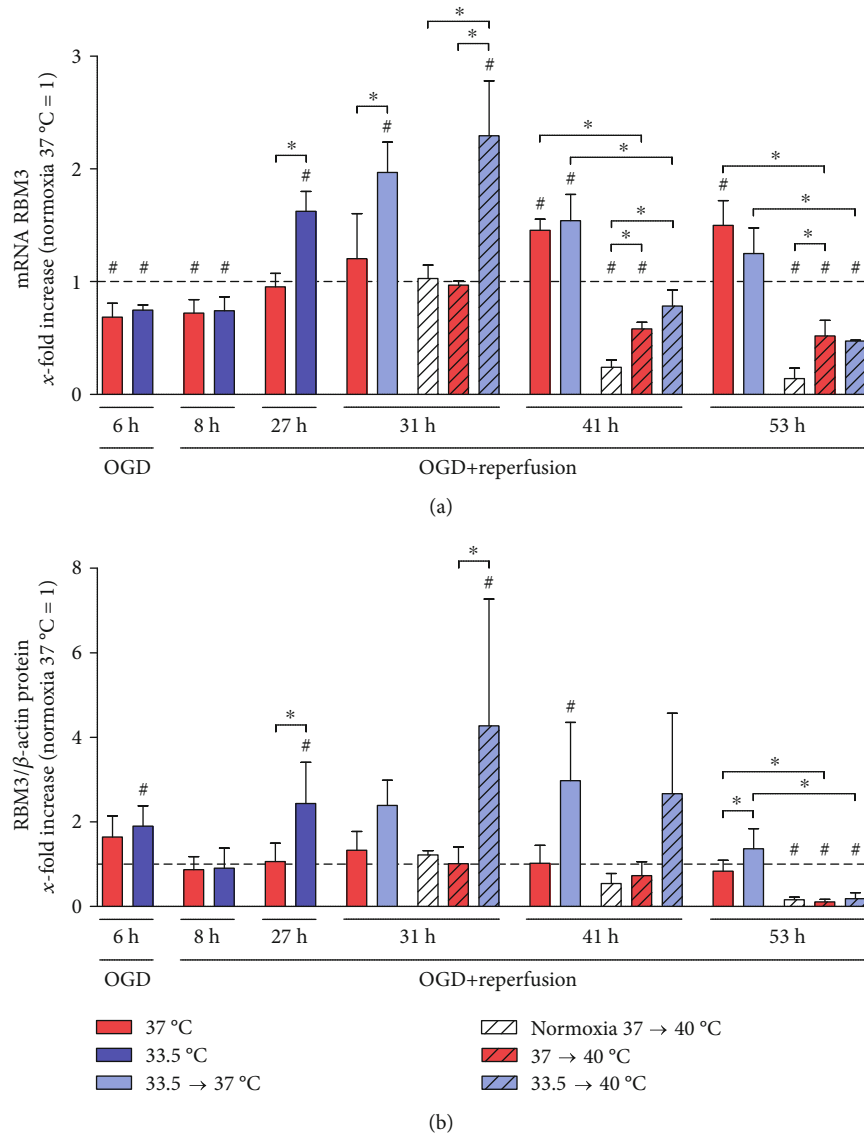


FIGURE 4: Hypothermia induces while pyrexia inhibits RBM3 (a) mRNA transcriptions and (b) intracellular protein levels in HL-1 cardiomyocytes. Data from 3 to 5 independent experiments is presented as mean \pm SD. * $p \leq 0.05$ and # $p \leq 0.05$ as compared to normoxia control at 37°C (normalized to 1).

mechanism, in OGD/R-injured cardiomyocytes after warming to pyrexia at 41 h and 53 h (see Figure 5). Previous treatment with cooling could temporarily attenuate caspase-3 cleavage at 41 h but could not maintain protection for a prolonged exposure to pyrexia (53 h). Pyrexia in noninjured cardiomyocytes also led to apoptosis (31 and 53 h), but to a significantly lesser extent than in the OGD/R-injured cells (41 and 53 h). Rewarming of the OGD/R-injured cardiomyocytes to normothermia however did not result in increased activation of caspase-3.

4. Discussion

Ischemia-reperfusion injury causes myocardial cell death by inducing intracellular calcium overload, oxidative stress, and inflammation, which can be exacerbated by pyrexia. IR induces necrotic cell death during the ischemic phase followed

by ATP-dependent apoptotic signaling cascades during the reperfusion phase, leading to an apoptosis-induced secondary cell death that can account for up to 50% of the infarct area [16]. Correspondingly, we previously observed that exposure to OGD induces mitochondrial dysfunction and cell death in the HL-1 cardiomyocytes that could be attenuated by hypothermia [15, 16]. OGD/R as well as changes in temperature can cause increased production of reactive oxygen species or free radicals, resulting in oxidative stress and terminal apoptosis and/or cell death [19]. In correlation with previous findings, we observed an increase in OGD/R-induced iNOS transcription that was also attenuated by cooling in the HL-1 cardiomyocytes, presumably due to the inhibition of nuclear factor kappa B (NF- κ B) translocation to the nucleus [20].

While necrosis is generally observed after an acute ischemic incident, apoptosis is the primary myocardial cell death mechanism following reperfusion. We did not observe

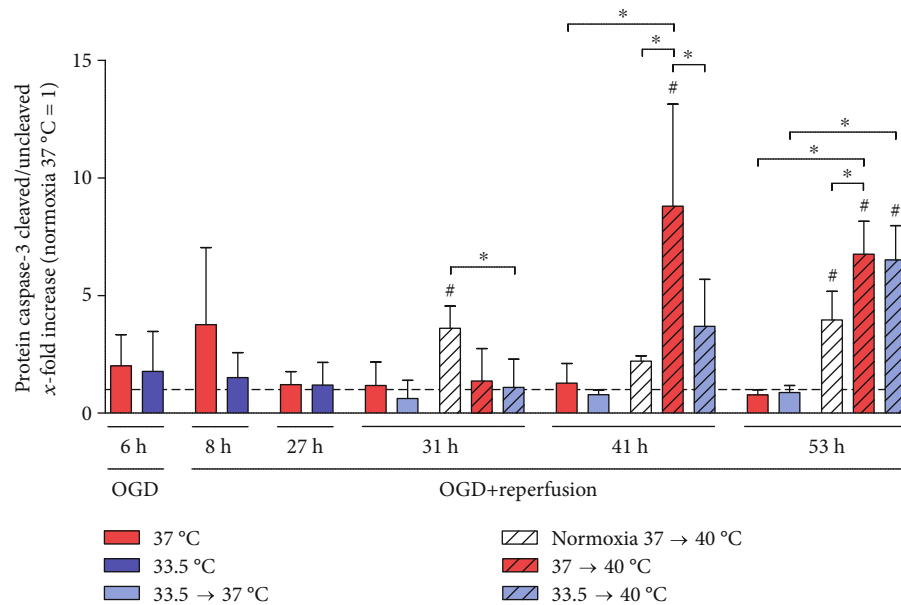


FIGURE 5: Pyrexia induces caspase-3 cleavage in the OGD/R-injured cardiomyocytes (41 and 53 h) that was briefly attenuated by hypothermia (41 h). Undamaged normoxia control cardiomyocytes warmed to pyrexia also showed increased cleavage of caspase-3 (31 and 53 h). Data from 3 to 4 independent experiments is presented as mean \pm SD. * $p \leq 0.05$ and # $p \leq 0.05$ as compared to normoxia control at 37°C (normalized to 1).

the induction of apoptosis in the reperfusion phase, but warming to pyrexia after OGD/R with or without hypothermia resulted in the induction of apoptosis, as evidenced by significant increases in the cleavage of caspase-3 (53 h). Unlike necrosis, apoptosis can have beneficial effects and be reversed by the activation of prosurvival pathways, including the Janus kinase- (JAK-) STAT signaling pathway in which cardiac-specific SOCS-3 plays a key role in promoting myocardial IR-induced injury [21]. Nagata et al. observed that induced cardiac-specific SOCS-3 expression correlated with decreased activation of prosurvival STAT3, AKT, and ERK1/2, as well as decreased expression of myeloid cell leukemia-1 (Mcl-1), a member of the antiapoptotic Bcl-2 family. Moreover, they also observed significantly reduced cleavage of caspase-3 and smaller infarct sizes in cardiac-specific SOCS-3-KO mice at 6 hours and 24 hours after reperfusion, respectively [22]. This is in correlation with our findings that pyrexia induces SOCS-3 expression, resulting in increased cleavage of caspase-3, which could be temporarily attenuated by hypothermia. We previously observed that hypothermia significantly increased the Bcl-2/Bax ratio to protect OGD/R-injured HL-1 cardiomyocytes from apoptosis [16] but did not observe any significant increases upon warming to pyrexia (data not shown). However, the expression of Mcl-1 warrants further investigation as a key STAT3 activator gene of apoptosis after myocardial IR-induced injury.

Moreover, our observation of suppressed RBM3 expression by pyrexia in the HL-1 cardiomyocytes corresponds with previous findings that showed that blood RBM3 mRNA levels were also decreased in febrile children [23]. RBM3 has been shown *in vitro* to have antiapoptotic effects in a variety of cellular stress situations, including OGD/R, staurosporine, H₂O₂, and nitric oxide (NO) treatment, by attenuating

caspase-3 activation and PARP cleavage, as well as inducing Bcl-2 expression [24–26]. Our observation of increased caspase-3 activation in conjunction with suppressed RBM3 expression by pyrexia in OGD/R-injured cardiomyocytes further supports the cytoprotective properties of RBM3 and warrants further investigation as a promising therapeutic strategy against IR injury.

The heart is normally not a key source of inflammatory cytokines and therefore is not considered an immunologically active organ [27]. However, a variety of stresses, including infection by pathogens, mechanical stretch, oxidative stress, and ischemia, can induce innate immune responses that can lead to acute inflammation, and the extent of the inflammatory response after an acute ischemic incident is a key factor that dictates the severity of damage to cardiac tissue. Moreover, IR injury induces the release of host damage-associated molecular patterns (DAMPs) into the extracellular matrix where they bind to various pattern recognition receptors (PRRs) on the surface of neighboring structural cardiac cells, such as cardiomyocytes, endothelial cells, and fibroblasts, or recruited immune cells to also activate endogenous inflammatory signaling cascades (see Figure 6). This activates various signaling transcription factors, in particular NF- κ B, to induce the expression of proinflammatory cytokines, including IL-1 β , IL-18, IL-6, and TNF- α [28].

In correlation with previous reported findings [27], we did not observe significant changes in IL-1 β transcription after exposure to OGD/R and hypothermia followed by rewarming to normothermia. However, we did observe significant increases in IL-1 β transcription after prolonged exposure to pyrexia (53 h), which could be attenuated by preceding hypothermia. Interestingly, this pyrexia-induced expression of IL-1 β correlates with the significant induction

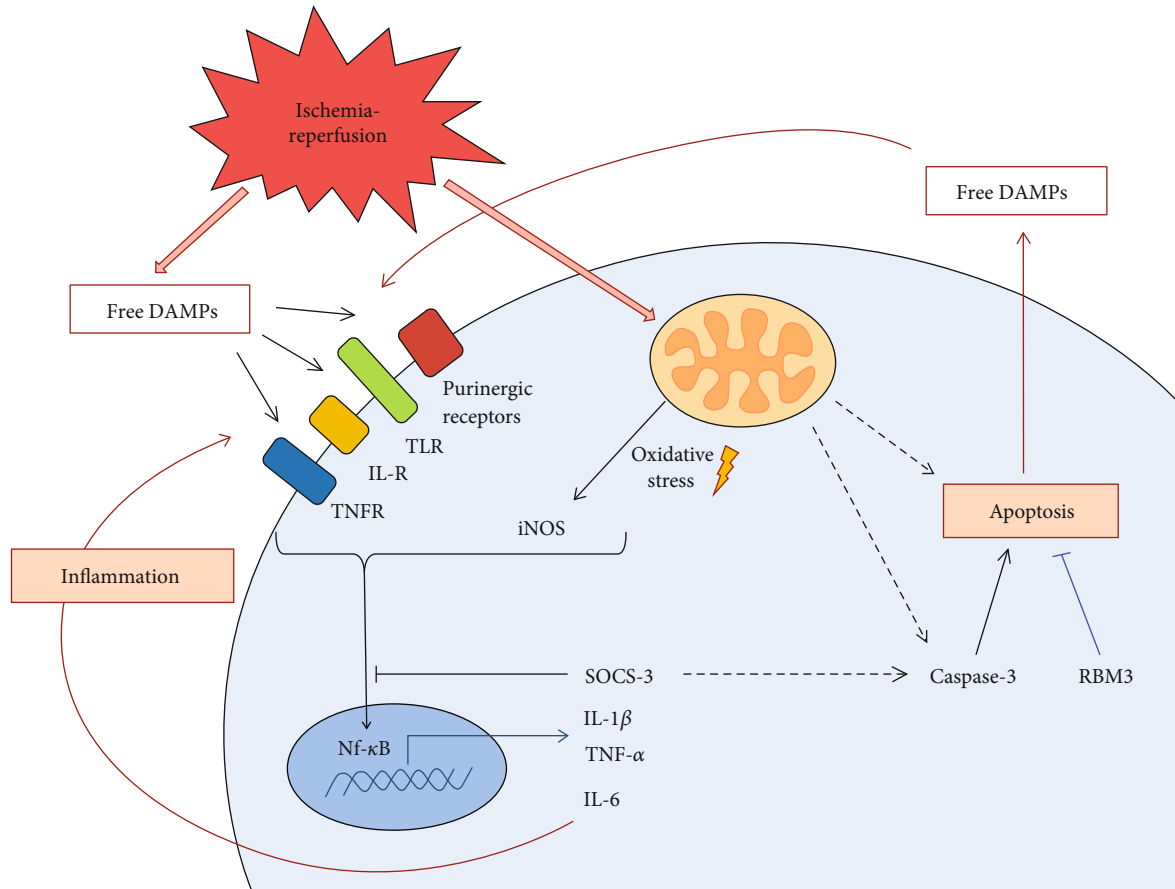


FIGURE 6: Synopsis of the sterile inflammatory response and myocardial apoptotic cell death induced by ischemia-reperfusion injury, hypothermia, and post-TTM rebound pyrexia in the HL-1 cardiomyocytes.

of IL-6 transcription observed at the same time point after warming to pyrexia. Our findings further support previous reports of increased IL-6 expression in cardiomyocytes in response to increased IL-1 β [28], which acts to recruit leukocytes and propagates inflammation in the heart [29]. We also observed a tendency towards increased MCP-1/CCL2 transcription after warming to pyrexia, though not to significance, that also plays a role in regulating leukocyte trafficking (data not shown).

IL-6 has been shown to have cardioprotective effects [29], but chronic or excessive expression of IL-6 can be fatal and has been shown to cause heart failure in a rodent model [30]. Additionally, IL-6 along with IL-1 β and TNF- α has been known to act as endogenous pyrogens, thus contributing to the induction of fever [31]. We observed that cooling effectively maintained IL-6 transcription at normoxia control levels at all investigated time points and throughout rewarming to 37°C. Therefore, attenuating IL-6 expression in cardiomyocytes may be an essential strategy to minimize the systemic inflammatory response often referred to as rebound pyrexia in hypothermia-treated cardiac arrest patients.

SOCS-3 is a member of the STAT-induced STAT inhibitor (SSI) family that functions as a negative regulator of cytokine signaling to control immune homeostasis in both physiological and pathological conditions. It therefore plays

an important role in restraining inflammation, yet allowing optimal immune response against infections. However, similar to the findings of Nagata et al., we also observed significant increases in TNF- α , IL-6, and IL-1 β transcriptions relative to normoxia control that correlated with significant increases in SOCS-3 in the OGD/R groups upon warming to pyrexia [20], whereas previously cooled OGD/R groups rewarmed to normothermia did not show this inflammatory response and even resulted in attenuated IL-1 β expression.

Limitations of our study lie in the use of a cardiomyocyte monoculture model, as our focus was to investigate the specific contribution of resident cardiomyocytes to the inflammatory response. Of course the interaction between leukocytes, cardiac fibroblasts, and resident cardiomyocytes plays an important role in the inflammatory response after IR-induced cardiac injury and warrants further investigation. Moreover, the release of cardiac-specific DAMPs from necrotic myocardial cells was not addressed in this study but is currently under investigation in a primary murine cardiomyocyte model in our lab.

5. Conclusion

Targeted temperature management is an effective therapeutic strategy for ischemia/reperfusion injury, but preventing post-

TTM rebound pyrexia is crucial to minimizing the sterile inflammatory response and subsequent cardiomyocyte apoptosis after an acute ischemia-reperfusion injury. Optimization of the TTM protocol for postcardiac arrest care is currently a topic of great research interest. Although most efforts are focused on the application of TTM, including optimal cooling temperature, rates of cooling and subsequent rewarming, practical methods of cooling that allow for adequate and consistent temperature control, and eligible patient cohort, preventing the onset of post-TTM rebound pyrexia warrants further investigation. Our findings show that maintaining a period of post-TTM normothermia, referred to as “therapeutic normothermia” by Leary et al., is effective in preventing secondary apoptosis-driven myocardial cell death, thus minimizing the infarct area and further release of various mediators of the innate sterile inflammatory response after an acute ischemia/reperfusion injury.

Abbreviations

AMI:	Acute myocardial infarction
AKT:	Protein kinase B
ATP:	Adenosine triphosphate
Bax:	Bcl-2-associated X protein
Bcl-2:	B-cell lymphoma 2
BSA:	Bovine serum albumin
DAMPs:	Damage-associated molecular patterns
EDTA:	Ethylenediaminetetraacetic acid
ERK1/2:	Extracellular signal-regulated protein kinases 1 and 2
FBA:	Fetal bovine serum
GAPDH:	Glyceraldehyde-3-phosphate dehydrogenase
HIE:	Hypoxic/ischemic encephalopathy
IL-1 β /-6/-18:	Interleukin-1 β /-6/-18
iNOS:	Inducible nitric oxide synthase
IOTH:	Intra-OGD therapeutic hypothermia
IR:	Ischemia-reperfusion
JAK-STAT:	Janus kinase/signal transducers and activators of transcription
Mcl-1:	Myeloid cell leukemia-1
MCP-1/CCL2:	Monocyte chemoattractant protein-1/CC-chemokine ligand 2
(m)RNA:	(Messenger) ribonucleic acid
NF- κ B:	Nuclear factor kappa B
NO:	Nitric oxide
OGD/R:	Oxygen-glucose deprivation/reperfusion
PARP:	Poly(ADP-ribose) polymerase 1
PRRs:	Pattern recognition receptors
PVDF:	Polyvinylidene difluoride
RBM3:	RNA binding motif 3
RIPA buffer:	Radioimmunoprecipitation assay buffer
SDS:	Sodium dodecyl sulfate
SOCS-3:	Suppressor of cytokine signaling 3
STAT3:	Signal transducer and activator of transcription 3
TH:	Therapeutic hypothermia
TNF- α :	Tumor necrosis factor-alpha
TTM:	Targeted temperature management.

Data Availability

The (experimental) data used to support the findings of this study are available from the corresponding author upon request.

Conflicts of Interest

The authors declare that they have no competing interests.

Authors' Contributions

Giang Tong and Nalina N. A. von Garlen contributed equally to the drafting of the manuscript.

Acknowledgments

We thank Nora Kuenzel for her expertise and technical assistance in experimental procedures. This study was supported by a research grant from the German Heart Research Foundation (Deutsche Stiftung für Herzforschung) (Project No. F/53/17). We acknowledge the support from the German Research Foundation (DFG) and the Open Access Publication Fund of Charité – Universitätsmedizin Berlin.




References

- [1] K. Martinello, A. R. Hart, S. Yap, S. Mitra, and N. J. Robertson, “Management and investigation of neonatal encephalopathy: 2017 update,” *Archives of Disease in Childhood - Fetal and Neonatal Edition*, vol. 102, no. 4, pp. F346–F358, 2017.
- [2] C. W. Callaway, M. W. Donnino, E. L. Fink et al., “Part 8: post-cardiac arrest care: 2015 American Heart Association guidelines update for cardiopulmonary resuscitation and emergency cardiovascular care,” *Circulation*, vol. 132, 18_Supplement_2, pp. S465–S482, 2015.
- [3] H. Kirkegaard, E. Soreide, I. de Haas et al., “Targeted temperature management for 48 vs 24 hours and neurologic outcome after out-of-hospital cardiac arrest: a randomized clinical trial,” *JAMA*, vol. 318, no. 4, pp. 341–350, 2017.
- [4] M. Leary, A. V. Grossestreuer, S. Iannacone et al., “Pyrexia and neurologic outcomes after therapeutic hypothermia for cardiac arrest,” *Resuscitation*, vol. 84, no. 8, pp. 1056–1061, 2013.
- [5] N. Nielsen, J. Wetterslev, T. Cronberg et al., “Targeted temperature management at 33°C versus 36°C after cardiac arrest,” *The New England Journal of Medicine*, vol. 369, no. 23, pp. 2197–2206, 2013.
- [6] A. Abu-Arafah, A. Rodriguez, R. L. Paterson, and P. J. D. Andrews, “Temperature variability in a modern targeted temperature management trial,” *Critical Care Medicine*, vol. 46, no. 2, pp. 223–228, 2018.
- [7] A. Rungtatscher, G. B. Luciani, D. Linardi et al., “Temperature variation after rewarming from deep hypothermic circulatory arrest is associated with survival and neurologic outcome,” *Therapeutic Hypothermia and Temperature Management*, vol. 7, no. 2, pp. 101–106, 2017.
- [8] R. C. Baena, R. Busto, W. D. Dietrich, M. Y. T. Globus, and M. D. Ginsberg, “Hyperthermia delayed by 24 hours aggravates neuronal damage in rat hippocampus following global ischemia,” *Neurology*, vol. 48, no. 3, pp. 768–773, 1997.

- [9] A. Diwan, T. Tran, A. Misra, and D. Mann, "Inflammatory mediators and the failing heart: a translational approach," *Current Molecular Medicine*, vol. 3, no. 2, pp. 161–182, 2003.
- [10] E. Mezzaroma, S. Toldo, D. Farkas et al., "The inflammasome promotes adverse cardiac remodeling following acute myocardial infarction in the mouse," *Proceedings of the National Academy of Sciences of the United States of America*, vol. 108, no. 49, pp. 19725–19730, 2011.
- [11] G. Torre-Amione, S. Kapadia, C. Benedict, H. Oral, J. B. Young, and D. L. Mann, "Proinflammatory cytokine levels in patients with depressed left ventricular ejection fraction: a report from the Studies of Left Ventricular Dysfunction (SOLVD)," *Journal of the American College of Cardiology*, vol. 27, no. 5, pp. 1201–1206, 1996.
- [12] D. Kalra, B. Bozkurt, A. Deswal, G. Torre-Amione, D. L. Mann, and D. L. Mann, "Experimental options in the treatment of heart failure: the role of cytokine antagonism," *Heart failure monitor*, vol. 1, no. 4, pp. 114–121, 2001.
- [13] K. E. Porter and N. A. Turner, "Cardiac fibroblasts: at the heart of myocardial remodeling," *Pharmacology & Therapeutics*, vol. 123, no. 2, pp. 255–278, 2009.
- [14] T. Aoyagi and T. Matsui, "The cardiomyocyte as a source of cytokines in cardiac injury," *Journal of Cell Science & Therapy*, vol. s5, 2012.
- [15] G. Tong, C. Walker, C. Bühner, F. Berger, O. Miera, and K. R. L. Schmitt, "Moderate hypothermia initiated during oxygen-glucose deprivation preserves HL-1 cardiomyocytes," *Cryobiology*, vol. 70, no. 2, pp. 101–108, 2015.
- [16] J. Krech, G. Tong, S. Wowro et al., "Moderate therapeutic hypothermia induces multimodal protective effects in oxygen-glucose deprivation/reperfusion injured cardiomyocytes," *Mitochondrion*, vol. 35, pp. 1–10, 2017.
- [17] W. C. Claycomb, N. A. Lanson Jr., B. S. Stallworth et al., "HL-1 cells: a cardiac muscle cell line that contracts and retains phenotypic characteristics of the adult cardiomyocyte," *Proceedings of the National Academy of Sciences of the United States of America*, vol. 95, no. 6, pp. 2979–2984, 1998.
- [18] J. P. Nolan and A. Cariou, "Post-resuscitation care: ERC-ESICM guidelines 2015," *Intensive Care Medicine*, vol. 41, no. 12, pp. 2204–2206, 2015.
- [19] J. K. Brunelle and N. S. Chandel, "Oxygen deprivation induced cell death: an update," *Apoptosis*, vol. 7, no. 6, pp. 475–482, 2002.
- [20] H. S. Han, Y. Qiao, M. Karabiyikoglu, R. G. Giffard, and M. A. Yenari, "Influence of mild hypothermia on inducible nitric oxide synthase expression and reactive nitrogen production in experimental stroke and inflammation," *Journal of Neuroscience*, vol. 22, no. 10, pp. 3921–3928, 2002.
- [21] B. Carow and M. E. Rottenberg, "SOCS3, a major regulator of infection and inflammation," *Frontiers in Immunology*, vol. 5, p. 58, 2014.
- [22] T. Nagata, H. Yasukawa, S. Kyogoku et al., "Cardiac-specific SOCS3 deletion prevents *in vivo* myocardial ischemia reperfusion injury through sustained activation of cardioprotective signaling molecules," *PLoS One*, vol. 10, no. 5, article e0127942, 2015.
- [23] J. J. L. Wong, A. Y. M. Au, D. Gao et al., "RBM3 regulates temperature sensitive miR-142-5p and miR-143 (thermomiRs), which target immune genes and control fever," *Nucleic Acids Research*, vol. 44, no. 6, pp. 2888–2897, 2016.
- [24] A. L. Ferry, P. W. Vanderklish, and E. E. Dupont-Versteegden, "Enhanced survival of skeletal muscle myoblasts in response to overexpression of cold shock protein RBM3," *American Journal of Physiology-Cell Physiology*, vol. 301, no. 2, pp. C392–C402, 2011.
- [25] S. Chip, A. Zelmer, O. O. Ogunshola et al., "The RNA-binding protein RBM3 is involved in hypothermia induced neuroprotection," *Neurobiology of Disease*, vol. 43, no. 2, pp. 388–396, 2011.
- [26] H. J. Yang, F. Ju, X. X. Guo et al., "RNA-binding protein RBM3 prevents NO-induced apoptosis in human neuroblastoma cells by modulating p38 signaling and miR-143," *Scientific Reports*, vol. 7, no. 1, article 41738, 2017.
- [27] S. Kapadia, Z. Dibbs, K. Kurrelmeyer et al., "The role of cytokines in the failing human heart," *Cardiology Clinics*, vol. 16, no. 4, pp. 645–656, 1998, viii.
- [28] F. Braza, S. Brouard, S. Chadban, and D. R. Goldstein, "Role of TLRs and DAMPs in allograft inflammation and transplant outcomes," *Nature Reviews Nephrology*, vol. 12, no. 5, pp. 281–290, 2016.
- [29] J. A. Fontes, N. R. Rose, and D. Čiháková, "The varying faces of IL-6: From cardiac protection to cardiac failure," *Cytokine*, vol. 74, no. 1, pp. 62–68, 2015.
- [30] T. Tanaka and T. Kishimoto, "Targeting interleukin-6: all the way to treat autoimmune and inflammatory diseases," *International Journal of Biological Sciences*, vol. 8, no. 9, pp. 1227–1236, 2012.
- [31] P. A. Mackowiak, "Concepts of fever," *Archives of Internal Medicine*, vol. 158, no. 17, pp. 1870–1881, 1998.

Research Article

Neutrophil Extracellular Trap Components Associate with Infarct Size, Ventricular Function, and Clinical Outcome in STEMI

Ragnhild Helseth ^{1,2}, Christian Shetelig,² Geir Øystein Andersen,²
Miriam Sjøstad Langseth,^{1,3,4} Shanmuganathan Limalanathan,⁵ Trine B. Opstad,^{1,4}
Harald Arnesen,^{1,4} Pavel Hoffmann ², Jan Eritsland,² and Ingebjørg Seljeflot ^{1,2,4}

¹Center for Clinical Heart Research, Oslo University Hospital Ullevål, Norway

²Department of Cardiology, Oslo University Hospital Ullevål, Norway

³Department of Internal Medicine, Drammen Hospital, Vestre Viken Hospital Trust, Norway

⁴University of Oslo, Norway

⁵The National Association for Heart and Lung Disease (LHL) Hospital, Gardermoen, Norway

Correspondence should be addressed to Ragnhild Helseth; ragnhild.helseth@gmail.com

Received 2 July 2019; Accepted 17 September 2019; Published 21 October 2019

Guest Editor: Alessio Rungtatscher

Copyright © 2019 Ragnhild Helseth et al. This is an open access article distributed under the Creative Commons Attribution License, which permits unrestricted use, distribution, and reproduction in any medium, provided the original work is properly cited.

Background. The relevance of neutrophil extracellular traps (NETs) in acute ST-elevation myocardial infarction (STEMI) is unclear. We explored the temporal profile of circulating NET markers and their associations to myocardial injury and function and to adverse clinical events in STEMI patients. **Methods and Results.** In 259 patients, blood samples were drawn before and after PCI, on day 1, and after 4 months. Double-stranded deoxyribonucleic acid (dsDNA) and myeloperoxidase-DNA (MPO-DNA) were measured in serum by a nucleic acid stain and ELISA. Cardiac magnetic resonance imaging assessed microvascular obstruction (MVO), area at risk, infarct size, myocardial salvage index, left ventricular ejection fraction (LVEF), and change in indexed left ventricular end-diastolic volume (LVEDVi). Clinical events were registered after 12 months. dsDNA and MPO-DNA levels were highest before PCI, with reduced levels thereafter (all $p \leq 0.02$). Patients with high vs. low day 1 dsDNA levels (>median; 366 ng/ml) more frequently had MVO, larger area at risk, larger infarct size acutely and after 4 months, and lower myocardial salvage index (all $p < 0.03$). Moreover, they had lower LVEF acutely and after 4 months, and larger change in LVEDVi (all $p \leq 0.014$). High day 1 dsDNA levels also associated with risk of having a large infarct size (>75th percentile) and low LVEF ($\leq 49\%$) after 4 months when adjusted for gender, time from symptoms to PCI, and infarct localization (OR 2.3 and 3.0, both $p < 0.021$), and patients with high day 1 dsDNA levels were more likely to experience an adverse clinical event, also when adjusting for peak troponin T (hazard ratio 5.1, $p = 0.012$). No such observations were encountered for MPO-DNA. **Conclusions.** High day 1 dsDNA levels after STEMI were associated with myocardial infarct size, adverse left ventricular remodeling, and clinical outcome. Although the origin of dsDNA could be discussed, these observations indicate a potential role for dsDNA in acute myocardial ischemia. This trial is registered with S-08421d, 2008/10614 (Regional Committee for Medical Research Ethics in South-East Norway (2008)).

1. Introduction

Despite today's state-of-the-art management of acute ST-elevation myocardial infarction (STEMI), including rapid revascularization with percutaneous coronary intervention (PCI) and modern antithrombotic treatment, one-year mortality still remains approximately 10% [1]. While the

inflammatory aspect of atherosclerosis and coronary artery disease (CAD) development is well established [2], data also indicate that the inflammatory response to acute myocardial ischemia affects infarct size and how the left ventricle is remodeled [3, 4]. The delicate interplay and transition from the early post-STEMI proinflammatory phase where myocardial ischemia and cell death lead to the production

of reactive oxygen species (ROS), the recruitment of immune cells, and a general proinflammatory “cytokine burst” to the subsequent reparative phase aimed at myocardial healing and scar formation, are complex and poorly understood [3, 4].

As first-line defenders against injury, circulating neutrophils infiltrate ischemic myocardium within hours of injury [3]. Neutrophils are key effectors in the early postinfarction proinflammatory phase by phagocytosing cellular debris, generating ROS, degrading extracellular matrix through neutrophil granule proteins, and chemotaxis involving monocytes [3–5]. Epidemiological data reporting that increased neutrophil count after PCI in STEMI patients associates with larger infarct size and deteriorated left ventricular function underpin the clinical importance of neutrophil actions in the early postinfarction phase [6].

Recently, it has been shown that neutrophils are able to release web-like structures comprising nuclear chromatin in the form of double-stranded deoxyribonucleic acid (dsDNA) and histones studded with neutrophil proteins into the extracellular space in a process termed NETosis [7]. Neutrophil extracellular traps (NETs) have gained attention in STEMI as they have been identified in coronary thrombi [8–10] and have prothrombotic properties including activation of platelets and the coagulation cascade [11, 12]. A certain association towards infarct size has been reported for circulating dsDNA in STEMI patients [13, 14], whereas NET burden within coronary thrombi has been shown to impact infarct size and ST-segment resolution, the latter representing an indirect measure of coronary no-reflow and ischemia reperfusion (IR) injury [8]. To what extent circulating NET markers in the acute phase of STEMI affect direct IR injury indices, as well as the post-MI left ventricular remodeling process and clinical outcome is unclear. Any contribution of NET components to myocardial injury and function or clinical outcome may pave the way for novel treatment strategies aimed at NET destruction or inhibition.

The aims of this study were, in a cohort of STEMI patients, to explore the temporal profile of the circulating NET markers dsDNA and myeloperoxidase-DNA (MPO-DNA) during the acute event and in a stable condition after 4 months. Whether the NET markers were associated with indices of myocardial injury, left ventricular function, and remodeling assessed by cardiac magnetic resonance (CMR), or with adverse clinical outcome, were further investigated. As the specificity of circulating dsDNA as a NET marker beyond a marker of cellular death can be questioned, gene expression of peptidylarginine deiminase 4 (PAD4), an assumed essential enzyme for NETosis, was also measured in circulating leukocytes in a subset of the cohort.

2. Material and Methods

This study was a substudy of the POSTEMI (Postconditioning in ST-elevation Myocardial Infarction) trial, a prospective, randomized, single-center nonblinded clinical trial aimed at investigating whether ischemic postconditioning has cardioprotective effects [15]. As previously reported, no cardioprotective effects on infarct size or other prespecified

study outcomes were observed [16]. The POSTEMI trial was approved by the Regional Committee for Medical Research Ethics in South-East Norway in 2008 (registration number S-08421d, 2008/10614), and all included patients gave written informed consent. The study conformed to the principles outlined in the Declaration of Helsinki. The supporting CONSORT (CONsolidated Standards Of Reporting Trials) checklist is provided in the Supplementary Materials. In brief, 272 patients with first-time STEMI admitted to Oslo University Hospital Ullevål within 6 hours of symptom onset were included between January 2009 and August 2012. Patients were randomized in a 1:1 fashion to ischemic postconditioning or standard care after angiographic verification of an acute coronary occlusion (Thrombolysis In Myocardial Infarction (TIMI) 0-1 flow) and successful revascularization (TIMI 2-3 flow) of the infarct-related artery (IRA). Patients with previous myocardial infarction (MI), renal failure, contraindications to CMR, clinical instability, or who were unable to give informed consent, were excluded.

2.1. Laboratory Analyses. Blood samples were drawn before and immediately after PCI, at day 1, and after 4 months. The median time from symptom onset to blood sampling before PCI was 2.8 hours, while the day 1 blood samples were drawn at a median of 18.3 hours after PCI. Serum was separated within 1 hour by centrifugation at 2500 g for 10 min and kept frozen at -80°C until analyzed for dsDNA and myeloperoxidase-deoxyribonucleic acid (MPO-DNA) in batches.

Levels of dsDNA were quantified by the fluorescent nucleic acid stain Quant-iT PicoGreen[®] (Invitrogen Ltd., Paisley, UK) and fluorometry (Fluoroskan Ascent[®] fluorometer, Thermo Fisher Scientific Oy, Vantaa, Finland). Levels of MPO-DNA were quantified by an in-house enzyme-linked immunosorbent assay (ELISA) technique [17] where plates were coated and incubated overnight with the capture antibody anti-MPO (AbD Serotec, Hercules, CA, USA) and, after blocking with bovine serum albumin (BSA), patient serum and a peroxidase-labeled anti-DNA antibody (Cell Death Detection Kit, Roche Diagnostics GmbH, Mannheim, Germany) were added. After 2 hours of incubation, a peroxidase substrate was added and absorbance was measured after 40 minutes as optical density (OD) units. The interassay CVs for dsDNA and MPO-DNA were 6.1% and 10.3%, respectively.

For gene expression of PAD4, PAXgene Blood RNA tubes collected immediately after PCI and on day 1 were used for RNA extraction from circulating leukocytes in a subset of 100 consecutively included patients. Total RNA was reversely transcribed into complementary DNA (cDNA) by the use of qScript cDNA SuperMix (Quanta BioSciences, Inc., Gaithersburg, USA), and expression of PAD4 mRNA was assessed by real-time polymerase chain reaction (RT-PCR) on the ViiA 7 Real-Time PCR System (Applied Biosystems, by Life Technologies, Foster City CA, USA) using TaqMan Universal PCR Master Mix, No AmpErase UNG, and the PAD4 TaqMan assay (Hs01057483_m1). PAD4 mRNA levels were measured as relative quantification (RQ) ($2^{-\Delta\Delta\text{Ct}}$ method) [18] with beta-2-microglobulin

(β_2M) as housekeeping gene (Assay ID Hs99999907_m1) (all Applied Biosystems).

Serial measurements of serum troponin T were performed by electrochemiluminescence technology (Elecsys 2010, Roche Diagnostics GmbH, Mannheim, Germany), and levels of N-terminal pro-B-type natriuretic peptide (NT-proBNP) were determined by an Elecsys proBNP sandwich immunoassay on an Elecsys 2010. C-reactive protein (CRP) was measured by conventional routine laboratory methods.

2.2. CMR Analyses. Details regarding the CMR protocol in the POSTEMI trial have been published previously [19]. In brief, CMR was performed at a median of 2 days after admission and repeated after 4 months. All images were taken with a 1.5T scanner (Philips Intera, release 11 or Philips Achieva, release 3.2, Philips Medical Systems, Best, The Netherlands). T2-weighted images in the short-axis plane were used for the determination of the “area at risk,” defined as myocardium with a signal intensity of >2 standard deviations above the signal intensity in remote, noninfarcted myocardium. Images with late gadolinium enhancement obtained 15 minutes after contrast injection (gadolinium-DTPA 469 mg/ml, 0.15 mmol/kg; Magnevist, Schering AG, Germany) in short-axis and 2- and 4-chamber long-axis views were used to calculate infarct size. Microvascular obstruction (MVO), defined as a dark area within the hyperintense area of infarcted myocardium, was determined in late enhancement images in the acute phase as present or not. Myocardial salvage index (%) was calculated as $[(\text{area at risk in the acute phase} - \text{infarct size after 4 months}) / \text{area at risk in the acute phase}] \times 100$. LV short-axis images were obtained for volume analyses including left ventricular ejection fraction (LVEF), indexed LV end-systolic volume (LVESVi), and indexed left ventricular end-diastolic volume (LVEDVi).

2.3. Adverse Clinical Events and Follow-Up. Adverse clinical events, defined as a composite endpoint of death, MI, unscheduled revascularisation ≥ 3 months after the index infarction, stroke, or rehospitalization for heart failure, were registered after 4 months and one year.

2.4. Statistics. Due to a skewed distribution of the NET markers, nonparametric statistics were used throughout. Correlation analyses were performed by Spearman's rho. For comparisons of NET marker levels at different time points, Friedman's test followed by Wilcoxon's signed rank test were used. For group comparisons of two or more continuous variables, the Mann-Whitney U test and the Kruskal-Wallis test were performed. Proportional data were compared using chi-square tests, including the Mantel-Haenszel test for linear-by-linear association. Logistic regression analyses were performed for dsDNA levels $>$ median on day 1 with large infarct size (defined as infarct size $>$ 75th percentile) and low LVEF ($<49\%$) as dependent variables. Covariates were entered into the multivariable models based on either clinical relevance, or an association with dsDNA levels on day 1 or the dependent variable with a p value of <0.10 . Cox's regression was used for the assessment of

dsDNA levels $>$ median on day 1 and risk of adverse clinical endpoints. Due to a modest number of endpoints and thus restriction in how many variables could be included into the model, the TIMI risk score, a composite risk score for the estimation of 1-year mortality in STEMI patients [20], was used. No correction for multiple comparisons was performed, as this was an exploratory, hypothesis-generating study. All statistical analyses were performed by IBM SPSS software version 25 (SPSS Inc., Chicago, Illinois).

3. Results

3.1. Baseline Characteristics. Baseline characteristics stratified according to below/above median dsDNA levels (median 366 ng/ml) on day 1 are shown in Table 1. Patients with high dsDNA levels on day 1 were significantly more often male and had more often anterior MIs, higher peak troponin T, and peak CRP, as well as higher creatinine levels at admission, than patients with low dsDNA levels on day 1 (Table 1). No significant differences in baseline characteristics were encountered for patients with MPO-DNA levels below/above median on day 1 (data not shown).

3.2. Temporal Profiles of NET Markers. Levels of dsDNA and MPO-DNA throughout the study period are shown in Figure 1. Both markers were highest before PCI. While dsDNA levels were significantly reduced at all subsequent time points (all $p < 0.01$), MPO-DNA levels were significantly reduced after PCI and at 4 months (Figure 1). The ischemic postconditioning procedure did not affect the NET marker levels at any time point (data not shown). The results are therefore presented for the total cohort.

The two NET markers intercorrelated moderately but significantly at all time points ($r = 0.22-0.40$, $p < 0.001$).

PAD4 mRNA levels were significantly higher after PCI compared to on day 1 (2.33 (1.54, 3.81) vs. 0.95 (0.60, 1.38), $p < 0.001$), but they did not correlate significantly to dsDNA or MPO-DNA levels neither after PCI nor on day 1, nor did PAD4 mRNA differ across NET marker quartiles (data not shown). The same pattern was observed for a change in PAD4 mRNA levels (data not shown).

3.3. Associations between NET Markers and Indices of Myocardial Infarct Size. dsDNA levels on day 1 correlated significantly to myocardial area at risk and infarct size measured in the acute phase ($r = 0.264$, $p < 0.001$ and $r = 0.298$, $p < 0.001$, respectively) and correlated inversely to myocardial salvage index and to final infarct size measured after 4 months ($r = -0.157$, $p = 0.033$ and $r = 0.139$, $p = 0.032$, respectively). Day 1 MPO-DNA levels correlated weakly to myocardial area at risk and infarct size in the acute phase ($r = 0.154$, $p = 0.032$ and $r = 0.137$, $p = 0.041$, respectively).

Based on trend analyses of quartiles of dsDNA and MPO-DNA on day 1, the median values were identified as a cut-off for low and high levels related to MVO, area at risk, infarct size, and myocardial salvage index (Supplementary Figure 2). As outlined in Figures 2(a)–2(e), patients with high dsDNA levels on day 1 had significantly more frequent MVO, larger area at risk, larger infarct size in the

TABLE 1: Baseline characteristics of the total population and according to levels of dsDNA on day 1.

	All patients (<i>n</i> = 272)	dsDNA levels (<i>n</i> = 251)		<i>p</i>
		<median	>median	
Age (years)	60 (53, 67)	60 (53, 68)	61 (53, 67)	0.934
Male gender	223 (82)	99 (77)	109 (89)	0.018
Current smoker	139 (51)	60 (47)	67 (55)	0.229
Body mass index (kg/m ²)	26.6 (24.4, 29.1)	26.8 (24.5, 29.2)	26.3 (24.3, 29.2)	0.701
Hypertension	73 (26.8)	35 (27)	35 (29)	0.844
Hypercholesterolemia	26 (9.6)	10 (8)	14 (11)	0.336
Diabetes mellitus	17 (6.3)	8 (6)	8 (7)	0.934
Time, symptoms to PCI (min)	185 (126, 265)	163 (113, 274)	198 (139, 265)	0.117
Anterior MI ¹	131 (48.2)	54 (42)	69 (56)	0.028
Peak troponin T (ng/l)	5865 (3302, 10337)	4918 (2463, 7186)	7760 (4702, 12984)	<0.001
Peak CRP (mg/l)	19 (7, 47)	12.4 (5.7, 35.5)	30.0 (11.8, 70.2)	<0.001
HbA1c (%)	6.0 (5.7, 6.2)	6.0 (5.7, 6.2)	6.0 (5.8, 6.2)	0.233
Admission creatinine (μmol/l)	70 (62, 81)	68 (60, 80)	73 (64, 84)	0.039
Admission cholesterol (mmol/l)	5.2 (4.5, 6.0)	5.2 (4.7, 6.0)	5.0 (4.3, 6.0)	0.308

Values are presented as median values with 25th and 75th percentiles or proportions (%). ≤median: dsDNA levels ≤ 366 ng/ml. >median: dsDNA levels > 367 ng/ml. CRP: C-reactive protein. HbA1c: glycosylated hemoglobin. MI: myocardial infarction. PCI: percutaneous coronary intervention. ¹Anterior vs. inferior or posterior MI.

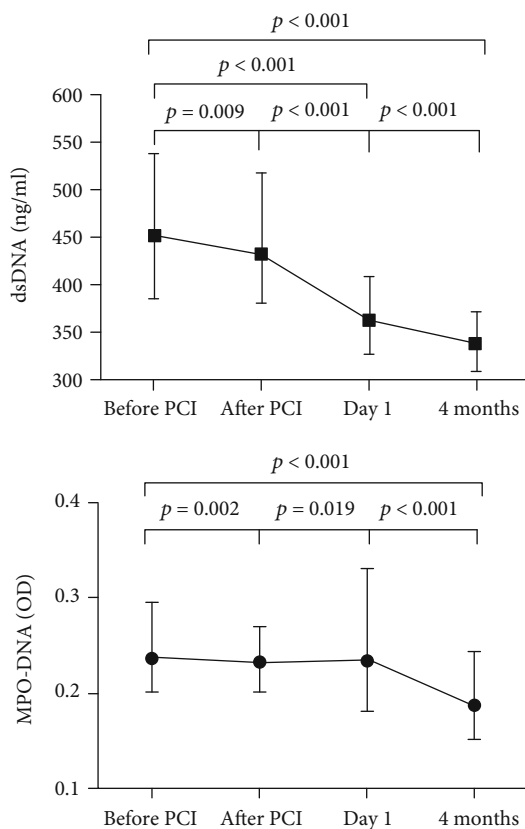


FIGURE 1: Temporal profiles of NET markers in the total population (*n* = 259 before PCI, *n* = 258 after PCI, *n* = 251/254 for dsDNA/MPO-DNA on day 1, and *n* = 258 at 4 months). Data are presented as median values with 25th and 75th percentiles. dsDNA: double-stranded deoxyribonucleic acid. MPO-DNA: myeloperoxidase-deoxyribonucleic acid. PCI: percutaneous coronary intervention. Friedman's test, Wilcoxon's signed rank test.

acute phase and after 4 months, and lower myocardial salvage index ($p \leq 0.03$ for all). No such relationships were encountered for MPO-DNA (data not shown).

In univariate regression analyses, patients with high dsDNA levels on day 1 had significantly higher risk of having a large final infarct (defined as >75th percentile) at 4-month follow-up (odds ratio (OR): 2.9; 95% confidence interval (CI): 1.5–5.4; $p = 0.001$) (Table 2). After adjustment for clinical covariates (gender, time from symptom onset to PCI, infarct localization, and ischemic postconditioning), the association remained significant (OR of 2.3, 95% CI 1.1–4.6, $p = 0.021$). After further adjustment for peak CRP and troponin T, however, the association between dsDNA and infarct size was lost (Table 2).

3.4. Associations between NET Markers and Left Ventricular Remodeling. Day 1 dsDNA levels were significantly inversely correlated to LVEF measured both in the acute phase and after 4 months ($r = -0.323$, $p < 0.001$ and $r = -0.285$, $p < 0.001$, respectively). The same pattern was observed for dsDNA measured immediately after PCI. MPO-DNA levels did not correlate with LVEF at any time point. Neither dsDNA nor MPO-DNA correlated significantly to a change in LVEDVi or LVESVi from the acute phase to 4 months.

Based on trend analyses for quartiles of dsDNA and MPO-DNA on day 1 (Supplementary Figure 3), the median was identified as a cut-off for low and high levels as related to LVEF and a change in LVEDVi at 4-month follow-up. As outlined in Figures 2(f)–2(h), patients with high levels of dsDNA on day 1 had significantly lower LVEF acutely and after 4 months, as well as a larger change in LVEDVi ($p \leq 0.014$ for all). No significant associations with LV remodeling indices were encountered for MPO-DNA beyond a larger change in LVEDVi at 4 months for low

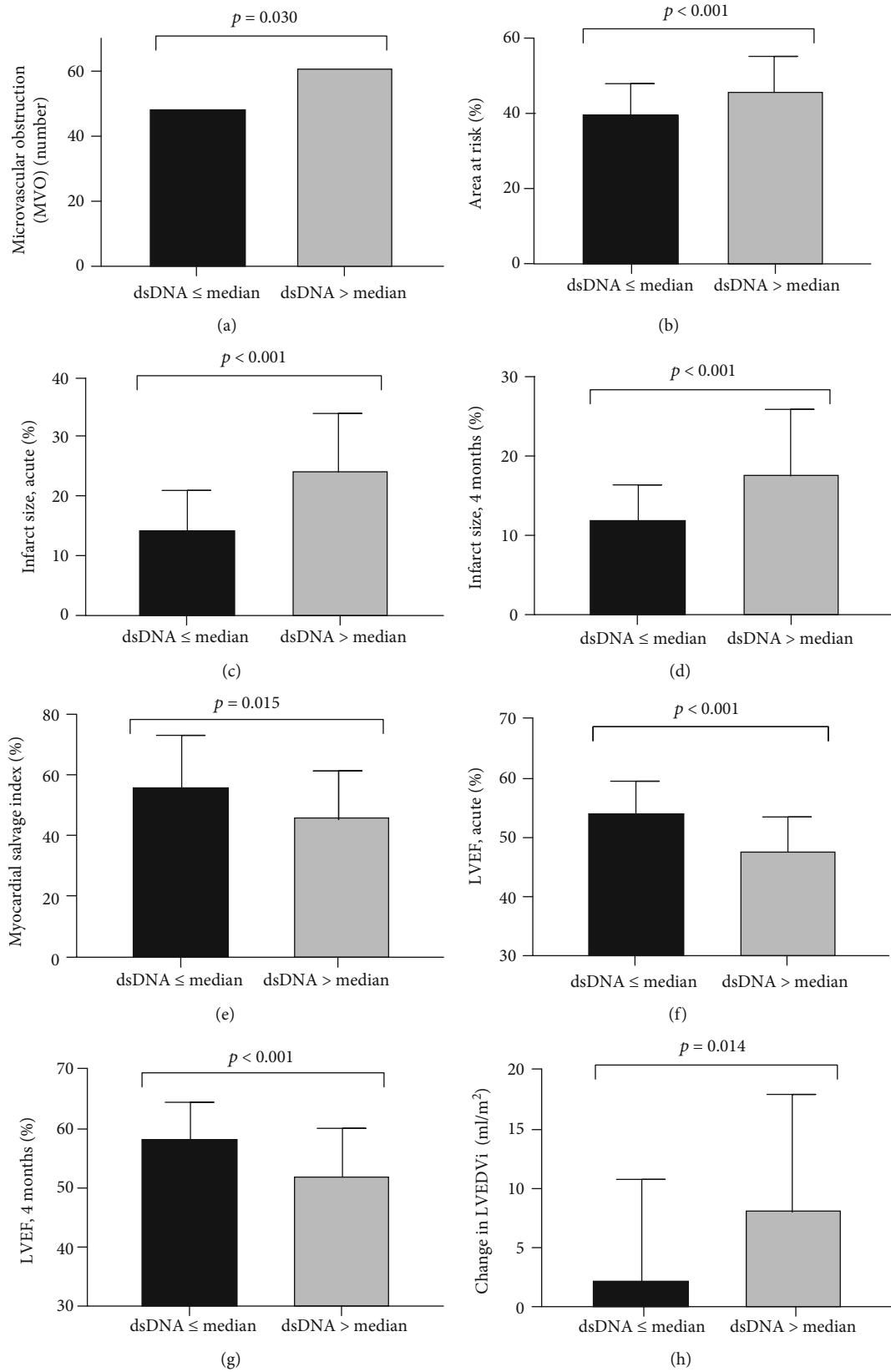


FIGURE 2: Indices of myocardial infarct size (a, b, c, d, e) and left ventricular remodeling (f, g, h) evaluated by CMR according to circulating levels of dsDNA measured on day 1. (a) $n = 218$, (b) $n = 192$, (c) $n = 219$, (d) $n = 231$, (e) $n = 185$, (f) $n = 223$, (g) $n = 232$, and (h) $n = 212$. LVEF: left ventricular ejection fraction. LVEDVi: left ventricular end-diastolic volume index. dsDNA: double-stranded deoxyribonucleic acid. dsDNA \leq median: ≤ 366 ng/ml. dsDNA $>$ median: > 367 ng/ml. Chi-square test in (a), Mann-Whitney's test in (b)–(h).

TABLE 2: Crude and multivariable adjusted odds ratio (OR) for large final infarct size.

	OR	95% CI	p value
<i>Univariate analyses</i>			
High dsDNA on day 1 ¹	2.9	1.5–5.4	0.001
Age, per year	0.99	0.96–1.02	0.400
Male gender	3.3	1.2–8.7	0.017
Time, symptoms to PCI (ln), per SD	1.2	0.9–1.6	0.275
Anterior MI	8.2	4.0–16.8	<0.001
Ischemic postconditioning	0.4	0.2–0.8	0.007
Total cholesterol (mmol/l), admission	0.94	0.72–1.23	0.668
Peak CRP (ln), per SD	3.6	2.3–5.6	<0.001
CRP after 4 months (ln), per SD	1.2	0.9–1.6	0.163
Peak troponin T (ln), per SD	21.3	9.3–48.9	<0.001
<i>Multivariable analyses</i>			
<i>Model 1</i>			
High dsDNA on day 1 ¹	2.3	1.1–4.6	0.021
Male gender	2.7	0.9–7.9	0.078
Time, symptoms to PCI (ln), per SD	1.4	0.96–1.99	0.082
Anterior MI	7.3	3.4–15.6	<0.001
Ischemic postconditioning	0.4	0.2–0.8	0.007
<i>Model 2</i>			
High dsDNA on day 1 ¹	1.4	0.6–3.1	0.458
Male gender	4.1	1.1–15.3	0.037
Time, symptoms to PCI (ln), per SD	1.4	0.9–2.2	0.095
Anterior MI	5.5	2.4–12.8	<0.001
Ischemic postconditioning	0.3	0.1–0.6	0.003
Peak CRP (ln), per SD	3.1	1.9–5.1	<0.001
<i>Model 3</i>			
High dsDNA on day 1 ¹	0.7	0.3–1.8	0.456
Male gender	1.5	0.4–6.1	0.535
Time, symptoms to PCI (ln), per SD	1.1	0.7–1.7	0.744
Anterior MI	3.1	1.3–7.7	0.014
Ischemic postconditioning	0.3	0.1–0.8	0.012
Peak troponin T (ln), per SD	16.6	6.5–42.2	<0.001

Large final infarct size is defined as >75th percentile (>22.8% of LV volume) at CMR 4 months after the STEMI. ¹>median (366 ng/ml). CI: confidence interval. CRP: C-reactive protein. dsDNA: double-stranded deoxyribonucleic acid. ln: natural logarithm. MI: myocardial infarction. PCI: percutaneous coronary intervention. SD: standard deviation.

levels of MPO-DNA on day 1 (6.1 (-1.1, 13.8) vs. 2.2 (-4.3, 12.1) ml/m², $p = 0.025$).

In univariate regression analyses, patients with high dsDNA levels on day 1 had significantly higher risk of having reduced LVEF (defined as $\leq 49\%$) at 4-month follow-up with an OR of 3.7 (95% CI 2.0–6.8, $p < 0.001$) (Table 3). After adjustment for potential covariates (gender, time from symptom onset to PCI and infarct localization), these patients were still significantly more likely to have reduced LVEF (OR 3.0, 95% CI 1.6–5.7, $p = 0.001$). After further adjustment for peak CRP and troponin T, however, the association was lost (Table 3). High dsDNA on day 1 was also significantly associated with a large change in LVEDVi (>10 ml/ml²) after

TABLE 3: Crude and multivariable adjusted odds ratio (OR) for reduced LVEF after 4 months.

	OR	95% CI	p value
<i>Univariate analyses</i>			
High dsDNA levels on day 1 ¹	3.7	2.0–6.8	<0.001
Age, per year	1.00	0.97–1.02	0.760
Male gender	3.7	1.4–9.7	0.009
Time, symptoms to PCI (ln), per SD	1.4	1.0–1.9	0.026
Anterior MI	3.6	2.0–6.5	<0.001
Ischemic postconditioning	0.9	0.5–1.5	0.641
Multivessel disease	0.9	0.5–1.6	0.667
Peak CRP (ln), per SD	3.1	2.1–4.6	<0.001
CRP after 4 months (ln), per SD	1.5	1.2–2.0	0.006
Peak troponin T (ln), per SD	10.5	5.6–20.0	<0.001
<i>Multivariable analyses</i>			
<i>Model 1</i>			
High dsDNA levels on day 1 ¹	3.0	1.6–5.7	0.001
Male gender	2.9	1.0–8.3	0.048
Time, symptoms to PCI (ln), per SD	1.5	1.1–2.1	0.022
Anterior MI	3.0	1.6–5.8	0.001
<i>Model 2</i>			
High dsDNA levels on day 1 ¹	2.1	0.99–4.33	0.052
Male gender	3.1	0.95–10.09	0.061
Time, symptoms to PCI (ln), per SD	1.5	1.0–2.2	0.042
Anterior MI	2.8	1.3–5.9	0.008
Peak CRP (ln), per SD	2.2	1.4–3.4	<0.001
CRP after 4 months (ln), per SD	1.4	0.96–1.95	0.085
<i>Model 3</i>			
High dsDNA levels on day 1 ¹	1.4	0.6–3.0	0.442
Male gender	2.2	0.6–7.2	0.212
Time, symptoms to PCI (ln), per SD	1.3	0.9–1.9	0.215
Anterior MI	1.2	0.5–2.6	0.692
Peak troponin T (ln), per SD	7.9	3.9–15.8	<0.001

Reduced LVEF is defined as LVEF $\leq 49\%$ measured by CMR 4 months after STEMI. ¹>median (366 ng/ml). CI: confidence interval. CRP: C-reactive protein. dsDNA: double-stranded deoxyribonucleic acid. ln: natural logarithm. MI: myocardial infarction. PCI: percutaneous coronary intervention. SD: standard deviation.

4 months (OR 2.1, 95% CI 1.2–3.8, $p = 0.010$), remaining statistically significant after adjustment for gender and infarct localization, but not when adjusting for peak troponin T or peak CRP (data not shown).

3.5. Associations between NET Markers and Adverse Clinical Events. During 12-month follow-up, 20 patients (7.3%) experienced an adverse clinical event. As previously outlined [21], these included 3 reinfarctions, 2 urgent revascularizations, 9 hospitalizations for heart failure, and 6 deaths.

Patients experiencing an adverse clinical event during follow-up had significantly higher dsDNA levels before PCI, immediately after PCI, and on day 1 and borderline

TABLE 4: NET marker levels according to adverse clinical events after 12-month follow-up.

	Adverse clinical event -	Adverse clinical event +	<i>p</i>
dsDNA (ng/ml)			
Before PCI	450 (385, 538)	506 (415, 745)	0.022
After PCI	433 (380, 506)	499 (387, 630)	0.037
Day 1	360 (327, 406)	402 (376, 436)	0.005
After 4 months	338 (310, 371)	349 (318, 368)	0.833
MPO-DNA (OD)			
Before PCI	0.239 (0.205, 0.294)	0.306 (0.196, 0.359)	0.210
After PCI	0.232 (0.203, 0.272)	0.225 (0.212, 0.254)	0.454
Day 1	0.230 (0.182, 0.341)	0.274 (0.189, 0.330)	0.484
After 4 months	0.195 (0.155, 0.247)	0.158 (0.140, 0.205)	0.045

Adverse clinical event is defined as a composite of death, myocardial infarction (MI), unscheduled revascularization ≥ 3 months after the index infarction, stroke, or rehospitalization for heart failure. dsDNA: double-stranded deoxyribonucleic acid. MPO-DNA: myeloperoxidase-deoxyribonucleic acid. OD: optical density units. PCI: percutaneous coronary intervention.

significantly lower MPO-DNA levels at 4-month follow-up than patients not experiencing an adverse clinical event (Table 4).

For further survival analyses, dsDNA and MPO-DNA levels were dichotomized into low and high levels with the median as the cut-off. Patients with high dsDNA levels before PCI and on day 1 were significantly more likely to experience an adverse clinical event during follow-up than patients with low dsDNA levels (before PCI log rank $p = 0.032$, Figure 3). No such association was observed for high/low MPO-DNA levels at any time point (data not shown). In Cox's regression analyses adjusted for either peak troponin T or TIMI risk score, dsDNA levels on day 1 were still associated with an increased risk of adverse clinical endpoints (hazard ratio (HR) 5.1, 95% CI 1.4–18.4, $p = 0.012$ and HR 5.2, 95% CI 1.5–18.5, $p = 0.009$, respectively) (Table 5).

4. Discussion

In this substudy of the POSTEMI trial, the main findings are as follows: (1) circulating NET markers were elevated in the acute phase of STEMI; (2) high levels of dsDNA the first day after STEMI were associated with larger myocardial infarcts and adverse left ventricular remodeling; and (3) high dsDNA levels the first day after STEMI were associated with adverse clinical outcome during 12-month follow-up, and also after adjustment for the degree of myocardial necrosis assessed by peak troponin T levels. In summary, these observations indicate that extracellular nuclear material could be involved in the post-STEMI inflammatory cascade, possibly impacting clinical outcomes.

The time profile of the NET markers with high levels in the acute phase is well in line with the results from our previous smaller study, in which dsDNA was elevated until five days after STEMI [14]. From these observations, it may be suggested that NETs are most abundant in the immediate post-STEMI proinflammatory phase. The fact that PAD4 mRNA levels were not linked to NET marker levels was somewhat surprising, but could be related to the type of

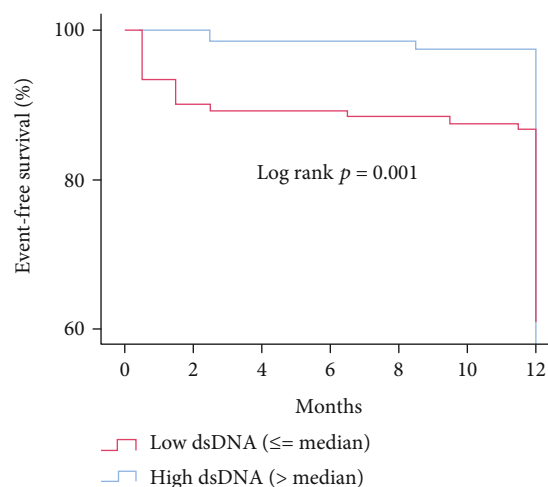


FIGURE 3: Adverse clinical events during 12-month follow-up according to dsDNA levels measured on day 1 ($n = 251$). dsDNA: double-stranded deoxyribonucleic acid. MPO-DNA: myeloperoxidase-deoxyribonucleic acid. PCI: percutaneous coronary intervention. dsDNA \leq median: ≤ 366 ng/ml. dsDNA $>$ median: > 366 ng/ml. Kaplan-Meier's survival plot.

NETosis, as the contribution of PAD4 in vital NETosis lately has been questioned [22, 23].

High dsDNA levels the first day after STEMI were associated with more frequent MVO and greater myocardial injury, the latter measured by area at risk, infarct size, and myocardial salvage index. MVO is part of the ischemia-reperfusion (IR) injury occurring immediately after reperfusion and is caused by the occlusion of coronary microvessels by atherosclerotic debris and cells including neutrophils [24]; thus, it seems likely that neutrophil-derived NETs also participate in MVO. The association between high dsDNA levels and infarct size measured by CMR is also in line with the scarce amount of comparable existing data [14]. The fact that high dsDNA levels in the acute phase of STEMI were associated with large infarcts (>75 th percentile) when adjusting for the ischemic time and infarct localization, but not peak CRP and troponin T, is worth noticing. As CRP was significantly

TABLE 5: Hazard ratios for experiencing an adverse clinical event during 12-month follow-up.

	HR	95% CI	<i>p</i>
Age, per year	0.98	0.94–1.02	0.294
Male gender	0.7	0.2–1.8	0.420
Ischemic postconditioning	0.5	0.2–1.3	0.179
Time, symptoms to PCI (ln), per SD	1.1	0.7–1.7	0.737
Peak troponin T (ln), per SD	1.7	1.0–2.8	0.037
Peak CRP (ln), per SD	3.1	1.7–5.5	<0.001
Baseline NT-proBNP (ln), per SD	1.1	0.7–1.8	0.650
TIMI risk score, per point	1.3	1.1–1.6	0.016
<i>High dsDNA before PCI</i>	2.9	1.0–8.0	0.043
Adjusted for peak troponin T	2.6	0.9–7.3	0.065
Adjusted for peak CRP	2.4	0.8–6.8	0.105
Adjusted for TIMI risk score	2.7	1.0–7.6	0.057
<i>High dsDNA on day 1</i>	5.9	1.7–20.3	0.005
Adjusted for male gender	6.7	1.9–23.2	0.003
Adjusted for peak troponin T	5.1	1.4–18.4	0.012
Adjusted for peak CRP	3.5	1.0–12.5	0.058
Adjusted for TIMI risk score	5.2	1.5–18.1	0.009

High dsDNA is defined as >median (before PCI: >452 ng/ml; day 1: >367 ng/ml). Adverse clinical event is defined as a composite of all-cause mortality, myocardial infarction, unscheduled revascularization \geq 3 months after the index infarction, rehospitalization for heart failure, or stroke. CI: confidence interval. CRP: C-reactive protein. HR: hazard ratio. PCI: percutaneous coronary intervention. SD: standard deviation. TIMI: thrombolysis in myocardial infarction.

correlated to dsDNA levels at day 1, they could both reflect the same proinflammatory milieu. Adjusting for troponin T might, however, not be justified in an explorative study like this as troponin T and infarct size are interdependent covariates. Nevertheless, the lack of association with infarct size when adjusting for troponin T renders the possibility that dsDNA measured in the peripheral circulation also reflect cardiomyocyte cell death, in addition to NETosis. The lack of correlation between PAD4 expression and NET markers in this cohort supports this. It is, however, interesting to observe that dsDNA was at its highest before revascularization (PCI), that is, prior to the usual peak of troponin T. Unfortunately, the exact time for peak troponin T was not available in this study. Whether high levels of dsDNA participate in the IR injury during revascularization, for instance through mediating MVO and thereby exacerbating cardiomyocyte cell death, troponin T release, and infarct size cannot be concluded from this observational study and warrants further investigation.

High dsDNA levels the first day after STEMI were also associated with lower LVEF and poorer left ventricular function at 4-month follow-up. The contribution of excessive or prolonged inflammation to adverse LV remodeling after STEMI is well established [3, 25], and neutrophils are suggested to play a pivotal role [5]. Experimental models have previously indicated the presence of NETs in IR-challenged myocardium based on improved LVEF in rats given a combination of tissue plasminogen activator and DNase and higher LVEF 24 hours after coronary occlusion

in PAD4^{-/-} mice compared to wild type mice [26, 27]. Reports on NET levels in association with left ventricular remodeling after STEMI in humans have, to the best of our knowledge, not been published so far. Again, the lack of significant associations to low LVEF and adverse LV remodeling by a large change in LVEDVi when adjusting for troponin T is worth noticing, but could follow the same line of reasoning as described above.

Lastly, patients with high dsDNA levels the first day after STEMI were more likely to experience an adverse clinical outcome during 12-month follow-up. This association remained statistically significant when adjusting for myocardial necrosis by troponin T, again underpinning the potential independent contribution of dsDNA beyond being a marker of cardiomyocyte necrosis. It is interesting to note that also in patients with stable CAD [28, 29], circulating NET markers have repeatedly been observed to associate with the risk of adverse clinical outcomes, suggesting that NET effects extend beyond those related to infarct size and LV remodeling after STEMI.

4.1. Limitations. The observational nature of the study impedes any causal interference. Inconsistent results for the two NET markers further hamper interpretation of the data. The moderate intercorrelations between dsDNA and MPO-DNA are, nevertheless, comparable to previous reports [14, 29], emphasizing that the structure and composition of circulating NETs, as well the optimal methods for detection, have yet to be identified. Moreover, plasma may be better than serum for the detection of NET components [30]. PAD4 expression was measured in all circulating leukocytes, complicating interpretation of these results in relation to neutrophil-specific activity. Lastly and of utmost importance, interpretation of the dsDNA findings is challenging as dsDNA could be a waste product of dying cardiomyocytes, an active effector of the neutrophil-mediated inflammatory response to myocardial damage, or actually represent both processes. Although the current study cannot dissect the origin of dsDNA, it gives rise to further embark the roles of NET-associated mediators in STEMI.

4.2. Conclusions. In this cohort of STEMI patients, high circulating day 1 dsDNA levels after PCI were associated with myocardial infarct size, more adverse left ventricular remodeling, and poor clinical outcome during 12-month follow-up. Although the origin of dsDNA could be discussed, these observations indicate a potential role for dsDNA in acute myocardial ischemia.

Data Availability

The data used to support the findings of this study are available from the corresponding author upon request.

Disclosure

Some data from the manuscript were presented as a conference abstract at the 2018 European Society of Cardiology (ESC) Congress in Munich.

Conflicts of Interest

The authors declare that there is no conflict of interest regarding the publication of this article.

Acknowledgments

The authors thank the staffs at the Section for Interventional Cardiology, the Intensive Coronary Unit, and Center for Clinical Heart Research at Oslo University Hospital Ullevål, as well as study nurses and CMR technicians for excellent support. This work was supported by Stein Erik Hagens Foundation for Clinical Heart Research, Oslo, Norway.

Supplementary Materials

CONSORT 2010 checklist. Supplementary Figure 1: study flow diagram. Supplementary Figure 2: indices of myocardial injury measured by CMR according to quartiles of dsDNA and MPO-DNA on day 1. Supplementary Figure 3: left ventricular remodeling measured by CMR according to quartiles of dsDNA and MPO-DNA on day 1. (*Supplementary Materials*)

References

- [1] B. Ibanez, S. James, S. Agewall et al., “2017 ESC guidelines for the management of acute myocardial infarction in patients presenting with ST-segment elevation: The Task Force for the management of acute myocardial infarction in patients presenting with ST-segment elevation of the European Society of Cardiology (ESC),” *European Heart Journal*, vol. 39, no. 2, pp. 119–177, 2018.
- [2] G. K. Hansson, “Inflammation, atherosclerosis, and coronary artery disease,” *New England Journal of Medicine*, vol. 352, no. 16, pp. 1685–1695, 2005.
- [3] P. C. Westman, M. J. Lipinski, D. Luger et al., “Inflammation as a driver of adverse left ventricular remodeling after acute myocardial infarction,” *Journal of the American College of Cardiology*, vol. 67, no. 17, pp. 2050–2060, 2016.
- [4] S. B. Ong, S. Hernandez-Resendiz, G. E. Crespo-Avilan et al., “Inflammation following acute myocardial infarction: multiple players, dynamic roles, and novel therapeutic opportunities,” *Pharmacology & Therapeutics*, vol. 186, pp. 73–87, 2018.
- [5] Y. Ma, A. Yabluchanskiy, and M. L. Lindsey, “Neutrophil roles in left ventricular remodeling following myocardial infarction,” *Fibrogenesis Tissue Repair*, vol. 6, no. 1, p. 11, 2013.
- [6] S. Chia, J. T. Nagurny, D. F. Brown et al., “Association of leukocyte and neutrophil counts with infarct size, left ventricular function and outcomes after percutaneous coronary intervention for ST-elevation myocardial infarction,” *The American Journal of Cardiology*, vol. 103, no. 3, pp. 333–337, 2009.
- [7] V. Brinkmann, U. Reichard, C. Goosmann et al., “Neutrophil extracellular traps kill bacteria,” *Science*, vol. 303, no. 5663, pp. 1532–1535, 2004.
- [8] A. Mangold, S. Alias, T. Scherz et al., “Coronary neutrophil extracellular trap burden and deoxyribonuclease activity in ST-elevation acute coronary syndrome are predictors of ST-segment resolution and infarct size,” *Circulation Research*, vol. 116, no. 7, pp. 1182–1192, 2015.
- [9] J. Riegger, R. A. Byrne, M. Joner et al., “Histopathological evaluation of thrombus in patients presenting with stent thrombosis. A multicenter European study: a report of the prevention of late stent thrombosis by an interdisciplinary global European effort consortium,” *European Heart Journal*, vol. 37, no. 19, pp. 1538–1549, 2016.
- [10] J. Novotny, S. Chandraratne, T. Weinberger et al., “Histological comparison of arterial thrombi in mice and men and the influence of Cl-amidine on thrombus formation,” *PLoS One*, vol. 13, no. 1, article e0190728, 2018.
- [11] T. A. Fuchs, A. Brill, D. Duerschmied et al., “Extracellular DNA traps promote thrombosis,” *Proceedings of the National Academy of Sciences*, vol. 107, no. 36, pp. 15880–15885, 2010.
- [12] B. Engelmann and S. Massberg, “Thrombosis as an intravascular effector of innate immunity,” *Nature Reviews Immunology*, vol. 13, no. 1, pp. 34–45, 2013.
- [13] A. Shimony, D. Zahger, H. Gilutz et al., “Cell free DNA detected by a novel method in acute ST-elevation myocardial infarction patients,” *Acute Cardiac Care*, vol. 12, no. 3, pp. 109–111, 2010.
- [14] R. Helseth, S. Solheim, H. Arnesen, I. Seljeflot, and T. B. Opstad, “The time course of markers of neutrophil extracellular traps in patients undergoing revascularisation for acute myocardial infarction or stable angina pectoris,” *Mediators of Inflammation*, vol. 2016, Article ID 2182358, 8 pages, 2016.
- [15] S. Limalanathan, G. Ø. Andersen, P. Hoffmann, N. E. Klow, M. Abdelnoor, and J. Eritsland, “Rationale and design of the POSTEMI (postconditioning in ST-elevation myocardial infarction) study,” *Cardiology*, vol. 116, no. 2, pp. 103–109, 2010.
- [16] S. Limalanathan, G. O. Andersen, N. E. Klow, M. Abdelnoor, P. Hoffmann, and J. Eritsland, “Effect of ischemic postconditioning on infarct size in patients with ST-elevation myocardial infarction treated by primary PCI results of the POSTEMI (POStconditioning in ST-Elevation Myocardial Infarction) randomized trial,” *Journal of the American Heart Association*, vol. 3, no. 2, article e000679, 2014.
- [17] K. Kessenbrock, M. Krumbholz, U. Schonermarck et al., “Netting neutrophils in autoimmune small-vessel vasculitis,” *Nature Medicine*, vol. 15, no. 6, pp. 623–625, 2009.
- [18] K. J. Livak and T. D. Schmittgen, “Analysis of relative gene expression data using real-time quantitative PCR and the $2^{-\Delta\Delta C_T}$ method,” *Methods*, vol. 25, no. 4, pp. 402–408, 2001.
- [19] S. Limalanathan, J. Eritsland, G. O. Andersen, N. E. Klow, M. Abdelnoor, and P. Hoffmann, “Myocardial salvage is reduced in primary PCI-treated STEMI patients with microvascular obstruction, demonstrated by early and late CMR,” *PLoS One*, vol. 8, no. 8, article e71780, 2013.
- [20] D. A. Morrow, E. M. Antman, A. Charlesworth et al., “TIMI risk score for ST-elevation myocardial infarction: a convenient, bedside, clinical score for risk assessment at presentation: an intravenous nPA for treatment of infarcting myocardium early II trial substudy,” *Circulation*, vol. 102, no. 17, pp. 2031–2037, 2000.
- [21] C. Shetelig, S. Limalanathan, P. Hoffmann et al., “Association of IL-8 with infarct size and clinical outcomes in patients with STEMI,” *Journal of the American College of Cardiology*, vol. 72, no. 2, pp. 187–198, 2018.
- [22] N. C. Rochael, A. B. Guimaraes-Costa, M. T. Nascimento et al., “Classical ROS-dependent and early/rapid ROS-independent release of neutrophil extracellular traps triggered by

- Leishmania* parasites,” *Scientific Reports*, vol. 5, no. 1, article 18302, 2015.
- [23] S. Masuda, D. Nakazawa, H. Shida et al., “NETosis markers: quest for specific, objective, and quantitative markers,” *Clinica Chimica Acta*, vol. 459, pp. 89–93, 2016.
- [24] D. M. Yellon and D. J. Hausenloy, “Myocardial reperfusion injury,” *New England Journal of Medicine*, vol. 357, no. 11, pp. 1121–1135, 2007.
- [25] N. G. Frangogiannis, “The inflammatory response in myocardial injury, repair, and remodelling,” *Nature Reviews Cardiology*, vol. 11, no. 5, pp. 255–265, 2014.
- [26] L. Ge, X. Zhou, W. J. Ji et al., “Neutrophil extracellular traps in ischemia-reperfusion injury-induced myocardial no-reflow: therapeutic potential of DNase-based reperfusion strategy,” *American Journal of Physiology-Heart and Circulatory Physiology*, vol. 308, no. 5, pp. H500–H509, 2015.
- [27] A. S. Savchenko, J. I. Borissoff, K. Martinod et al., “VWF-mediated leukocyte recruitment with chromatin decondensation by PAD4 increases myocardial ischemia/reperfusion injury in mice,” *Blood*, vol. 123, no. 1, pp. 141–148, 2014.
- [28] J. I. Borissoff, I. A. Joosen, M. O. Versteyleen et al., “Elevated levels of circulating DNA and chromatin are independently associated with severe coronary atherosclerosis and a prothrombotic state,” *Arteriosclerosis, Thrombosis, and Vascular Biology*, vol. 33, no. 8, pp. 2032–2040, 2013.
- [29] M. S. Langseth, T. B. Opstad, V. Bratseth et al., “Markers of neutrophil extracellular traps are associated with adverse clinical outcome in stable coronary artery disease,” *European Journal of Preventive Cardiology*, vol. 25, no. 7, pp. 762–769, 2018.
- [30] G. A. Ramirez, A. A. Manfredi, P. Rovere-Querini, and N. Maugeri, “Bet on NETs! Or on how to translate basic science into clinical practice,” *Frontiers in Immunology*, vol. 7, p. 417, 2016.

Research Article

Enhanced Activity by NKCC1 and Slc26a6 Mediates Acidic pH and Cl⁻ Movement after Cardioplegia-Induced Arrest of db/db Diabetic Heart

Minjeong Ji,¹ Seok In Lee,² Sang Ah Lee,³ Kuk Hui Son ², and Jeong Hee Hong ^{1,3}

¹Department of Physiology, College of Medicine, Gachon University, Lee Gil Ya Cancer and Diabetes Institute, 155 Getbeolro, Yeonsu-gu, Incheon 21999, Republic of Korea

²Department of Thoracic and Cardiovascular Surgery, Gachon University Gil Medical Center, Gachon University, Incheon 21565, Republic of Korea

³Department of Health Sciences and Technology, GAIHST, Gachon University, 155 Getbeolro, Yeonsu-gu, Incheon 21999, Republic of Korea

Correspondence should be addressed to Kuk Hui Son; dr632@gilhospital.com and Jeong Hee Hong; minicleo@gachon.ac.kr

Received 19 June 2019; Revised 26 July 2019; Accepted 13 August 2019; Published 8 September 2019

Guest Editor: Alessio Rungtatscher

Copyright © 2019 Minjeong Ji et al. This is an open access article distributed under the Creative Commons Attribution License, which permits unrestricted use, distribution, and reproduction in any medium, provided the original work is properly cited.

Diabetic heart dysfunctions during cardiac surgeries have revealed several clinical problems associated with ion imbalance. However, the mechanism of ion imbalance mediated by cardioplegia and a diabetic heart is largely unclear. We hypothesized that ion transporters might be regulated differently in the diabetic heart and that the differentially regulated ion transporters may involve in ion imbalance of the diabetic heart after cardioplegic arrest. In this study, we modified the Langendorff-free cardioplegia method and identified the involved ion transporters after cardioplegia-induced arrest between wild type and db/db heart. Enhanced expression of Na⁺-K⁺-2Cl⁻ cotransporter 1 (NKCC1) was observed in the db/db heart compared to the wild type heart. Enhanced NKCC1 activity was observed in the left ventricle of db/db mice compared to that of wild type after cardioplegia-induced arrest. The expression and activity of Slc26a6, a dominant Cl⁻/HCO₃⁻ exchanger in cardiac tissues, were enhanced in left ventricle strips of db/db mice compared to that of wild type. The Cl⁻ transporting activity in left ventricle strips of db/db mice was dramatically increased as compared to that of wild type. Interestingly, expression of Slc26a6, as well as carbonic anhydrase IV as a supportive enzyme of Slc26a6, was increased in db/db cardiac strips compared to wild type cardiac strips. Thus, the enhanced Cl⁻ transporting activity and expression by NKCC1 and Slc26a6 in db/db cardiac tissues after cardioplegia-induced arrest provide greater insight into enhanced acidosis and Cl⁻ movement-mediated db/db heart dysfunction. Thus, we suggested that enhanced Cl⁻ influx and HCO₃⁻ efflux through NKCC1 and Slc26a6 offer more acidic circumstances in the diabetic heart after cardioplegic arrest. These transporters should be considered as potential therapeutic targets to develop the next generation of cardioplegia solution for protection against ischemia-reperfusion injury in diabetic hearts.

1. Introduction

In cardiac surgeries under cardiopulmonary bypass and sporadic cardioplegia, damages may arise during intraoperative ischemia between multidose infusions of cardioplegia solutions or as a result of misdistribution of solutions distal to total coronary occlusions [1]. Additionally, potential reperfusion injuries occurred during each infusion of cardioplegia

solutions and following removal of the aortic cross-clamp [1]. However, it is well known that ischemia-reperfusion (IR) injury during cardiac surgery is associated with increased mortality and morbidity [2]. Cardioplegia solutions provide protective effects regarding the myocardial global IR injury by maintaining the pH level during the ischemia [3, 4]. However, protective effect of cardioplegia on IR injuries was restrictive. Thus, combinational challenges of cardioplegic

solutions and pharmacological agents to acquire further protective effect have been addressed [5–7].

Type 2 diabetes affects nearly four hundred million people worldwide. Between 2012 and 2030, there is a projected 69% and 20% increase in the number of adults with diabetes in developing and developed countries, respectively [1]. These patients show worse clinical outcomes following cardiac surgeries as compared with patients without diabetes [3, 8–10]. During ischemia, the accumulation of cytosolic H^+ provides a greater driving force for the Na^+-H^+ exchanger (NHE). Accumulation of intracellular Na^+ by NHE stimulates Ca^{2+} influx through the Na^+/Ca^{2+} exchanger (NCX). Subsequent accumulation of cytosolic Ca^{2+} has been associated with the pathogenesis of cardiac dysfunction [1, 11, 12]. While cardioprotective methods have improved outcomes for the past several decades, there are still clinical problems associated with diabetic heart dysfunction, such as arrhythmias, apoptosis, and heart failure [13], which results in increased ion imbalance. It is known that IR injuries or cardioplegia-induced injuries following cardiac surgery are contributed by ion channel abnormalities in myocytes; there have been no studies that focused on whether ion channels work differently following cardioplegia-induced arrest in the myocardium of diabetic patients. The proper myocardial protection with specialized cardioplegia for diabetic patients is needed to decrease morbidity after cardiac surgeries.

The abundance and diversity of ion transporters of the heart are involved in the ion homeostasis. Therefore, studies that examine ion transporter changes in a diabetic myocardium after cardioplegia-induced arrest are essential. In this study, our goal was to address the following requests. Which transporters contribute to the pH modulation after cardioplegic arrest? And is there any difference between wild type (WT) and diabetic hearts? Although the ionic properties have been well established in cardiac myocytes [14, 15], whether the activities of ion transporters are maintained in cardioplegic arrested type 2 diabetic hearts remains unknown. Thus, we hypothesized that difference of the expression level and activity of ion transporters between WT and diabetic hearts will occur and that the difference may help to understand the mechanism of a diabetic heart after cardioplegic arrest. In the present study, we evaluated the differences in ion transporter function between db/db and WT mice following cardioplegia-induced arrest.

2. Material and Methods

2.1. Animals. An experimental mouse model of high glucose type 2 diabetes mellitus (db/db, BKS.Cg-Dock7m^{+/+}Leprdb/J; male, 8 weeks of age) and normal glucose WT mice (C57BL/6, male, 8 weeks of age) was housed in the specific pathogen-free animal facility of the Lee Gil Ya Cancer and Diabetes Institute, Gachon University. The mice were housed in individually ventilated cages under controlled humidity (50%) and temperature (21.4°C). All experimental procedures for mouse maintenance and isolation of the heart from mice followed the Gachon University guidelines and were approved by the Gachon Animal

Care and Use Committee of Gachon University (ACUC, LCDI-2016-0037).

2.2. Cardioplegia Infusion. All animal experiments were performed by a single cardiac surgeon. Animals were sedated with 5% isoflurane in an anesthetic chamber. We delivered cardioplegia by modifying the Langendorff-free cardioplegia method [16]. Following sedation, sternotomy and clam shell incision were quickly performed to expose the entire thorax; dissection around the aorta was carried out for aortic clamping. The right atrial auricle was excised to prevent left heart distension during cardioplegia infusion. A 23G needle was inserted in the left ventricle (LV); the needle insertion site was the apex of LV, and it was carefully chosen to avoid injuring coronary arteries. The above procedures were carried out prior to the start of heart fibrillation. The 23G needle was connected to either the cardioplegia or Regular solution. The histidine-tryptophan-ketoglutarate (HTK) solution at 5°C (Custodiol, Chemie GMBH, Alsbach-Hähnline, Germany) was administered using a roller pump at 1 mL/min per gram heart weight. During infusion, the ascending aorta was clamped with nontoothed DeBakey forceps. During cardioplegia infusion, care was taken to ensure that no LV distension was present and that coronary arteries were properly cleared by the cardioplegia solution. All procedures and infusion volume were identical between Regular and HTK solution infusions.

2.3. Cardiac Strip Preparation. Following cardioplegia infusion, the heart was harvested, and LV separation was performed. Briefly, minced cardiac strips (~100 × 150 μm) were incubated in each HTK solution on ice. The separated LV was preserved in HTK or Regular solutions until needed for subsequent experiments. Imaging of isolated cardiac strips was completed within 1 hr. The compositions of HTK and Regular solutions are shown in Table 1. The Regular solution can be considered as HEPES-buffered physiological salt solution which consists of the same electrolyte composition like blood serum. To understand the cardioplegia delivery method and isolation of cardiac strip after harvesting the heart, we have schematically represented in Figure 1.

2.4. Analysis of $Cl^-HCO_3^-$ Exchanger (CBE) Activity of Cardiac Strips. Intracellular pH (pH_i) was measured using the 2',7'-bis-(carboxyethyl)-5-(and-6)-carboxyfluorescein (BCECF-AM, #0061, Teflabs, Austin, TX) at dual excitation wavelengths of 440 and 495 nm and an emission wavelength of 530 nm. Isolated cardiac strips on coverslips were incubated with 6 μM BCECF-AM and 0.05% Pluronic F-127 (P3000MP, Invitrogen) in the chamber for 15 min at room temperature. The strips were perfused with cardioplegia solution for at least 5 min before measuring the pH_i at 37°C. The cardioplegic resting pH level was obtained from the initial BCECF fluorescence ratio (ratio = $F_{495/440}$) of the first 60 sec of pH imaging during perfusion. The cardioplegic resting pH level was defined as the resting pH after cardioplegia-induced arrest. Slc26a6 is one of $Cl^-HCO_3^-$ exchangers (CBE) family. The CBE activity was measured in the presence of CO_2 -saturated HCO_3^- media. Measurement was initiated

TABLE 1: Composition of solutions (mM).

	Regular	0 Ca ²⁺	HTK	HCO ₃ ⁻	0 Cl ⁻ /HCO ₃ ⁻	0 Na ⁺
NaCl	140	140	15	120	—	—
KCl	5	5	9	5	—	5
MgCl	1	1	4	1	—	1
CaCl ₂	1	—	0.015	1	—	1
HEPES	20	20	—	2.5	2.5	2.5
D-Glucose	10	10	—	10	10	10
Histidine	—	—	198	—	—	—
Tryptophan	—	—	2	—	—	—
Ketoglutarate	—	—	1	—	—	—
Mannitol	38	38	30	38.4	38.4	38.4
NaHCO ₃	—	—	—	25	25	—
Na-gluconate	—	—	—	—	120	—
Ca-gluconate	—	—	—	—	0.5	—
K-gluconate	—	— </tr				

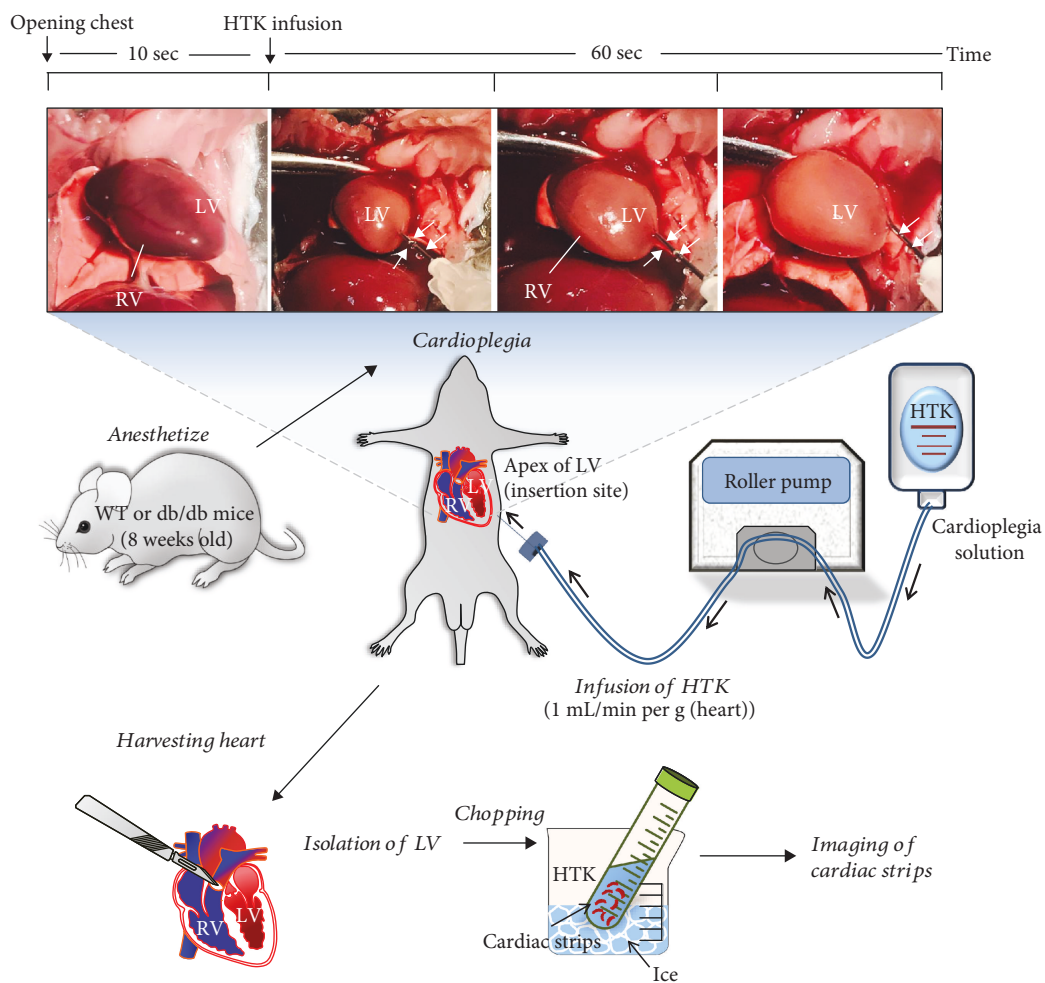


FIGURE 1: Langendorff-free cardioplegia method. Summary of the cardiac strip isolation followed by the Langendorff-free cardioplegia method. LV: left ventricle; RV: right ventricle. White arrows indicated the inserted needle for cardioplegia infusion.

by perfusing the tissues with the free $\text{Cl}^-/\text{HCO}_3^-$ media (0 $\text{Cl}^-/\text{HCO}_3^-$, Table 1). The determination of CBE activity was from the derivatives of the slopes ($\Delta\text{pH}_i/\text{sec}$) of the beginning of increase of pH_i in the free $\text{Cl}^-/\text{HCO}_3^-$ media. The emitted wavelength was monitored with a CCD camera (Photometrics) attached to a microscope (Olympus, Japan); all images were analyzed with a MetaFluor system (Molecular Devices).

2.5. Analysis of $\text{Na}^+/\text{K}^+-2\text{Cl}^-$ Cotransporter 1 (NKCC1) Activity in Cardiac Strips. NKCC1 activity was measured based on the rate of pH_i decrease, which was induced by intracellular NH_4^+ uptake [17]. Administration of 20 mM NH_4Cl in the Regular solution mediated initial alkalization by NH_3 diffusion; then, pH_i was decreased due to NH_4^+ pulse. In the second phase, the pH_i recovery rate following the NH_4^+ pulse was defined as the acidification rate ($\Delta\text{pH}_i/\text{sec}$). The initial linear acidification rate was fitted to a linear equation using the Origin software (version 8.0, OriginLab Inc.). The difference between acidification rates with or without bumetanide was used to calculate bumetanide-sensitive NKCC1 activity.

2.6. Analysis of Cl^- -Transporting Activity by MQAE in Cardiac Strips. Intracellular Cl^- was measured using N-(ethoxycarbonylmethyl)-6-methoxyquinolinium bromide (MQAE, E3101, Thermo Fisher). The increased MQAE fluorescence represents decreased Cl^- concentration, while decreased fluorescence represents increased Cl^- concentration. LV strips on the coverslip were incubated with 5 mM MQAE for 30 min at room temperature and then washed with HTK or Regular solution until reaching the stabilization of the baseline signal. The MQAE fluorescence signal was recorded for at least 3 min to obtain the baseline signal, after which the perfusion solution was switched to free $\text{Cl}^-/\text{HCO}_3^-$ media (0 $\text{Cl}^-/\text{HCO}_3^-$, Table 1). This was followed by addition of HCO_3^- solution (HCO_3^- , Table 1). The MQAE fluorescence was measured at 360 nm for excitation, and light emitted at 530 nm was collected with a CCD camera (Photometrics). The Cl^- transporting activity was determined from the derivatives of the slopes (MQAE fluorescence unit/sec) of the first 35-55 sec of fluorescence trace in free $\text{Cl}^-/\text{HCO}_3^-$ media.

2.7. Confocal Imaging of Cardiac Tissues. For immunofluorescence studies, frozen cardiac tissue sections (10 μm thick) were fixed with chilled methanol (for Slc26a6, ZO-1) or 4% paraformaldehyde (for NKCC1) for 10 min. Immunostaining was performed as previously described [18] using a 1:100 dilution of NKCC1 (ab59791, Abcam), ZO-1 (#33-9100, Thermo Fisher), and Slc26a6 (PA5-37970, Thermo Fisher) antibodies. Briefly, the bound antibodies were detected with Rhodamine (715-025-151, Jackson ImmunoResearch) and FITC (713-095-003, Jackson ImmunoResearch) (1:100 dilution). Coverslips were placed onto glass slides (Frost^{plus}, Fisher) with DAPI-included Fluoromount-GTM (Electron Microscopy Sciences, Hatfield, PA), and images were analyzed using a LSM 700 confocal microscope

through Fluo-view software (Carl Zeiss, Germany). The unstained sample was used as the negative control (NC).

2.8. Analysis of Na^+/H^+ Exchanger (NHE) Activity of Cardiac Strips. NHE activity was measured based on the recovery rate of pH_i , induced by intracellular Na^+ uptake in Regular solution as previously described [19, 20]. Briefly, after the decrease of the intracellular pH level by perfusing 20 mM NH_4Cl solution, 0 Na^+ solution was perfused. There was no recovery from acidification in 0 Na^+ solution. And then, the intracellular pH_i was recovered by Na^+ -containing Regular solution, and the recovery rate was defined as NHE activity by measuring from the derivatives of the slopes of the first 35-55 sec of pH_i recovery trace.

2.9. Measurement of Serum Glucose Concentration. Mice were anesthetized with isoflurane ($\approx 3\%$ in air) by inhalation. The chest was opened to fully expose the heart, and blood was collected using 25G needle (Kovax-syringe 1 mL, Republic of Korea) from the heart. And then, collected blood was centrifuged for 15 min at 1,500 rpm. Then, the supernatant was collected, and the serum glucose level was measured using a blood glucose meter (Green Cross Mark, Republic of Korea).

2.10. Western Blotting. Cardiac tissues were isolated from mice and stimulated with the indicated cardioplegia solutions for 1 hr. Lysates of cardiac tissue homogenates were obtained with lysis buffer (containing (mM) 150 NaCl, 20 Tris, 2 EDTA, 1% Triton X-100, and a protease inhibitor mixture) and were treated as previously described [18]. 30 μg denatured protein samples was subjected to SDS-PAGE. Proteins were visualized with NKCC1 (ab59191, Abcam), phosphoNKCC1 (#ABS1004, Millipore), Slc26a6 (ab172684, Abcam), CA IV (sc-74527, Santa Cruz Biotechnology), GAPDH (MA5-15738, Thermo Fisher), NHE1 (NBP1-76847, Novusbio), and β -actin (A3854, Sigma) antibodies using the enhanced luminescence (ECL) solution (Thermo Scientific). The intensity of protein band was normalized with that of β -actin as a protein loading control.

2.11. Isolation of Single Cardiac Myocytes for Di-8-ANEPPS Staining. Cardiac myocyte isolation was performed according to a previously generated protocol [16]. The LV from 8-week-old mice was injected with EDTA buffer containing (mM) 130 NaCl, 5 KCl, 0.5 Na_2PO_4 , 10 HEPES, 10 Taurine, 10 glucose, 10 (2,3)-butanedione monoxime (BDM, Sigma Aldrich, B0753), and 5 EDTA. The heart was removed, and 10 mL EDTA buffer was injected into the left ventricle. Perfusion buffer (3 mL) was injected into LV containing (mM) 130 NaCl, 5 KCl, 0.5 Na_2PO_4 , 10 HEPES, 10 Taurine, 10 glucose, 10 BDM, and 1 MgCl_2 . Collagenase buffer (30 mL) containing 0.5 mg/mL Collagenase type II (17101515, Thermo Scientific) and 0.05 mg/mL protease XIV (P5147, Sigma Aldrich) was injected into the LV until the heart is transparent and soft. Tissues were gently teased into 1 mm^3 pieces and were transferred into 50 mL conical tubes. Stop buffer containing the perfusion buffer with 5% FBS was then added to cell suspension. Suspension was filtered with a 100 μm strainer and was centrifuged for 3 min at 300 \times g. The supernatant was removed to isolate the cell pellet containing

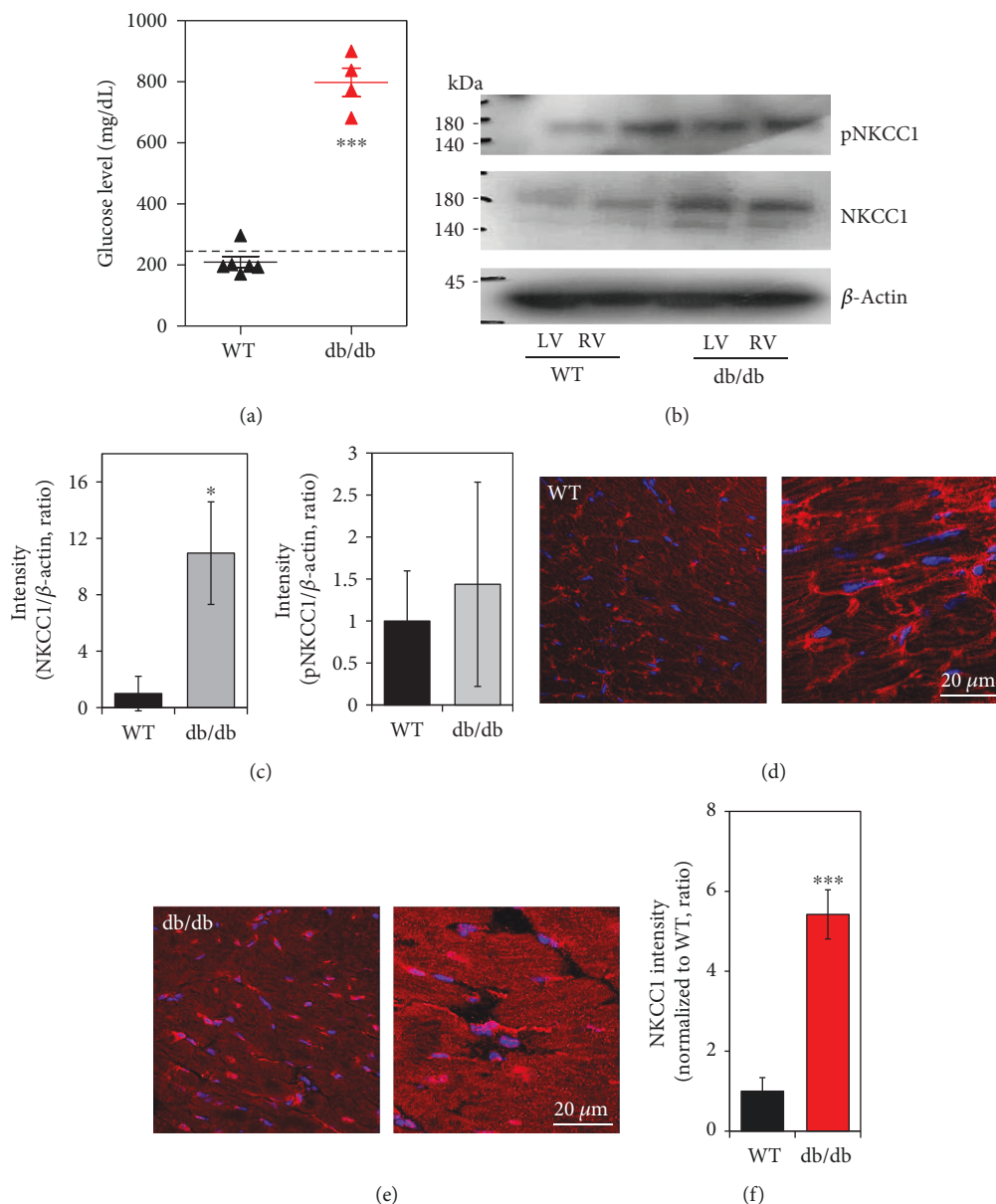


FIGURE 2: Enhanced NKCC1 protein in db/db cardiac tissues. (a) Serum glucose concentration in the WT ($n = 6$) and db/db ($n = 4$) mice (** $P < 0.001$). Dotted line represents glucose 250 mg/dL. (b) Expression of phosphoNKCC1 (pNKCC1) and NKCC1 protein level in LV and RV cardiac strips of WT and db/db mice following cardioplegia-induced arrest. The β -actin was used as the loading control. (c) Analysis of band intensity of NKCC1 and pNKCC1 in LV. The bars show the mean \pm SEM ($n = 3$, * $P < 0.05$). Immunolocalization of NKCC1 (red) and DAPI (blue) in LV of WT (d) and db/db mice (e). Right images of (d, e) are magnified. The scale bars represent 20 μ m. (f) Analysis of intensity of NKCC1 between WT and db/db LVs. The bars show the mean \pm SEM ($n = 5$, *** $P < 0.001$).

cardiac myocytes. To determine the T-tubule structure, 3 μ L of 10 mM di-8-ANEPPS (19541, Cayman, Ann Arbor, MI) and 2.5 μ L of 20% Pluronic F-127 were mixed. The freshly isolated cardiac myocytes were transferred to poly-L-lysine-coated cover slips and were incubated with mixed di-8-ANEPPS dye at 4°C (10 min). After staining, the mixed dye was washed with DMEM prior to confocal imaging.

2.12. Intracellular pH Calibration. Ratios of BCECF-AM (Teflabs) were converted to pH unit as described previously [21, 22]. Briefly, cardiac strips were incubated in the

calibration solution (pH 5.5, 6.0, 6.5, 7.0, 7.5, 8.0, and 8.5) for 5 min at room temperature. The equation of the pH calibration curve was $\text{pH} = \text{pKa} + \log \left(\frac{R_{\text{max}} - R}{R - R_{\text{min}}} \right)$ (R : ratio value of BCECF; R_{max} : maximum ratio; R_{min} : minimum ratio; pKa value of BCECF: 6.97). The BCECF fluorescence ratio was converted to the changes in the pH_i (ΔpH_i) value, followed by the calibration curve.

2.13. DNA Transfection. Human SLC26A6 and human CA IV were developed in pCMV6-AC-mKate vectors; the original clones were provided by Dr. Shmuel Muallem (National

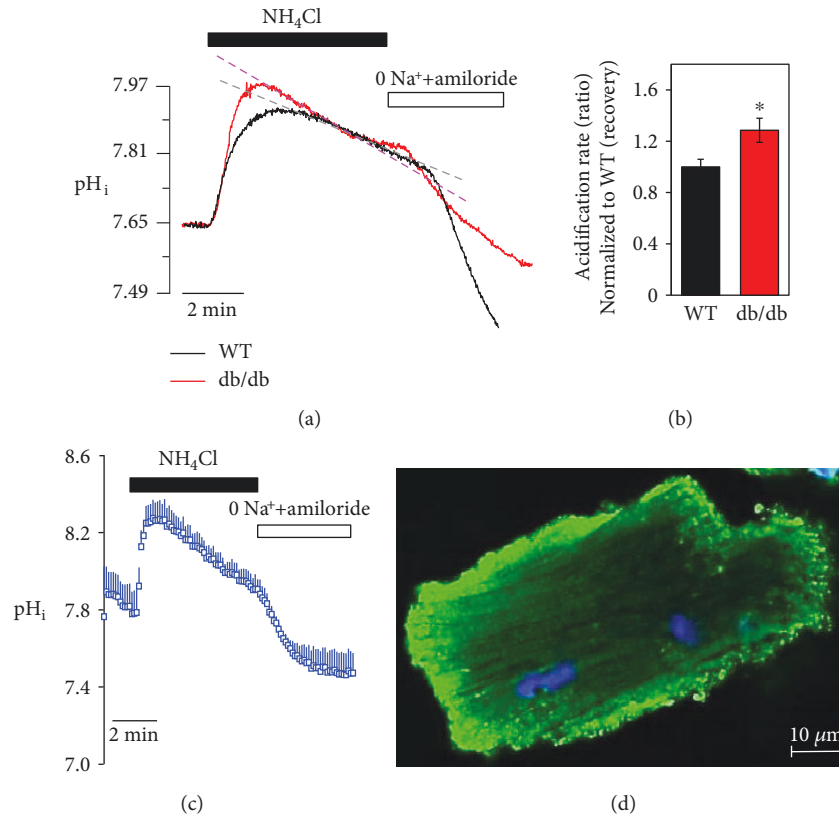


FIGURE 3: Enhanced NKCC1 activity in LV of db/db cardiac strips after HTK-induced arrest. (a) Changes in pH_i by NH_4Cl pulse technique between WT and db/db cardiac strips. (b) Analysis of the acidification rate between HTK-arrested cardiac strips between WT and db/db ($n = 5$, $*P < 0.05$). (c) Changes in pH_i by NH_4Cl pulse technique in isolated cardiac myocyte. (d) Image of ANEPPS staining (green) of isolated cardiac myocyte. The scale bar represents $10 \mu m$.

Institutes of Health, Bethesda). Plasmid DNA transfection by Lipofectamine 2000 followed the manufacturer's protocol (11668019, Invitrogen) and was previously described [23].

2.14. Statistical Analysis. Results are expressed as the mean \pm standard error of the mean (SEM). Significance was statistically determined by the analysis of variance in each experiment ($*P < 0.05$, $**P < 0.01$, and $***P < 0.001$). Statistical differences between the mean values from the two sample groups were analyzed using Student's *t*-tests.

3. Results

3.1. Enhanced NKCC1 Protein in db/db Cardiac Tissues. We first determined the diabetic mouse model with a high glucose level. The db/db mice provide a type 2 diabetes mouse model [24–26], and we confirmed the higher glucose level of db/db mouse serum (Figure 2(a)). We speculated that the $[Na^+]_i$ alteration by the NKCC1 cotransporter in the diabetic myocardium is higher than that in the normal myocardium, which may result in myocardial injury after cardioplegia-induced arrest. We measured differences in NKCC1 protein expression between wild type and db/db cardiac tissues. Enhanced NKCC1 protein expression was observed in $LV^{db/db}$, whereas no difference in expression of phosphorylated NKCC1 (pNKCC1) protein was detected between wild type and db/db

cardiac strips, and total NKCC1 protein was increased in db/db (Figures 2(b) and 2(c)). Next, we also examined expression of NKCC1 proteins in cardiac tissues with immunostaining. As shown in Figures 2(d)–2(f), NKCC1 expression was enhanced in db/db compared to wild type cardiac tissue.

3.2. Enhanced NKCC1 Activity in LV of db/db Cardiac Strips after HTK-Induced Arrest. NKCC activity in cardiac tissue strips was examined with 20 mM NH_4Cl pulse technique and determined via sensitivity to bumetanide, a selective NKCC1 inhibitor. Interestingly, cardioplegic arrest by HTK preserved the acidification property, not the initial alkalization, mediated by the NH_4^+ pulse (data not shown). Thus, we determined the recovery state of NH_4^+ pulse technique (Regular solution perfusion followed by HTK arrest for 1 min) to mimic the reperfusion followed by cardiac arrest. The alkalized NH_4^+ pulse was observed in LV^{WT} and $LV^{db/db}$ (Figure 3(a)). The acidification rate of $LV^{db/db}$ strips was increased compared to LV^{WT} strips (Figure 3(b)). To confirm the NH_4^+ pulse-induced changes in pH_i , we measured pH_i in isolated single cardiomyocyte and compared pH changes of cardiac strips (Figure 3(c)). NH_4^+ pulse-induced pH trace between the cardiac strip and cardiomyocyte has the same pattern. Additionally, we determined the T-tubule structure in freshly isolated cardiac myocytes using the membrane-specific dye di-8-ANEPPS. Confocal images from cardiac

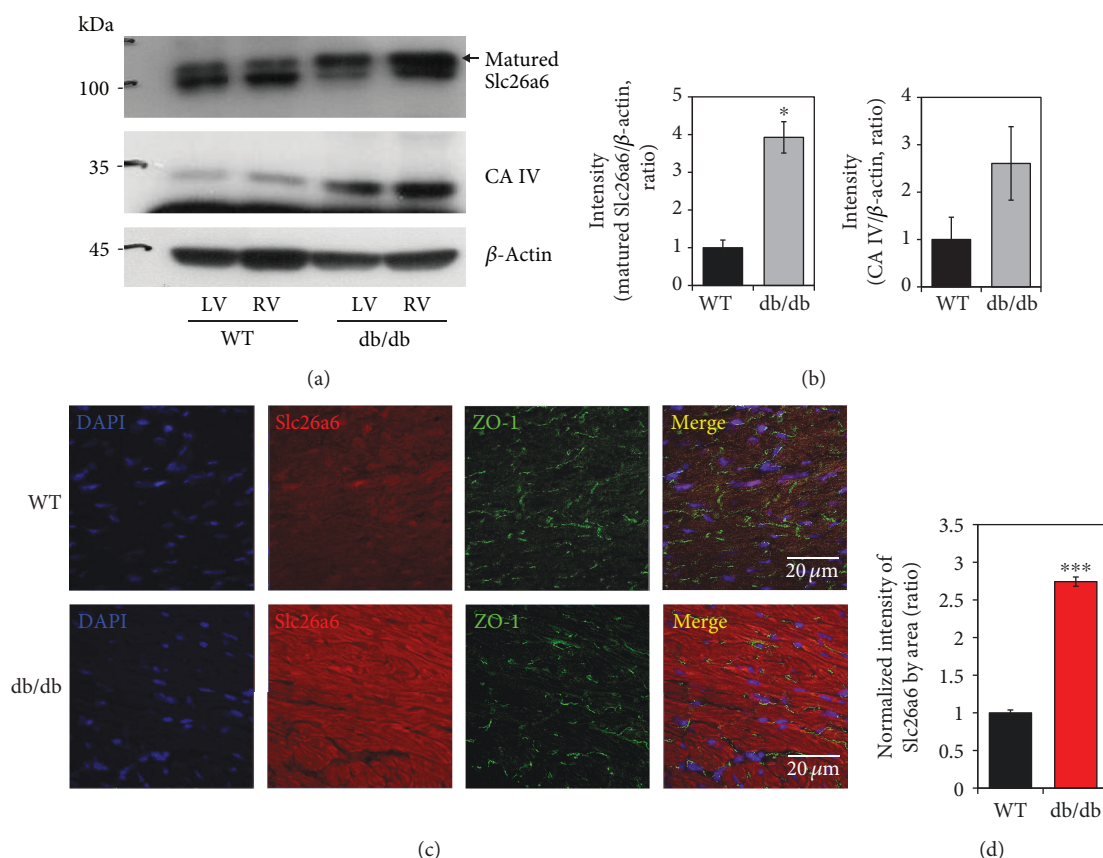


FIGURE 4: Increased expression of Slc26a6 in db/db cardiac tissue. (a) Protein expression of Slc26a6 and CA IV in cardiac tissues of WT and db/db mice. (b) Analysis of band intensity of mature Slc26a6 and CA IV in LV. β -Actin was used as the loading control. Bars present the mean \pm SEM ($n = 3$, * $P < 0.05$). (c) Immunolocalization of Slc26a6 (red), intercalated disc marker ZO-1 (green), and nucleus (DAPI, blue) in cardiac tissues of WT and db/db mice. The scale bars represent 20 μ m. (d) Analysis of normalized intensity (total intensity/measuring area) of Slc26a6. Bars present the mean \pm SEM ($n = 4$, *** $P < 0.001$).

myocytes stained with di-8-ANEPPS (green, Figure 3(d)) were obtained. The pH calibration curve of cardiac strips was applied to all changes in pH experiments (Supplementary Figure 1).

3.3. Increased Expression of Slc26a6 in db/db Cardiac Tissue. The $\text{Cl}^-/\text{HCO}_3^-$ exchanger (CBE) mediates Cl^- uptake and acidification of pH_i through the HCO_3^- efflux. Although AE3 is involved in CBE, we focused on Slc26a6, which dominantly expresses in the mouse heart compared to AE3 [27, 28]. To evaluate the expression of Slc26a6 in WT and db/db mice, we performed western blot analysis in WT and db/db cardiac tissues. Interestingly, Slc26a6 expression was enhanced in db/db mice (Figures 4(a) and 4(b)). In db/db cardiac tissues, the expression of CA IV was moderately increased, however, not statistically different (Figures 4(a) and 4(b)). Membrane-associated CA IV interacts with HCO_3^- transporters to facilitate formation of HCO_3^- transport metabolons [29]. We confirmed immunolocalization of Slc26a6 in cardiac tissues. The expression of Slc26a6 in $\text{LV}^{\text{db/db}}$ was 2.7 times that of LV^{WT} (Figures 4(c) and 4(d)). These results suggested that the enhanced expression of the Slc26a6 facilitate Cl^- flux in db/db cardiac tissues.

3.4. Supportive Function of CA IV on SLC26A6 Activity and Enhanced CBE Activity in db/db Cardiac Strips. Whether CBE activity is maintained after cardioplegic arrest remains unknown. The CBE activity of $\text{LV}^{\text{db/db}}$ strips was moderately increased as compared with that of LV^{WT} strips after the cardioplegic arrest (Figures 5(a) and 5(b)). Enhanced protein expression of Slc26a6 and CA IV will provide the increased CBE activity. Thus, we explored the mechanism underlying CA IV and SLC26A6-mediated changes *in vitro*. CA IV enhanced SLC26A6 activity (Figures 5(c) and 5(d)). Both CA IV and SLC26A6 did not interact with each other (data not shown); however, CA IV facilitated the $\text{Cl}^-/\text{HCO}_3^-$ exchange activity of SLC26A6. To confirm the involvement of Slc26a6, protein kinase C agonist phorbol 12-myristate 13-acetate (PMA), known as a Slc26a6 inhibitor [30, 31], was added in cardioplegia solution. The CBE activity was inhibited by the treatment of PMA in cardiac strips (Figures 5(e) and 5(f)). To confirm the effect of Cl^- movement through NKCC and Slc26a6, changes in intracellular Cl^- concentration in LV^{WT} and $\text{LV}^{\text{db/db}}$ strips were examined by the MQAE fluorescence quenching technique. MQAE fluorescence usually increases in the presence of 0 Cl^- media due to the decrease in intracellular Cl^- concentration [32].

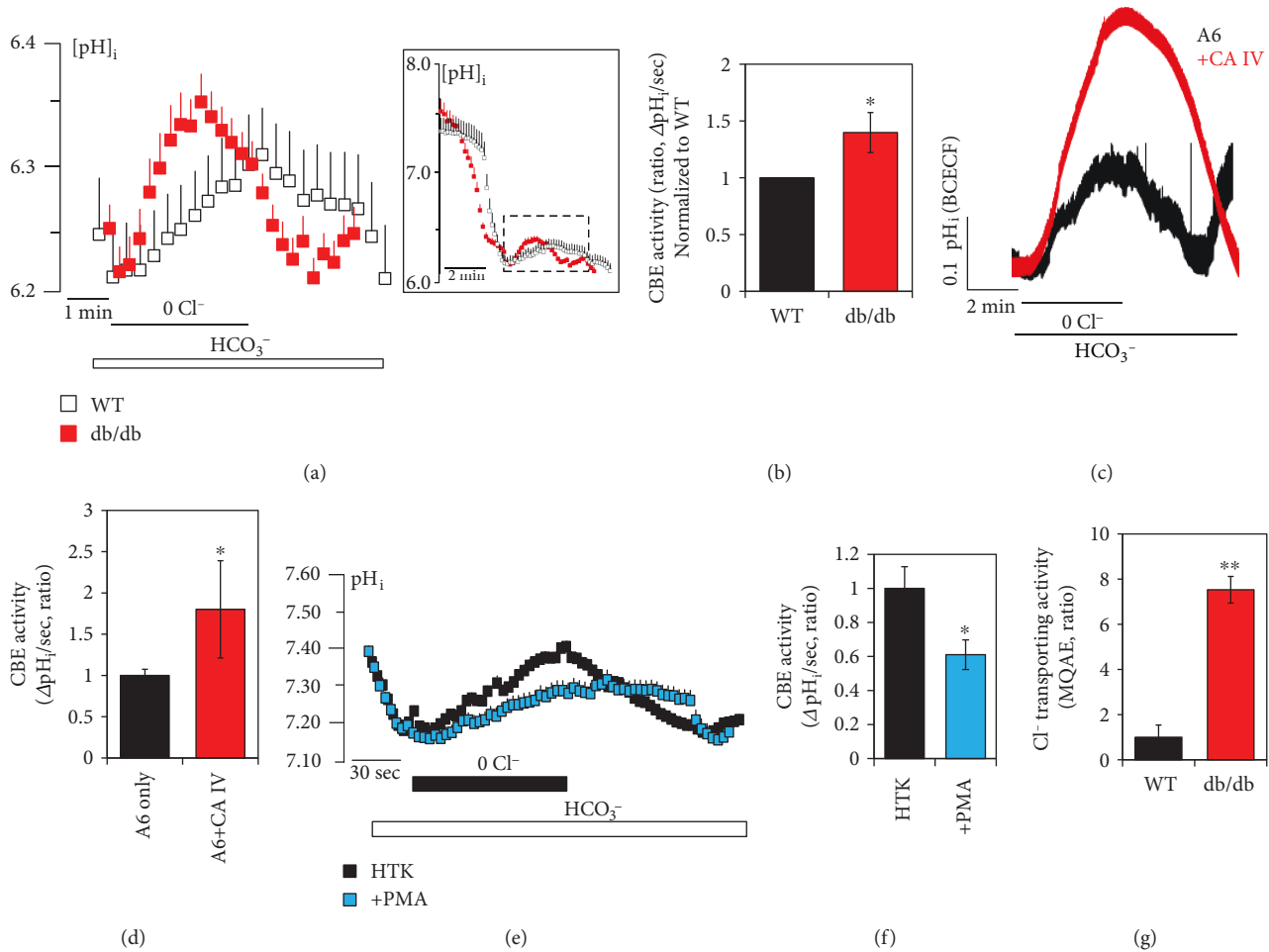


FIGURE 5: Supportive function of CAIV on SLC26A6 activity and enhanced CBE activity in db/db cardiac strips. (a) CBE activity was assessed by measuring changes in pH_i in LV cardiac strips of WT (open black square) and db/db (closed red square) mice following cardioplegia-induced arrest. Full image of CBE activity was represented in the square box, and magnified images were obtained from the dotted line. (b) Analysis of CBE activity. The slope of pH_i was measured as CBE activity in $0 Cl^-$. The bars show the mean \pm SEM ($n = 3$, $*P < 0.05$). (c) Changes in pH_i by CBE activity of human SLC26A6- (A6-) overexpressed HEK293T cells with and without human CA IV. (d) Analysis of CBE activity. The slope of pH_i was measured in CBE activity in the $0 Cl^-$. The bars represent the mean \pm SEM ($n = 3$, $*P < 0.05$). (e) Changes in pH_i by CBE activity with (closed blue square) and without (closed black square) 50 nM PMA and (f) analysis of CBE activity. The bars represent the mean \pm SEM ($n = 3$, $*P < 0.05$). (g) Analysis of Cl^- transporting activity with MQAE technique between WT and db/db LV strips. The bars represent mean \pm SEM ($n = 4$, $**P < 0.01$).

Interestingly, the Cl^- transporting activity of $LV^{db/db}$ strips was dramatically increased in $0 Cl^-$ media with MQAE fluorescence quenching technique (Figure 5(g)). These results suggested that the enhanced expression of SLC26a6 facilitates Cl^- transporting activity in db/db cardiac tissues after cardioplegia-induced arrest.

3.5. Activity and Protein Expression of NHE1 between WT and db/db after HTK-Induced Arrest. The Cl^-/HCO_3^- exchange facilitates Na^+ -loading, associated with Na^+ -dependent acid extrusion mechanisms such as NHE1, a major pH regulator [28]. We verified the role of NHE activity and protein expression after the cardioplegia-induced arrest. After the cardioplegia, there was no difference of NHE activity (Figures 6(a)–6(c)). The protein expression of NHE1 has no difference between LV^{WT} strips and $LV^{db/db}$ strips (Figures 6(d) and 6(e)).

4. Discussion

We hypothesized that the diabetic myocardium is more vulnerable after cardioplegia infusion than the myocardium in the condition of normal glucose, as the various ion channels that are involved in $[Na^+]_i$ homeostasis are altered. Cation flux via NKCC following ischemia was shown to be expressively increased in type 1 diabetic hearts, and inhibition of NKCC revealed the reduced ischemic injury in diabetic hearts [33]. In this study, we found enhanced NKCC1 protein and increased NKCC1 activity in $LV^{db/db}$. NKCC upregulation and its glycosylation disrupt Cl^- homeostasis [34]. Enhanced expression of NKCC1 in the db/db heart may provide synergistic dysregulation of Cl^- concentration in company with the enhanced SLC26a6. As enhanced CBE activity in $LV^{db/db}$, the Cl^- transporting activity of SLC26a6 in $LV^{db/db}$ was increased as compared with that of LV^{WT} .

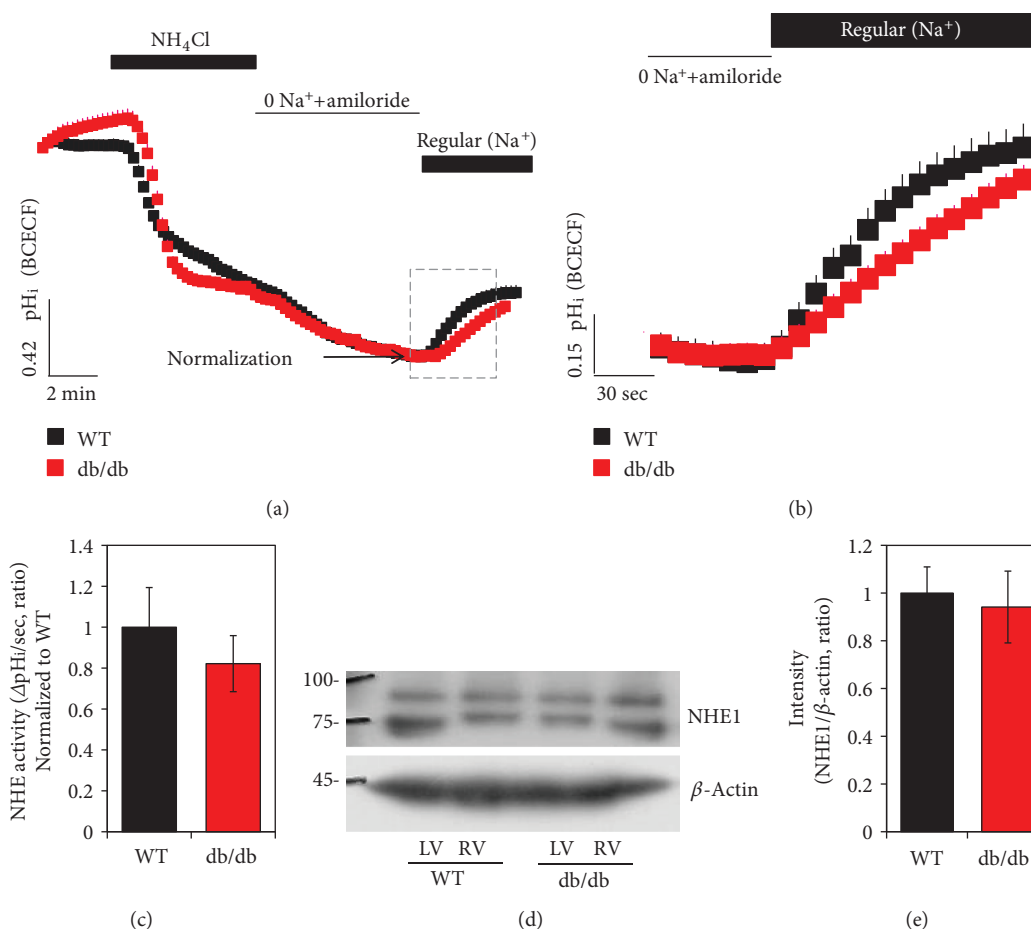


FIGURE 6: Activity and protein expression of NHE1 between WT and db/db after HTK-induced arrest. (a) NHE activity was assessed by NH₄Cl pulse technique in LV cardiac strips of WT (closed black square) and db/db (closed red square) mice following cardioplegia-induced arrest. Full image of NHE activity was represented in the square box, and magnified images were obtained from the dotted line. (b) NHE activity in LV of WT after cardioplegia-induced arrest. (c) Analysis of NHE activity. The slope of pHi was measured in NHE activity in the Na⁺-containing Regular solution. The bars represent the mean ± SEM ($n = 3$). (d) Expression of NHE1 protein in LV and RV cardiac strips of WT and db/db following cardioplegia-induced arrest. (e) Analysis of band intensity of NHE1 in LV. The β -actin was used as the loading control. The bars show the mean ± SEM ($n = 3$).

In addition, activity of Slc26a6 in db/db may be further enhanced due to the involvement of CA IV. The kinetics of Cl⁻ flux was partly addressed in diabetic mice almost 40 years ago [35]. The Cl⁻/HCO₃⁻ exchangers, encoded *Slc4a3* and *Slc26a6* genes, are expressed in heart tissue [27, 28, 36]. They are also called acid loaders and mediate HCO₃⁻ efflux and Cl⁻ influx to induce acidification of pHi. Slc26a6 is known as a dominant transporter in the heart ventricle [27]. Although complicated regulatory mechanisms underlie the various ion transporters, we found enhanced expression of Slc26a6 and Cl⁻ transporting activity in the db/db heart, suggesting that effective Slc26a6 blockers may be efficient in modulating pH of type 2 diabetic hearts.

In this study, we addressed that the pH modulation after cardioplegic arrest was differentially regulated between WT and diabetic hearts. During the cardioplegia, the intracellular acidosis provides the primary source of ischemic reperfusion injury, and the mechanism is postulated in Figure 7. Based on our results, the db/db hearts were observed to increase NKCC, CBE, and Cl⁻ transporting activities caused by

enhanced NKCC and Slc26a6 expression. It has been addressed that the enhanced expression and function of cardiac NKCC were observed during congestive heart failure and myocardial remodeling [37]. Enhanced NKCC activity of the db/db heart in the current study may also provide the pathological clue for the diabetic heart.

The HCO₃⁻ modulation of Slc26a6 in the heart was revealed in several reports [27, 28]. It also has been addressed that the role of Slc26a6 was Cl⁻/oxalate exchanger to secrete oxalate rather than Cl⁻/HCO₃⁻ exchanger in salivary glands [38]. Although we addressed enhanced Slc26a6 expression in the db/db heart, Cl⁻ window of Slc26a6 transporter needs to be clarified. It also has been carefully considered the enhanced Cl⁻ transporting activity in the db/db heart. Moreover, the physiological and pathological roles and cross-linked role of cardiac NKCC and Slc26a6 are currently unclear, and the mechanisms behind the Cl⁻ regulation cannot be concluded from the current results. Possibly, the elevated NKCC and Slc26a6 will provide the favorable circumstances to elevate Cl⁻ transporting activity in the db/db

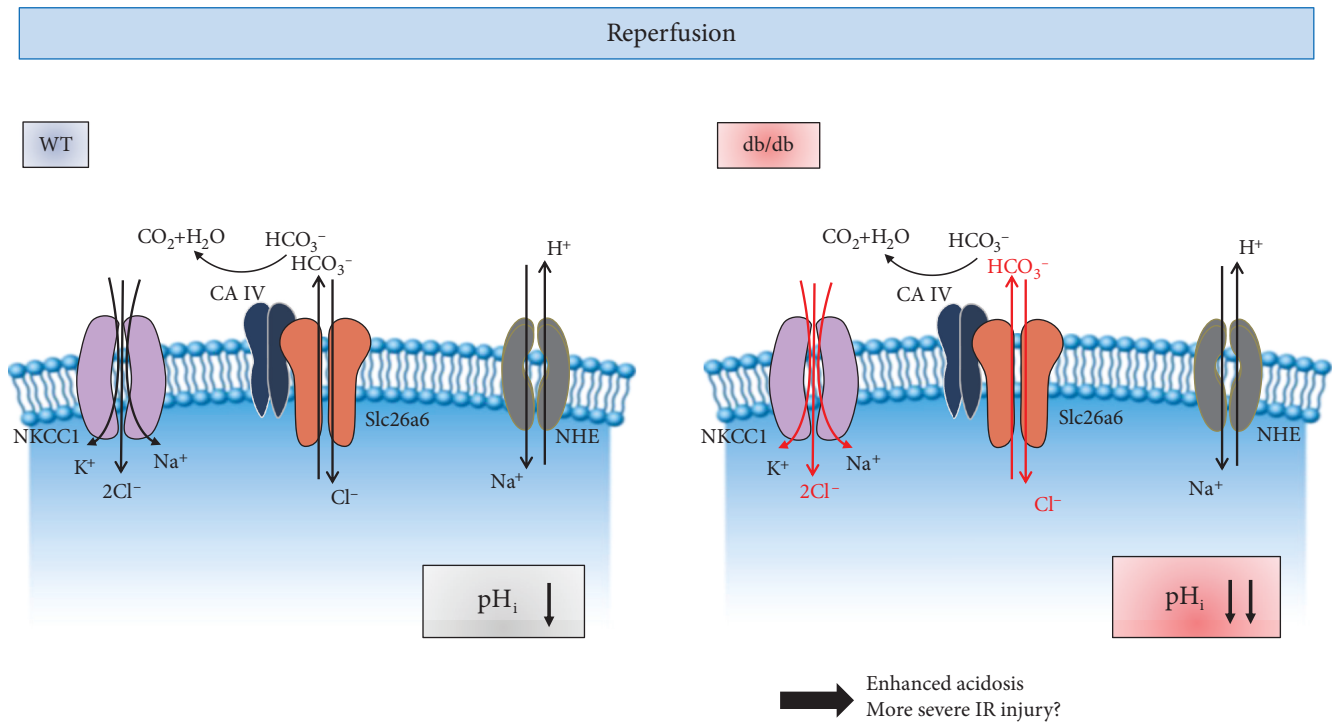


FIGURE 7: Schematic model of involvement of ion transporters followed by cardioplegia-induced arrest and ion imbalance in the db/db heart. Enhanced Slc26a6 and NKCC1 in the db/db heart may be involved in dysregulated pH_i and Cl^- modulation after cardioplegia-induced arrest. Abbreviation: NHE: $Na^+ - H^+$ exchanger; Slc26a6: solute carrier transporter 26 family a6; NKCC1: $Na^+ - K^+ - 2Cl^-$ cotransporter 1; CA IV: carbonic anhydrase IV.

heart. In addition, the Cl^- influx and HCO_3^- efflux by Slc26a6 may facilitate intracellular acidification during cardioplegia-induced arrest in the diabetic myocardium.

The results of the current study revealed several important limitations. For technical limitation, the current study was performed in normothermic temperatures, deviation from the cardiac surgery situation as Egar et al. mentioned [39]. However, the strength of our studies places in the fact that we modified the Langendorff-free method, which mimics immediately after aortic cross-clamp application and initial phase of cardioplegia-induced arrest during cardiac surgeries. In addition, the type 2 diabetes model (db/db mouse) with a high serum glucose level was used to evaluate the cardioplegia effect on the myocardium. Clinically, type 2 diabetes patients are more prone to cardiac diseases as compared to type 1 diabetes and require cardiac surgeries. Since the pathophysiological meaning of type 1 and 2 diabetes and their effect on the myocardium are different, our study is relevant in a clinical setting. Our study results suggested that it is necessary to develop cardioplegia that is specialized for diabetic patients. As such, this study suggests that modulation of ion-transporting activity in the db/db heart may be an effective strategy for preventing cardiac damage including acidosis and edema in diabetic patients after cardioplegia infusion.

Data Availability

All data and figures used to support the findings of this study are included within the article.

Conflicts of Interest

The authors declare that they have no conflicts of interest with the contents of this article.

Authors' Contributions

JHH and KHS contributed to conception and design of manuscript and acquisition and analysis of data in the cardioplegia-induced model; SAL reanalyzed and confirmed data; MJJ, SIL, and SAL made the draft of the article, acquired data, or reorganize and revise it critically for important intellectual content; and JHH drew all schematic animations. Minjeong Ji, Seok In Lee, and Sang Ah Lee contributed equally to this work. The drawings of Figures 1 and 7 were drawn by Dr. Jeong Hee Hong and Minjeong Ji.

Acknowledgments

This work was supported by the National Research Foundation of Korea (NRF) grant funded by the Korea government (MSIT) (2016R1D1A1B03933680 (KHS)) and grant from the Gil Medical Center, Gachon University, project (FRD 2018-07, JHH; FRD 2017-16, SIL).

Supplementary Materials

Supplementary Figure 1: pH calibration curve for LV cardiac strips at pH 5.5, 6.0, 6.5, 7.0, 7.5, 8.0, and 8.5. Ratios of BCECF-AM (Teflabs) were converted to pH unit as described previously [21, 22]. Briefly, cardiac strips were

incubated in the calibration solution (pH 5.5, 6.0, 6.5, 7.0, 7.5, 8.0, and 8.5) for 5 min at room temperature. The equation of the pH calibration curve was $\text{pH} = \text{pKa} + \log \left(\frac{(R_{\text{max}} - R)}{(R - R_{\text{min}})} \right)$ (R : ratio value of BCECF; R_{max} : maximum ratio; R_{min} : minimum ratio; pKa value of BCECF: 6.97). The BCECF fluorescence ratio was converted to the changes in pH_i (ΔpH_i) value, followed by the calibration curve. (*Supplementary Materials*)

References

- [1] S. Muraki, C. D. Morris, J. M. Budde, Z. Q. Zhao, R. A. Guyton, and J. Vinten-Johansen, "Blood cardioplegia supplementation with the sodium-hydrogen ion exchange inhibitor cariporide to attenuate infarct size and coronary artery endothelial dysfunction after severe regional ischemia in a canine model," *The Journal of Thoracic and Cardiovascular Surgery*, vol. 125, no. 1, pp. 155–164, 2003.
- [2] L. H. Opie, "Postischemic stunning—the case for calcium as the ultimate culprit," *Cardiovascular Drugs and Therapy*, vol. 5, no. 5, pp. 895–899, 1991.
- [3] D. J. Chambers and H. B. Fallouh, "Cardioplegia and cardiac surgery: pharmacological arrest and cardioprotection during global ischemia and reperfusion," *Pharmacology & Therapeutics*, vol. 127, no. 1, pp. 41–52, 2010.
- [4] G. P. Dobson, G. Faggian, F. Onorati, and J. Vinten-Johansen, "Hyperkalemic cardioplegia for adult and pediatric surgery: end of an era?," *Frontiers in Physiology*, vol. 4, p. 228, 2013.
- [5] A. Camara, J. An, Q. Chen et al., "Na⁺/H⁺ exchange inhibition with cardioplegia reduces cytosolic [Ca²⁺] and myocardial damage after cold ischemia," *Journal of Cardiovascular Pharmacology*, vol. 41, no. 5, pp. 686–698, 2003.
- [6] P. Nardi, S. R. Vacirca, M. Russo et al., "Cold crystalloid versus warm blood cardioplegia in patients undergoing aortic valve replacement," *Journal of Thoracic Disease*, vol. 10, no. 3, pp. 1490–1499, 2018.
- [7] C. H. Yeh, T. P. Chen, Y. C. Wang, Y. M. Lin, and S. W. Fang, "AMP-activated protein kinase activation during cardioplegia-induced hypoxia/reoxygenation injury attenuates cardiomyocyte apoptosis via reduction of endoplasmic reticulum stress," *Mediators of Inflammation*, vol. 2010, Article ID 130636, 9 pages, 2010.
- [8] J. Feng and F. Sellke, "Microvascular dysfunction in patients with diabetes after cardioplegic arrest and cardiopulmonary bypass," *Current Opinion in Cardiology*, vol. 31, no. 6, pp. 618–624, 2016.
- [9] O. Frolich and M. Karmazyn, "The Na–H exchanger revisited: an update on Na–H exchange regulation and the role of the exchanger in hypertension and cardiac function in health and disease," *Cardiovascular Research*, vol. 36, no. 2, pp. 138–148, 1997.
- [10] M. Karmazyn and M. P. Moffat, "Role of Na⁺/H⁺ exchange in cardiac physiology and pathophysiology: mediation of myocardial reperfusion injury by the pH paradox," *Cardiovascular Research*, vol. 27, no. 6, pp. 915–924, 1993.
- [11] M. M. Pike, C. S. Luo, M. D. Clark et al., "NMR measurements of Na⁺ and cellular energy in ischemic rat heart: role of Na⁺-H⁺ exchange," *American Journal of Physiology-Heart and Circulatory Physiology*, vol. 265, no. 6, pp. H2017–H2026, 1993.
- [12] X. H. Xiao and D. G. Allen, "Activity of the Na⁺/H⁺ exchanger is critical to reperfusion damage and preconditioning in the isolated rat heart," *Cardiovascular Research*, vol. 48, no. 2, pp. 244–253, 2000.
- [13] L. Daniels, J. R. Bell, L. M. D. Delbridge, F. J. McDonald, R. R. Lamberts, and J. R. Erickson, "The role of CaMKII in diabetic heart dysfunction," *Heart Failure Reviews*, vol. 20, no. 5, pp. 589–600, 2015.
- [14] E. Balse and H. E. Boycott, "Ion channel trafficking: control of ion channel density as a target for arrhythmias?," *Frontiers in Physiology*, vol. 8, p. 808, 2017.
- [15] P. Eder, "Cardiac remodeling and disease: SOCE and TRPC signaling in cardiac pathology," *Advances in Experimental Medicine and Biology*, vol. 993, pp. 505–521, 2017.
- [16] M. Ackers-Johnson, P. Y. Li, A. P. Holmes, S.-M. O'Brien, D. Pavlovic, and R. S. Foo, "A simplified, Langendorff-free method for concomitant isolation of viable cardiac myocytes and nonmyocytes from the adult mouse heart," *Circulation Research*, vol. 119, no. 8, pp. 909–920, 2016.
- [17] R. L. Evans and R. J. Turner, "Upregulation of Na⁽⁺⁾-K⁽⁺⁾-2Cl⁻ cotransporter activity in rat parotid acinar cells by muscarinic stimulation," *The Journal of Physiology*, vol. 499, no. 2, pp. 351–359, 1997.
- [18] D. U. Lee, D. M. Shin, and J. H. Hong, "The regulatory role of rolipram on inflammatory mediators and cholinergic/adrenergic stimulation-induced signals in isolated primary mouse submandibular gland cells," *Mediators of Inflammation*, vol. 2016, Article ID 3745961, 11 pages, 2016.
- [19] L. F. Hu, Y. Li, K. L. Neo et al., "Hydrogen sulfide regulates Na⁺/H⁺ exchanger activity via stimulation of phosphoinositide 3-kinase/Akt and protein kinase G pathways," *The Journal of Pharmacology and Experimental Therapeutics*, vol. 339, no. 2, pp. 726–735, 2011.
- [20] S. Nishio, Y. Teshima, N. Takahashi et al., "Activation of CaMKII as a key regulator of reactive oxygen species production in diabetic rat heart," *Journal of Molecular and Cellular Cardiology*, vol. 52, no. 5, pp. 1103–1111, 2012.
- [21] K. Nehrke, "Intracellular pH measurements in vivo using green fluorescent protein variants," *Methods in Molecular Biology*, vol. 351, pp. 223–239, 2006.
- [22] P. Rochon, M. Jourdain, J. Mangalaboyi et al., "Evaluation of BCECF fluorescence ratio imaging to properly measure gastric intramucosal pH variations in vivo," *Journal of Biomedical Optics*, vol. 12, no. 6, article 064014, 2007.
- [23] J. H. Hong, E. Muhammad, C. Zheng et al., "Essential role of carbonic anhydrase XII in secretory gland fluid and HCO₃⁻ secretion revealed by disease causing human mutation," *The Journal of Physiology*, vol. 593, no. 24, pp. 5299–5312, 2015.
- [24] M. K. Cavaghan, D. A. Ehrmann, and K. S. Polonsky, "Interactions between insulin resistance and insulin secretion in the development of glucose intolerance," *The Journal of Clinical Investigation*, vol. 106, no. 3, pp. 329–333, 2000.
- [25] L. A. Gallo, M. S. Ward, A. K. Fotheringham et al., "Once daily administration of the SGLT2 inhibitor, empagliflozin, attenuates markers of renal fibrosis without improving albuminuria in diabetic *db/db* mice," *Scientific Reports*, vol. 6, no. 1, article 26428, 2016.
- [26] R. L. Leibel, W. K. Chung, and S. C. Chua Jr., "The molecular genetics of rodent single gene obesities," *The Journal of Biological Chemistry*, vol. 272, no. 51, pp. 31937–31940, 1997.
- [27] B. V. Alvarez, D. M. Kieller, A. L. Quon, D. Markovich, and J. R. Casey, "Slc26a6: a cardiac chloride-hydroxyl exchanger

- and predominant chloride-bicarbonate exchanger of the mouse heart," *The Journal of Physiology*, vol. 561, no. 3, pp. 721–734, 2004.
- [28] H. S. Wang, Y. Chen, K. Vairamani, and G. E. Shull, "Critical role of bicarbonate and bicarbonate transporters in cardiac function," *World Journal of Biological Chemistry*, vol. 5, no. 3, pp. 334–345, 2014.
- [29] G. J. Schwartz, A. M. Kittelberger, D. A. Barnhart, and S. Vijayakumar, "Carbonic anhydrase IV is expressed in H(+)-secreting cells of rabbit kidney," *American Journal of Physiology-Renal Physiology*, vol. 278, no. 6, pp. F894–F904, 2000.
- [30] H. A. Hassan, S. Mentone, L. P. Karniski, V. M. Rajendran, and P. S. Aronson, "Regulation of anion exchanger Slc26a6 by protein kinase C," *American Journal of Physiology-Cell Physiology*, vol. 292, no. 4, pp. C1485–C1492, 2007.
- [31] D. Lee, S. A. Lee, D. M. Shin, and J. H. Hong, "Chloride influx of anion exchanger 2 was modulated by calcium-dependent spinophilin in submandibular glands," *Frontiers in Physiology*, vol. 9, 2018.
- [32] Y. S. Jeong and J. H. Hong, "Governing effect of regulatory proteins for Cl⁻/HCO₃⁻ exchanger 2 activity," *Channels*, vol. 10, no. 3, pp. 214–224, 2016.
- [33] R. Ramasamy, J. A. Payne, J. Whang, S. R. Bergmann, and S. Schaefer, "Protection of ischemic myocardium in diabetics by inhibition of electroneutral Na⁺-K⁺-2Cl⁻ cotransporter," *American Journal of Physiology-Heart and Circulatory Physiology*, vol. 281, no. 2, pp. H515–H522, 2001.
- [34] Z. Y. Ye, D. P. Li, H. S. Byun, L. Li, and H. L. Pan, "NKCC1 upregulation disrupts chloride homeostasis in the hypothalamus and increases neuronal activity-sympathetic drive in hypertension," *The Journal of Neuroscience*, vol. 32, no. 25, pp. 8560–8568, 2012.
- [35] O. Berglund, "Disturbed fluxes of Rb⁺(K⁺) and Cl⁻ in islets of spontaneously diabetic mice (C57BL/KsJ-db/db)," *Acta Biologica et Medica Germanica*, vol. 40, no. 1, pp. 23–30, 1981.
- [36] H. J. Kim, R. Myers, C. R. Sihm, S. Rafizadeh, and X. D. Zhang, "Slc26a6 functions as an electrogenic Cl⁻/HCO₃⁻ exchanger in cardiac myocytes," *Cardiovascular Research*, vol. 100, no. 3, pp. 383–391, 2013.
- [37] G. O. Andersen, E. Øie, L. E. Vinge et al., "Increased expression and function of the myocardial Na-K-2Cl cotransporter in failing rat hearts," *Basic Research in Cardiology*, vol. 101, no. 6, pp. 471–478, 2006.
- [38] T. Mukaibo, T. Munemasa, A. T. George et al., "The apical anion exchanger Slc26a6 promotes oxalate secretion by murine submandibular gland acinar cells," *The Journal of Biological Chemistry*, vol. 293, no. 17, pp. 6259–6268, 2018.
- [39] J. Egar, A. Ali, S. E. Howlett, C. H. Friesen, and S. O'Blenes, "The Na⁺/Ca²⁺ exchange inhibitor SEA0400 limits intracellular Ca²⁺ accumulation and improves recovery of ventricular function when added to cardioplegia," *Journal of Cardiothoracic Surgery*, vol. 9, no. 1, 2014.